



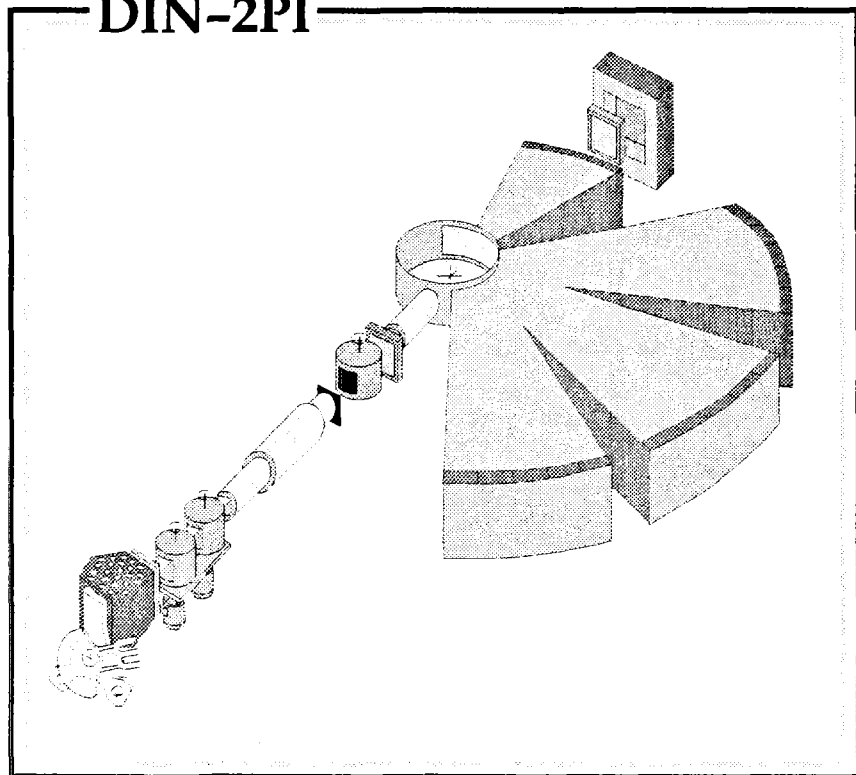
The Ministry of Russian Federation for Atomic Energy  
The State Scientific Center of Russian Federation  
**INSTITUTE OF PHYSICS AND POWER ENGINEERING**  
named after Acad. A.I.Leipunsky

**Nuclear Physics Department**

# **ANNUAL REPORT**

## **2000**

**DIN-2PI**



**OBNINSK**



# **Annual Report**

---

## **Nuclear Physics Department**

**The Ministry of Russian Federation for Atomic Energy  
The State Scientific Center of Russian Federation  
INSTITUTE OF PHYSICS AND POWER ENGINEERING  
named after Acad. A.I.Leipunsky**

---

**For the year 1 January to 31 December 2000**

**Contacts:**

**Nuclear Physics Department  
The State Scientific Center of Russian Federation  
Institute of Physics and Power Engineering  
named after Acad. A.I.Leypunsky.  
The Ministry of the Russian Federation for  
Atomic Energy.  
249020, Obninsk, Kaluga Region, Russia  
FAX: (095) 230 23 26, 8833112  
e-mail: kuzminov@ippe.obninsk.ru**

**Editor:**

**B.D.Kuzminov**

© Institute for Physics and Power Engineering  
named after Acad. A.I.Leipunsky,  
Nuclear Physics Department, 2001

Printed at IPPE, Obninsk, Russia.

# CONTENTS

---

## PREFACE

<b>1. DEPARTMENT STRUCTURE.....</b>	<b>5</b>
<b>2. SCIENTIFIC RESEARCH</b>	
<b>2.1 Nuclear Fission .....</b>	<b>7</b>
<b>2.2 Nuclear Structure and         Nuclear Reactions .....</b>	<b>23</b>
<b>2.3 Nuclear Data .....</b>	<b>33</b>
<b>2.4 Transmutation.....</b>	<b>47</b>
<b>2.5 Condensed Matter Physics.....</b>	<b>60</b>
<b>2.6 Mathematical Modeling.....</b>	<b>76</b>
<b>2.7 Applied Research .....</b>	<b>86</b>
<b>3. ACCELERATOR COMPLEX .....</b>	<b>96</b>
<b>4. PUBLICATIONS .....</b>	<b>97</b>
<b>5. PARTICIPATION IN INTERNATIONAL AND     NATIONAL CONFERENCES AND MEETINGS .....</b>	<b>106</b>
<b>6. COOPERATION.....</b>	<b>107</b>

---

## PREFACE

This edition covers a period from January 1 2000 to December 31 2000.

For the last year the investigations were carried out to improve the knowledge in field of nuclear physics, nuclear data, condensed matter physics, mathematical modeling and to develop accelerator facilities and nuclear measurement techniques for nuclear and non-nuclear applications.

Some of the principal investigations were: cold fragmentation in fission  $^{238}\text{U}$  by 5 Mev neutrons; fission fragment mass-energy and angular distributions at 1.2 Mev and 5.0 MeV neutron induced fission of  $^{232}\text{Th}$ ; the energy spectrum of delayed neutrons from fission of  $^{235}\text{U}$  and  $^{237}\text{Np}$ ; direct neutron capture in a microscopic model; neutron cross section evaluations for  $^{232}\text{Th}$  and  $^{238}\text{U}$  up to 150 MeV; radiological aspects of heavy metal liquid targets for accelerator-driven systems as intense neutron sources; neutron scattering microscopic investigation of liquid lead and lead-potassium eutectic alloy; surface excitations in a thin helium film in silica aerogels; nonlinear breather vibrations of crystals in the vicinity of defect generation threshold; numerical simulation of anomalous doping effect in Ge single crystals grown by FZ-technique aboard the space crafts; the fission fragment interaction with polymeric compounds and formation of a latent track; low - rated wear and corrosion monitoring by a thin layer activation technique.

In the end of 2000 several long-term programs of fundamental investigations were worked out. The objective of these programs was to develop nuclear technologies, specifically to create a new version of the Russian library recommended evaluated neutron data – BROND-3.



B. Fursov  
Director of Nuclear Physics Department

# 1. DEPARTMENT STRUCTURE

## DIRECTORATE:

Director: B.I.FURSOV  
Deputy Directors: B.D.KUZMINOV  
V.E.RUDNIKOV

## THEORETICAL NUCLEAR PHYSICS DIVISION

Head: A.V.IGNATYUK

### THEORETICAL NUCLEAR PHYSICS LABORATORY

Head: Yu.N.SHUBIN

### NUCLEAR DATA CENTER

Head: V.N.MANOKHIN

## EXPERIMENTAL NUCLEAR PHYSICS DIVISION

Head: A.A.GOVERDOVSKI

### NUCLEAR FISSION PHYSICS LABORATORY

Head: M.I.SVIRIN

### NEUTRON SPECTROMETRY LABORATORY

Head: B.V.ZHURAVLEV

### NUCLEAR REACTIONS LABORATORY

Head: V.M.PIKSAIKIN

### NUCLEAR FISSION DYNAMICS LABORATORY

Head: A.A.GOVERDOVSKI

### APPLIED NUCLEAR PHYSICS LABORATORY

Head: A.A.TUMANOV

## HIGH-VOLTAGE ACCELERATORS DIVISION

Head: A.I.GLOTOV

## CONDENSED MATTER PHYSICS LABORATORY

Head: A.V.PUCHKOV

## MATHEMATICS AND SOFTWARE DIVISION

Head: V.P.GINKIN

### NUMERICAL METHODS LABORATORY

Head: V.P.GINKIN

### PRECISION METHODS LABORATORY

Head: V.K.ARTEMYEV

### STATISTICAL METHODS LABORATORY

Head: S.V.PUPKO

## 2. SCIENTIFIC RESEARCH

### 2.1 NUCLEAR FISSION

#### Fission Fragment Mass-Energy Distribution for 5 MeV Neutron Fission of $^{238}\text{U}$

*V.A. Khriachkov, M.V. Dunaev, I.V. Dunaeva,  
N.N. Semenova, A.I. Sergachev*

##### Introduction

The spectra of cold fragmentation were investigated in detail practically for all thermal induced fission nuclei. This data supply the information for the earliest stages of evolution of fissioning system. For the last 10 years the experiments investigated of cold fragmentation by fast neutrons were carried out in IPPE. The  $^{236}\text{U}$ ,  $^{237}\text{Np}$  and  $^{232}\text{Th}$  nuclei which may be fissioned only by fast neutrons were investigated. In this work we present new result for cold fragmentation  $^{238}\text{U}$  by 5 MeV neutrons.

##### Experiment

The detector of fission fragments was a double Frisch grided ionisation chamber connected with waveform digitizer. The anode signals from each chamber, as digital oscillograms, were stored on the hard disk of computer. The subsequent analysis by digital signal processing methods allowed determinate the kinetic energy, mass and emission angle, for each complementary fragment, simultaneously. The energies of fragments were corrected on grid inefficiency, energy losses in the target and pulse height defect. In addition each of signal was careful check on the pileup with  $\alpha$ -particles or recoiled protons. In detail the method of measurement was described in [1,2,3]. After the correction the experimental data were calibrated with average energy of light fragments estimated in [4] for wide energy range of incident neutrons. We used only one figure for calibration, but reproduced mass, angular and TKE distributions of work [4] with high accuracy. The value of an average total kinetic energy (TKE) in our experiment was 169.8 MeV (170.15 in work [4]).

##### Result and discussion

The spectra of  $^{238}\text{U}$  cold fragmentation for different values of light fragment energy are shown in a Fig.1. It is interesting to highlight, that for high kinetic energies of a light fragment, the peak corresponding to mass 134 is splitted on three components with distances between them 3 mass unites. Such phenomenon is typical for charge-odd fissioning systems (for example,  $^{237}\text{Np}$  [5]), that is explained of free migration of a not paired proton. For charge - even fissioning system, as uranium, it can mean than proton pair is broken near a saddle point. For  $^{238}\text{U}$  fission by neutrons with energy 5 MeV, the excitation energy of a compound nucleus in a saddle point is 3.34 MeV, that is enough for a proton pair breaking.

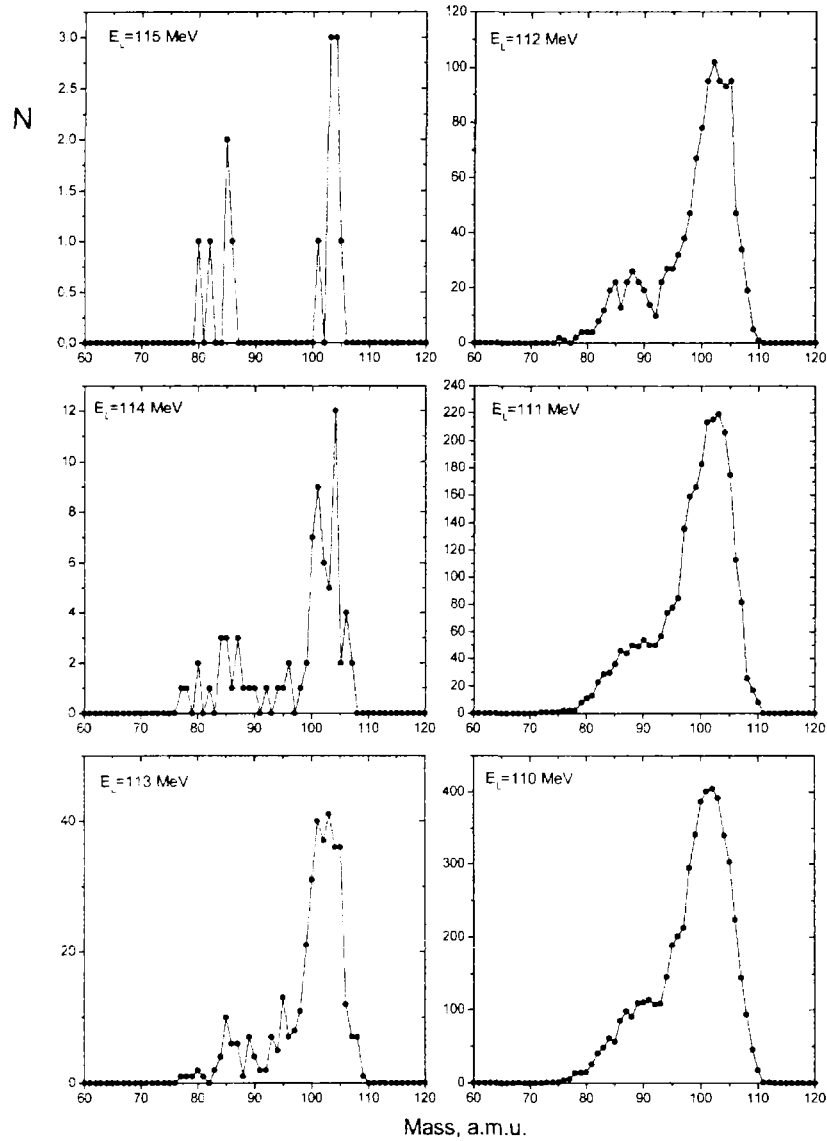


Fig. 1. Mass distributions of light fragments from  $^{238}\text{U}$  for given windows of kinetic energy

The total kinetic energy distributions for fragments with mass 130 and 140 a.m.u. are shown in a Fig. 2. For high values of TKE, the shape of distribution is not gaussian and has the clearly visible border. It seems, that for some masses the highest TKE values equal to total available energy ( $Q^* = \text{mass defect } (Q) + \text{neutron binding energy } (B_n) + \text{neutron kinetic energy } (T_n)$ ). The similar phenomenon was observed in our previous work [6] for  $^{232}\text{Th}$ . The difference between the peak value of TKE achieved in experiment and  $Q^*$  versus mass are shown in Fig. 3. The total kinetic energy reaches total available energy in the region between 134 and 140 masses, and also for masses 128, 129. Having in mind, that the total available energy for different masses varies up to 15 MeV, it is impossible to explain this energy limit by experimental systematic error. Despite of small number of events corresponding to limiting values of TKE, we can definitely conclude that they correspond to real fission events. The actual anode signals, which correspond, to one of two events for mass 140, are shown in a Fig. 4. The

density of ionisation losses (are shown at the bottom of a figure) corresponds to light and heavy fragments. Cosines of emission angles defined independently for each fragment, coincide with precision 0.007. It seems that total excitation energy of compound nucleus (9.8 MeV, including 3.34 MeV in a saddle point) was transformed in the fragment kinetic energy. Probably the fissioning system breaks up near the saddle point into two fragments with equilibrium (main) deformation. Attempts to detect similar decay for  $^{233}\text{U}$  and  $^{235}\text{U}$  thermal neutron fission [7,8], have shown that only 2-3 MeV value of free energy ( $Q^* - \text{TKE}_{\text{Max}}$ ) was reached. This fact can be explained by the analysis of the Thomas diagram [9] (see Fig.5). If the excitation energy is equal or less to fission barrier in the saddle point, the system has no enough energy to generate a surface of two separated fragments. Therefore fissioning system should descends from a barrier on 2-3 MeV and then the necessary energy will be obtained from a Coulomb interaction. Probably intrinsic excitation energy of fragments can be zero but its will not have main deformation. It seems that in our experiment the system has extra energy ( $\sim 3.3$  MeV) to separate nucleus into two fragments near the saddle point. The products of such system decay will be in the main deformation and will not have considerable excitation energy. All these facts allows us to assume that we observe the process when the fissioning system populates the fusion valley well known in heavy ion physics. At usual fission, when there is stage of descent, the fragments are born elongated in comparison with their main deformation. Let's note that a "separated fragments" valley is not the same as a "fusion valley". In the first case the fragments have more long shape. It is possible to assume, that between a saddle point and fusion valley there is  $\sim 3$  MeV potential barrier, and this fission process is inverse to heavy ion fusion process.

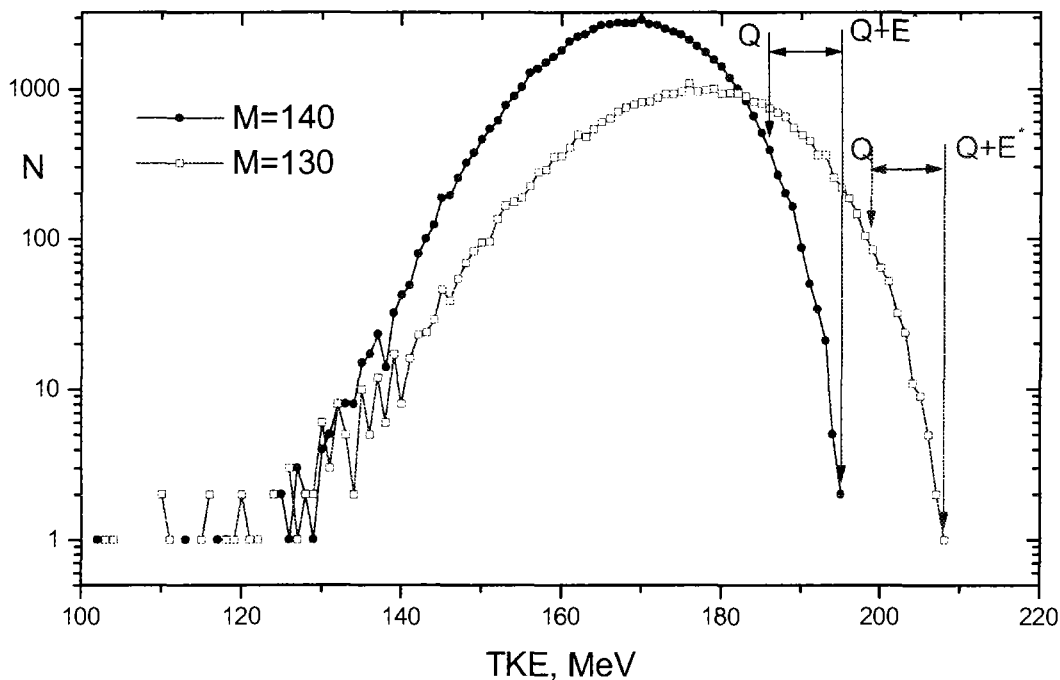


Fig. 2. The total kinetic energy distribution of fission fragment with masses 130 and 140 a.m.u.

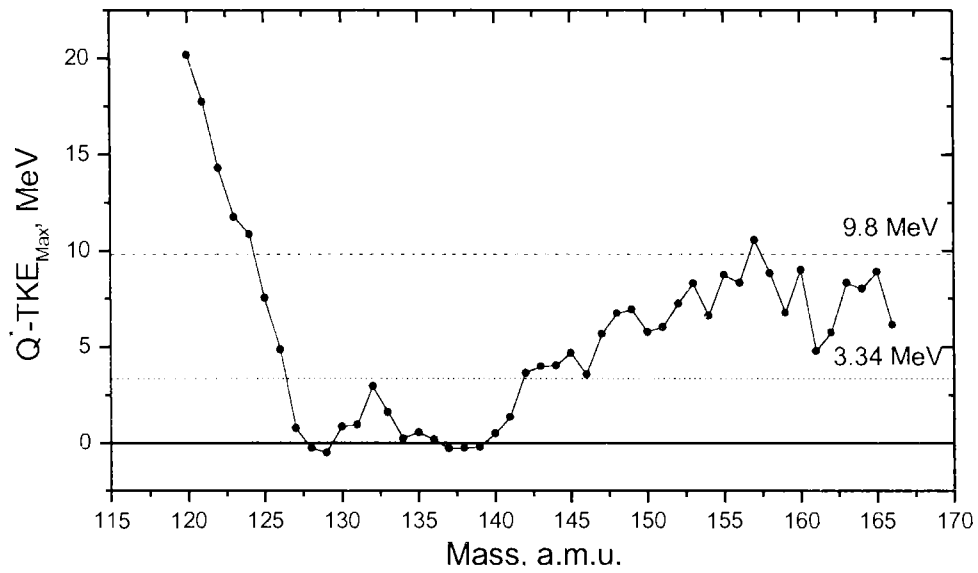


Fig. 3. The limit of total kinetic energy distribution vs. fission fragment mass

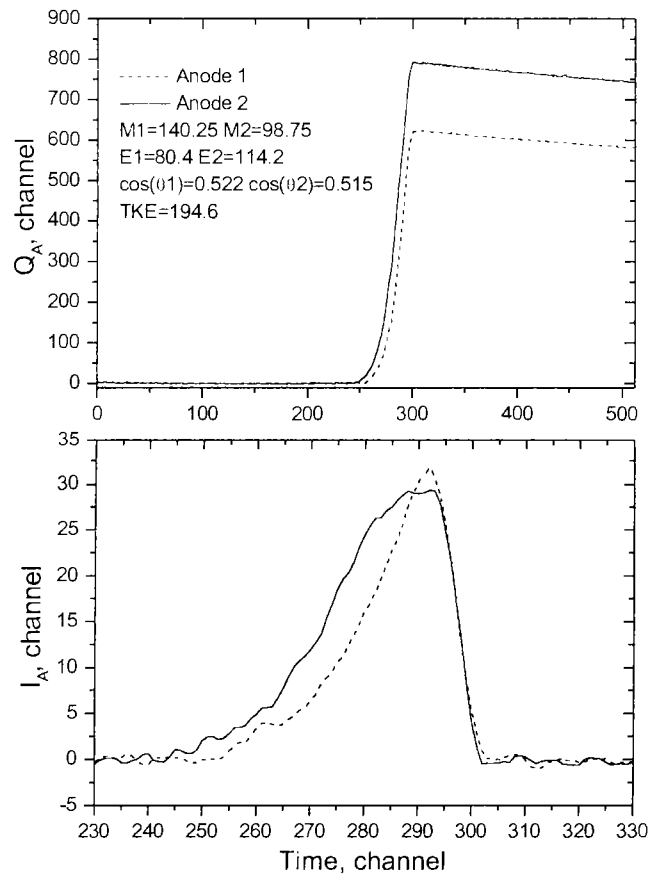


Fig. 4. The actual anode signals and ionisation losses density, which correspond to events with a limiting kinetic energy for mass 140

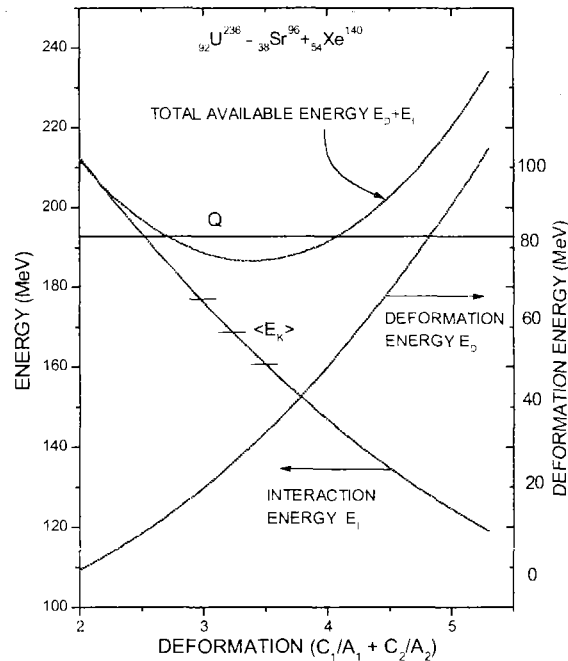


Fig. 5. Deformation energy, Coulomb interaction energy, and total potential energy at scission point vs. deformation [9]

We are grateful to B.D.Kuzminov, A.V.Ignatyuk and N.V.Kornilov for stimulating discussions.

## References

1. Goverdovski A.A., Khryachkov V.A., Ketlerov V.V. et al. Proc. Int. Conf. On nucl. Data for Science and Technology Trieste, Italy, May 19-24, 1997, v. 1, p. 676-678.
2. Khriachkov V.A., Goverdovski A.A., Ketlerov V.V. et al. NIM A394 (1997), pp.261-264
3. Khriachkov V.A., Ketlerov V.V., Mitrofanov V.F., Semenova N.N. NIM A444(3), pp.614-621. 2000.
4. Vives F., Hambsch F.-J., Oberstedt S. et al. Proc. Int. Conf. Nuclear fission and fission-product spectroscopy, Seyssins, France, 1998, pp.435-442.
5. Goverdovski A.A., Ketlerov V.V., Mitrofanov V.F. et al. Physics of Atomic Nuclei., Vol.62, no.6, pp.901-909, 1999.
6. Goverdovskiy A.A., Ketlerov V.V., Mitrofanov V.F. et al. JETP LETTERS, v.67, n.10, pp.793-795, 1998.
7. Quade U., Rudolph K., Skorka S. et al., Nucl. Phys, A487,1 (1988)
8. Khryachkov V.A., Goverdovski A.A., Kuz'minov B.D. et al., Sov.J.Nucl.Phys.53. 387(1991).
9. Thomas T.D., Gibson W.M. and Safford G.J. in Proc. Symp. Physics and Chemistry of Fission. Vol.1, IAEA, Vienna, 1966, 467.

## Fission Fragment Mass-Energy Distribution at 1.2 MeV and 5 MeV Neutron Induced Fission of $^{232}\text{Th}$

*V.A. Khriachkov, M.V. Dunaev, I.V. Dunaeva, N.N. Semenova, A.I. Sergachev*

Fission cross-section and angular distribution of fission fragments in the threshold region of  $^{232}\text{Th}$  fission induced by neutrons are subject to significant fluctuations. This region is of a specific interest to understand the evolution of a fissioning nucleus at early stages of fission process. Taking measurements of fission fragment yields in this range of Th-233 fissioning nucleus excitation energy is a very labour-consuming process due to an extremely small size of fission cross-section. The experiments require the instruments with high luminosity and reliability in their identification of a small number of fission fragments against a background of a great number of signals from  $\alpha$ -particles, recoil protons and gamma-quanta. A fission fragment spectrometer based on a two-section ionization chamber with Frish grids was used in the work. The signals from chamber anodes were stored in the computer memory in the form of digital oscillograms, each being 512 points long. The subsequent processing made it possible to determine the kinetic energy, mass and emission angle for each fragment. The required corrections for fragment energy losses in the target, Frish grid inefficiency and pulse pile-up were introduced. The measurements were taken with the continuous beam of the KG-2.5 accelerator at the SSC-RF IPPE.

Two energies of incident neutrons – 1.2 MeV and 5 MeV – were studied. The data obtained for the 5 MeV energy were used as the reference data for the spectrometer calibration. For the 1.2 MeV energy a record statistics was accumulated equal to ~70 thousand fission events, thus making it possible to get not only the integral spectra of mass, energy and fragment emission angles but also the data on the value of average kinetic energy and its dispersion as a function of fragment mass. The measurements show that at the neutron energy of 1.2 MeV the fragment mass distribution has a pronounced fine structure, thus confirming the results obtained at the IPPE earlier. The comparison of fragment mass distributions for the 1.2 MeV and 5 MeV energies showed that there was a significant difference in both the symmetric and asymmetric regions. By means of a special procedure partial angular distributions were obtained for the fragments which refer to standard modes 1 and 2 according to the Broze model.

The statistics gained is not sufficient to give an unambiguous answer to the principal question about possible differences in fragment angular distributions for these modes at the same excitation energy of fissioning  $^{232}\text{Th}$ - nucleus. There are plans to go on with this work.

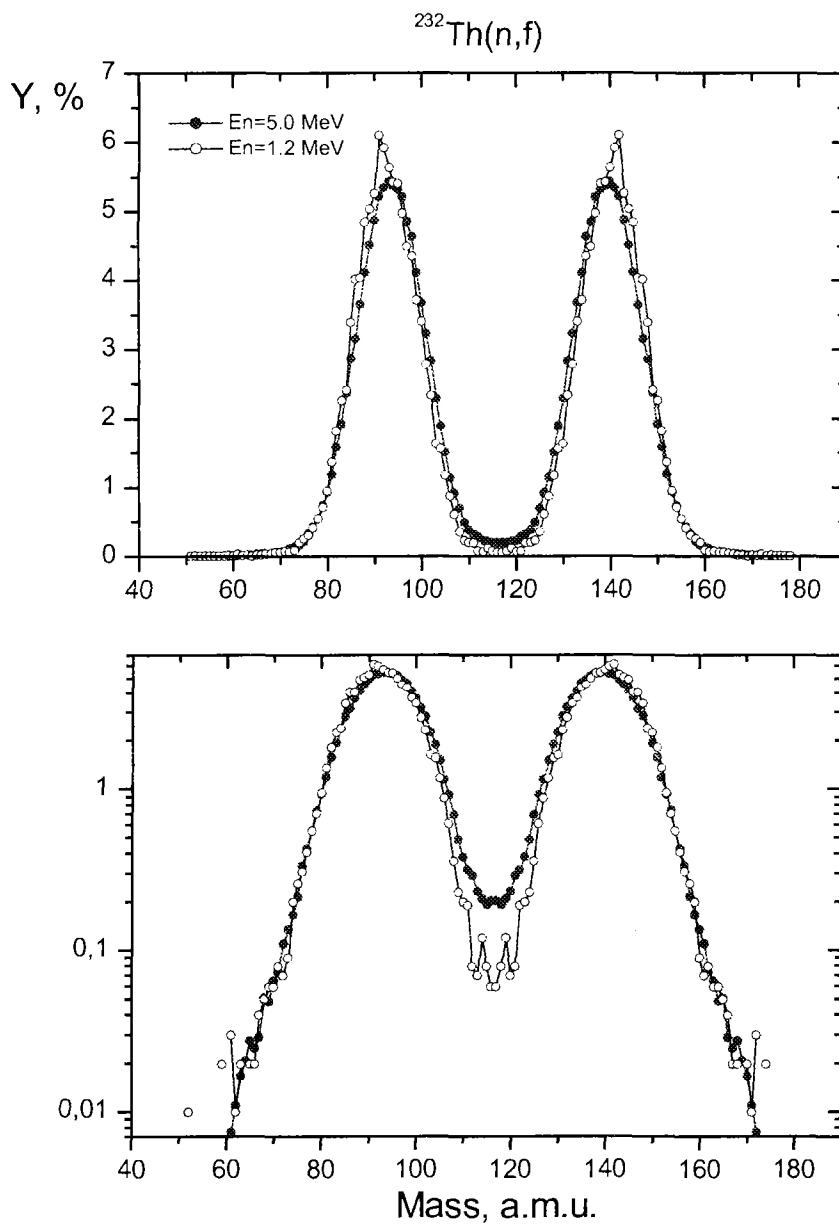


Fig. 1. Fragment mass distributions for  $^{232}\text{Th}$  fission by 1.2 MeV and 5.0 MeV neutrons

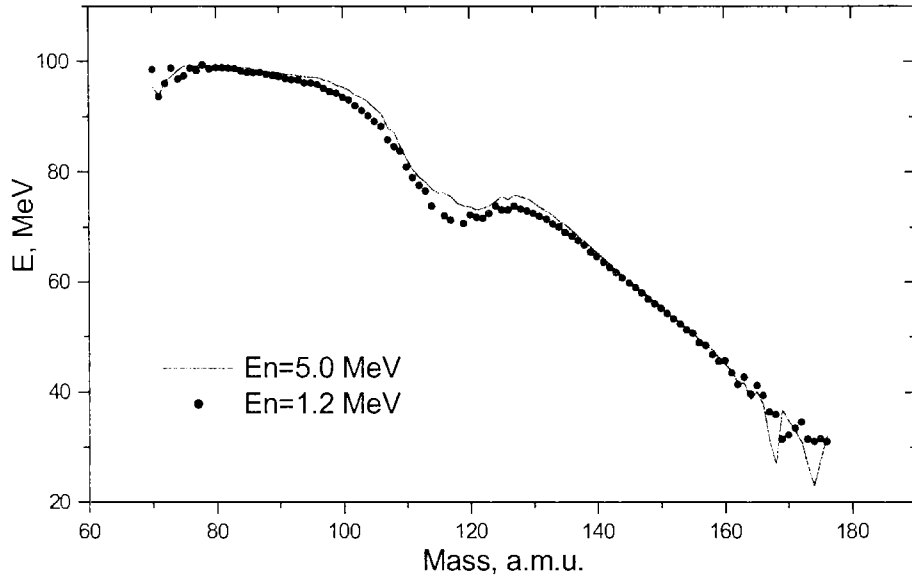


Fig. 2. Fission fragment kinetic energy distributions

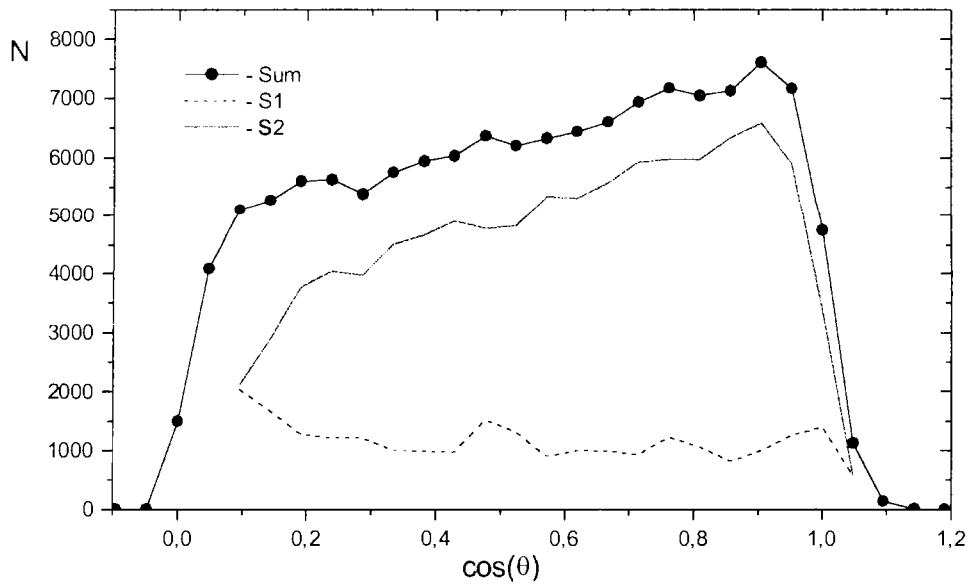


Fig. 3. Fragment angular distributions for fission of  $^{232}\text{Th}$  by 1.2 MeV neutrons

## Relative Abundances and Periods of Delayed Neutrons from Fission of $^{239}\text{Pu}$ by Fast Neutrons

*V.M. Piksaikin, L.E. Kazakov, S.G. Isaev, G.G. Korolev,  
V.A. Roshchenko, R.G. Tertytchny*

The fundamental role of delayed neutrons in the kinetic behaviour, control, and safety of nuclear reactors is well known today, being a matter of practical experience in hundreds of installations around the world. Not only are delayed neutrons of interest in the field of reactor physics, but they are also of interest in the field of nuclear physics and astrophysics. In spite of great efforts devoted to the investigation of delayed-neutron physics, the fundamental delayed-neutron parameters of several of the most common fissionable isotopes encountered in reactor systems are still poorly known. For example, delayed-neutron parameters used in most reactor physics applications are usually associated with either thermal or fast fission spectrum. It is difficult for the reactor designer to select the most applicable delayed neutron data set for an intermediate-spectrum system. In cases like this, the problem is further exacerbated because there is no clear-cut method to combine thermal and fast delayed-neutron sets since the group decay constants are different. This variation in decay constants is the direct result of the high correlation that naturally occurs amongst the various parameters (i.e., the group abundances and decay constants) in the delayed neutron model when performing the least-squares fit. Without the benefit of a consistent set of decay constants from energy-to-energy, the choice of which decay constants best characterise the delayed neutrons for a particular energy spectrum may not be obvious.

The primary objective of the present work was to measure the energy-dependent delayed neutron group parameters for  $^{239}\text{Pu}$  for incident-neutron energies ranging from thermal spectrum up to 4.9 MeV.



# The Energy Spectrum of Delayed Neutrons from Thermal Neutron Induced Fission of $^{235}\text{U}$ and its Analytical Approximation

*A.Yu. Doroshenko, V.M. Piksaikin, M.Z. Tarasko*

The energy spectrum of delayed neutrons from fission of heavy nuclei is the poorest known of all input data in reactor calculations (i.e. in the calculation of effective delayed neutron yields and fractions). At present there are two sources of information on delayed neutron spectrum – experimental data on the aggregate delayed neutron spectrum and experimental data on delayed neutron spectra from individual precursors. In frame of so-called “microscopic approach” the delayed neutron spectra from individual precursors are used for calculating the group and composite spectra by summing the contributions by individual precursors [1]. There is another approach in deriving the group and composite spectra of delayed neutrons in frame of microscopic approach. It was concluded by the authors [1] that some of the delayed neutron spectra are not adequate in the measured energy range and therefore these data was supplemented with nuclear model calculations. Namely this approach was put at the basis of the ENDF/B-VI delayed neutron database.

In the present work these two representative spectra ([1] and [2]) as well as some of the additional aggregate data were analyzed with the help of the analytical approximation taken in the form of the gamma-function. The effectiveness of this approximation is that the gamma-function depending on the values of its parameters can approximate both the Maxwell and evaporation type of energy distribution. As a result of the present analyses it was found a large difference between the values of the mean energy of the composite energy distributions of  $^{235}\text{U}$  delayed neutrons corresponding to each of the considered approach - [1], [2] – 70 keV. In addition to this on the basis of data from [2] it was shown that overall form of the composite spectrum of delayed neutrons from fission of  $^{235}\text{U}$  can not be approximated by the Maxwell or evaporation type of distribution. According to obtained approximation this spectrum has an overall form that is in between these two types of distribution.

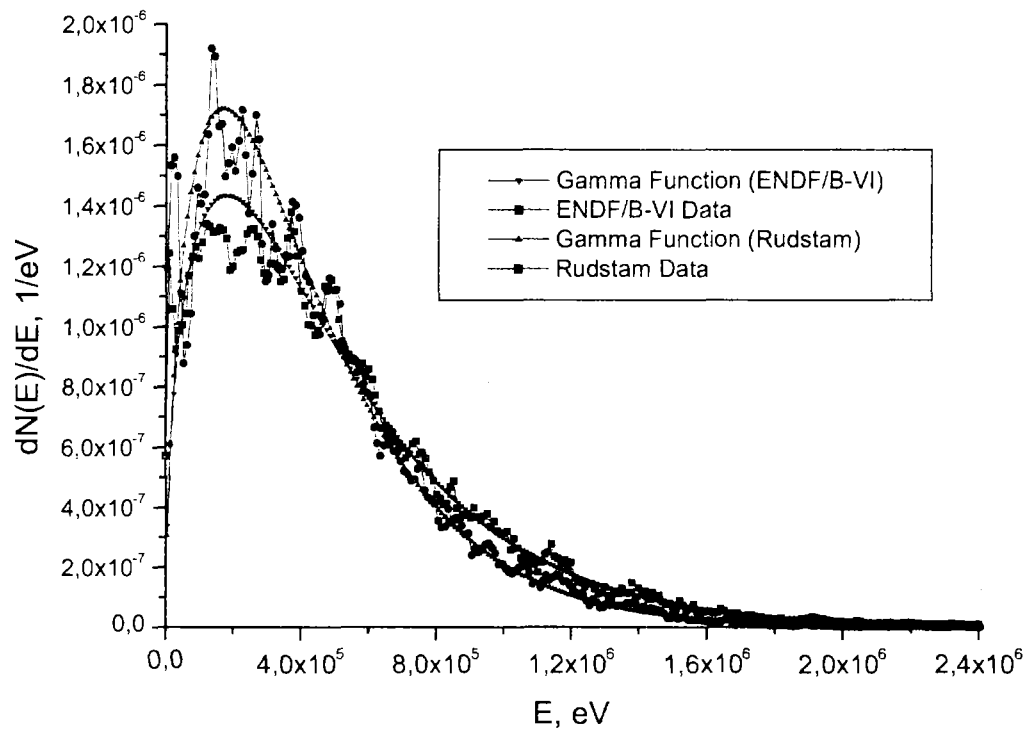


Fig. 1. Aggregate DN-spectra and its approximation by gamma function

#### References

1. M.C. Brady, T.R. England, Nucl. Sci. Eng., v.103, p.129, 1989.
2. G. Rudstam, Nucl. Sci. and Engineering, 1982, v.80, p.238.

# The Energy Spectrum of Delayed Neutrons from Fast Neutron Fission of $^{237}\text{Np}$

*A.Yu. Doroshenko, V.M. Piksaikin, M.Z. Tarasko*

The energy spectrum of delayed neutrons from fast neutron induced fission was obtained on the basis of group spectra of  $^{235}\text{U}$  which have been derived from the nuclear data and fission yields of the individual precursors for six delayed neutron groups according to the following procedure. Grouping of the precursors was made on the basis of half-life bounds using the  $^{235}\text{U}$  six group evaluation. Taking into account the known half life each precursor nuclide was assigned to a particular delayed neutron group. The group spectra were calculated by summing the individual precursor spectra weighted by emission probabilities and fission yields according to their group designation. The group parameters (decay constants and abundances) for determination of the aggregate spectrum of  $^{235}\text{U}$  were obtained as the average for the group using the precursor contribution as a weight function. It must be noted that there is another approach to calculate the group parameters, which is independent of fixing the half life bounds.

In the present work there was the task to obtain the total delayed neutron spectrum for fast neutron induced fission of  $^{237}\text{Np}$ . The calculations were made assuming that there is no difference between the group spectra for  $^{235}\text{U}$  and  $^{237}\text{Np}$  and that the group spectra do not depend on the energy of incident neutrons. The basis for such assumption is that in both cases we have the same precursors of delayed neutrons. Possible difference in grouping of the precursors according to the group constants of the nuclide under investigation does not introduce large uncertainties in the final results of total delayed neutron spectrum.

The calculations were made using the following formula

$$\Phi(E_n)dE_n = \sum_{i=1}^{i=6} a_i \varphi_i(E_n)dE_n,$$

where  $\Phi(E_n)$ - composite delayed neutron spectrum,

$\varphi_i(E_n)$ - delayed neutron spectrum of  $I$ - group number of  $^{235}\text{U}$  (thermal fission) taken from [26],

$a_i$  - abundance of  $I$ -group of  $^{237}\text{Np}$  delayed neutrons.

Abundances  $a_i$  were measured in the present experiment for the average incident neutron energy of  $1.154 \pm 0.025$  MeV. The numerical results of the total delayed neutron spectrum for fast neutron induced fission of  $^{237}\text{Np}$  are presented on diskette and shown in Fig. 1. Uncertainties of the data are derived on the basis of the uncertainties of  $^{235}\text{U}$  group spectra.

## Analytical approximation of delayed neutron spectrum

In the framework of the present project the new approach was developed for approximation of the delayed neutron spectrum by analytical expression. This approach on one hand gives the convenient analytical expression for representation of the delayed neutron spectrum, on the other hand it gives the opportunity to make some conclusion on the overall shape of the delayed neutron spectrum. Additional advantage of the proposed approach is possibility to obtain the data near the limits of the delayed neutron spectrum ( $100 \text{ keV} > E_n > 1.5 \text{ MeV}$ ) where experimental data are scarce or not available.

The analytical expression was taken in the form of the gamma-distribution

$$f(E) = \frac{\beta}{\Gamma(\alpha)} (\beta \cdot E)^{\alpha-1} \exp(-\beta \cdot E),$$

where  $\alpha$  and  $\beta$  - parameters of the distribution,

$$\Gamma(\alpha) = \int_0^{\infty} x^{\alpha-1} e^{-x} dx - \text{gamma function.}$$

The average energy and dispersion of the gamma-distribution can be represented by  $\alpha$  and  $\beta$  parameters

$$\langle E \rangle = \frac{\alpha}{\beta}, \quad D = \frac{\alpha}{\beta^2}$$

If one defines the temperature parameter  $T$  as  $1/\beta$  then  $\alpha = \langle E \rangle / T$  and the gamma distribution (1) can be rewritten in the form

$$f(E) = \frac{C_o}{T \cdot \Gamma(\alpha)} \left(\frac{E}{T}\right)^{\alpha-1} \exp\left(-\frac{E}{T}\right),$$

where  $C_o$  - normalization factor. It is easy to check that distribution  $f(E)$  transforms into the Maxwell distribution in case of  $\alpha=3/2$  and the evaporation distribution in case of  $\alpha=2$ .

In the present work the composite (total) delayed neutron spectrum for  $^{237}\text{Np}$  was approximated by the gamma-distribution (1) using the average energy and dispersion of the  $^{237}\text{Np}$  delayed neutron spectrum obtained on the basis of group data for  $^{235}\text{U}$ . The results are presented in Fig. 1 by solid line. The obtained value  $\alpha=1.72$  makes indication that the overall shape of the composite delayed neutron spectrum is different from both the evaporation and the Maxwell distribution. In the Table 1 parameters of the composite spectra are presented for  $^{237}\text{Np}$ .

Analyses of the uncertainties obtained for the group parameters  $\langle E \rangle$  and  $T$  for  $^{235}\text{U}$  show very large uncertainty values for fifth group parameters. Most probably there are too large errors in the  $^{235}\text{U}$  data for the delayed neutron spectrum related to the fifth group.

**Table 1**  
 **$^{237}\text{Np}$  delayed neutrons energy spectrum parameters for composite spectrum**

Composite DN spectrum			Correlation matrix		
Parameters		Uncertainties	$C_o$	$\langle E \rangle$	$T$
$C_o$	1.003	0.021	1		
$\langle E \rangle$ , keV	416.86	6.76	-0.85	1	
$T$ , keV	241.62	5.11	0.65	-0.71	1

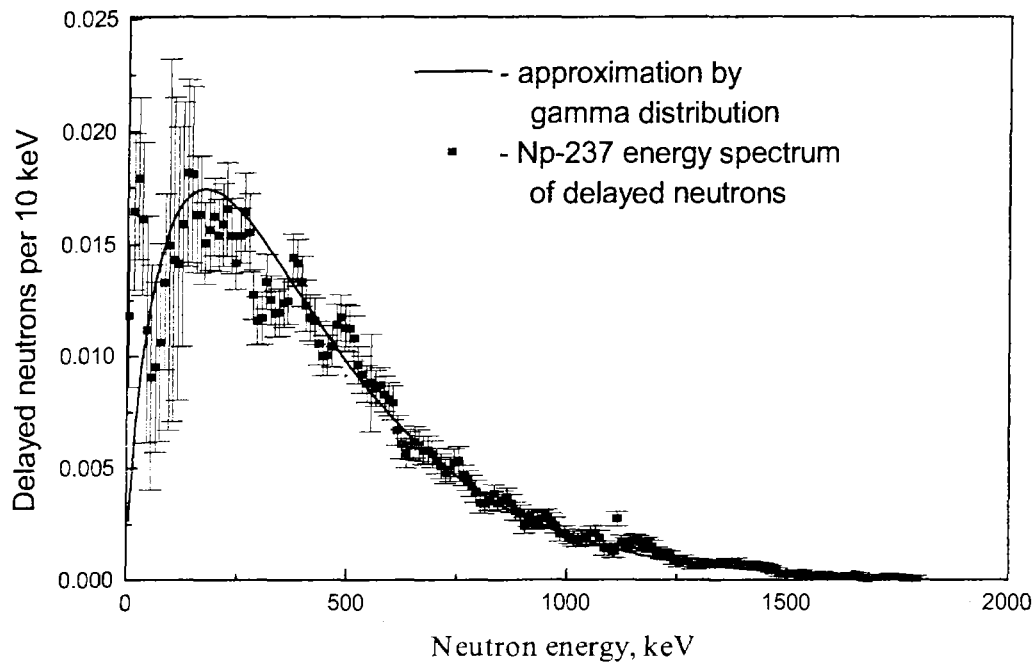


Fig.1. The delayed neutron energy spectrum of  $^{237}\text{Np}$

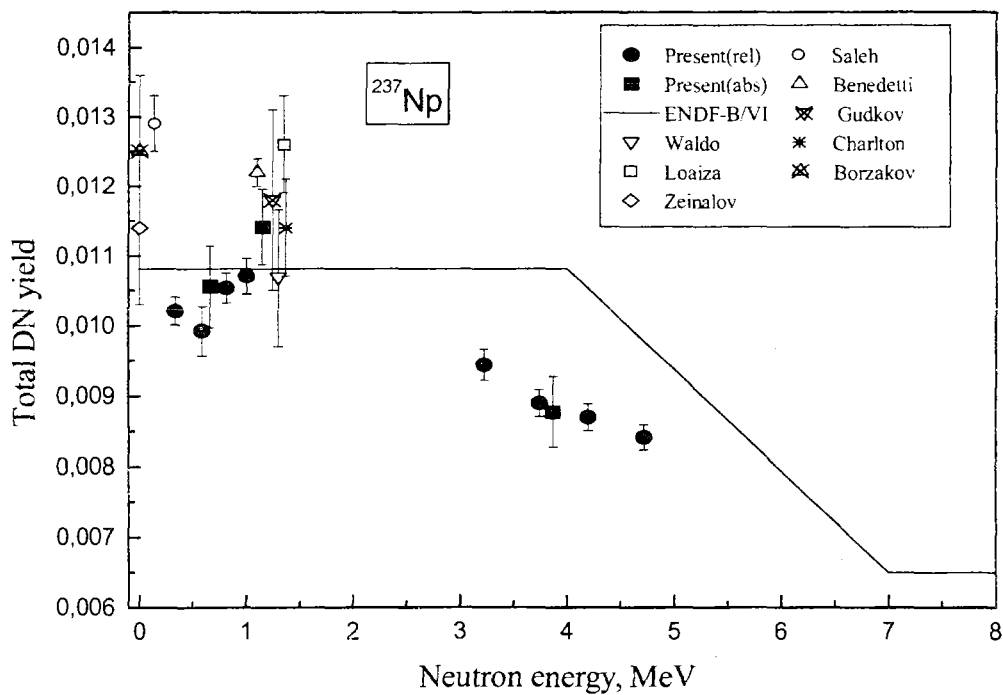


Fig.2. Energy dependence of total DN yield for  $^{237}\text{Np}$

# Investigation of the $^{232}\text{Th}$ Neutron Cross Sections in Resonance Energy Range

*Yu.V. Grigoriev, V.Ya. Kitaev, V.V. Sinitsa, B.V. Zhuravlev, S.B. Borzakov<sup>1</sup>,  
H. Faikov-Stanchik<sup>1</sup>, G.L. Ilchev<sup>1</sup>, Ts.Ts. Pantelev<sup>1</sup>, G.N. Kim<sup>2</sup>*

<sup>1</sup>*Joint Institute for Nuclear Research, Dubna, Russia*

<sup>2</sup>*Pohang Accelerator Laboratory, POSTECH, Korea*

The measurements of the  $^{232}\text{Th}$  neutron capture and total cross-sections in resonance energy range have been carried out the gamma-ray multisection liquid detector and neutron detector as a battery of boron counters on the 120 m flight path of the pulsed fast reactor IBR-30. As the filter samples were used the metallic disks of various thickness and in diameter of 45 mm. Two plates from metallic thorium with thickness of 0.2 mm and with the square of  $4.5 \times 4.5 \text{ cm}^2$  were used as the radiator samples. The group neutron total and radiative capture cross-sections within the accuracy of 2-7% in the energy range of (10 eV-10 keV) were obtained from the transmissions and the sum spectra of  $\gamma$ -rays from the fourth multiplicity to the seventh one. The radiative capture group cross-sections of  $^{238}\text{U}$  were used as the standard ones for obtaining of thorium ones. Analogous values were calculated on the GRUCON code with the ENDF/B-6, JENDL-3 evaluated data libraries. Within the limits of experimental errors there is observed an agreement between the experiment and calculation, but in some groups the experimental values are larger than the calculated ones.

## Reference

1. Back W.Y., Kim G.N., Cho M.N., Ko I.S., Namkung W., Grigoriev Yu.V., Faikov-Stanchik H., Shvetshov V.N., Furman W.I. Investigation of  $\gamma$ -multiplicity Spectra and Neutron Capture Cross-sections of  $^{232}\text{Th}$  in Energy Region 21.5 - 215 eV. In Proceeding Workshop on Nuclear Data Production and Evaluation. PAL, Pohang, Korea, August 7-8, 1998

## 2.2 NUCLEAR STRUCTURE AND NUCLEAR REACTIONS

### The $\beta^+$ -Strength in Heavy Nuclei and Electron Anti-Neutrino Capture

*I.N. Borzov*

The current scenarios of the r-process: a "hot bubble" expanding off a surface of proto-neutron star during a core-collapsed supernova, or neutron star merger, assume an existence of extreme neutrino fluxes of all three flavors. Although neutrino (anti-neutrino) capture on free nucleons has a stronger impact on the r-process in a neutrino-rich environment, the charged-current  $\bar{\nu}$ -A capture has to be included to the reaction network for completeness.

The case of  $\bar{\nu}$ -A capture on unstable  $N \leq Z$  nuclei is of special interest, as the total capture rate is mainly due to the  $\bar{\nu}$ -induced de-excitation to the isobaric-analog (IAS) and Gamow-Teller (GT) states in the daughter nucleus. The same final states can be also reached via the  $\beta^+$ -decay of very neutron-deficient nuclei. Recently, systematic experimental study of the  $\beta^+$ -decay strength distributions in nuclei close to  $^{100}\text{Sn}$  has been performed using a combination of the high resolution array of six Euroball-Cluster Ge-detectors (Cluster-cube) and total absorption spectrometer (TAS) [1]. As the experimental data on the supernova  $\bar{\nu}$ -capture are not available, the comparison with the  $\beta^+$ -decay data [1] can be helpful to estimate the predictive power of the theoretical methods used to calculate the  $\bar{\nu}$ -A capture rates.

Within the context of the project to treat all nuclear data needed for the astrophysical explosive processes on a unified microscopic basis, we have performed the ETFSI+cQRPA calculations of both the  $\beta^+$ -strength distributions and electron anti-neutrino capture rates in  $N \leq Z$  nuclei with  $A > 40$ .

The ground state description is based on the so-called Extended Tomas-Fermi approach with Strutinski Integral correction (ETFSI), previously used for the calculations of the nuclear masses [2], as well as the  $\beta$ -decay and  $\nu$ -capture rates [3]. The main features of the cQRPA framework are: an exact account for the particle-hole (ph) continuum and the use of a mass-independent finite-range ph effective NN-interaction of the Landau-Migdal type. Its strength parameter  $g$  is fixed from the GTR position in  $^{208}\text{Pb}$ . The delta-function particle-particle pp interaction is used, its strength is fixed from the experimental  $\beta^\pm$ -strength distributions.

#### The $\beta^+$ -decay strength distributions in vicinity of $^{100}\text{Sn}$

First, we have compared our calculations with the recent experimental data on the mass hindrance of total  $\beta^+$ -strength strength in the neutron deficient  $^{98}\text{Cd}$ ,  $^{97-99}\text{Ag}$  and  $^{103-107}\text{In}$  [1]. As seen from the Table, the calculations overestimate the observed strength: the reduction factor  $\eta$  needed to match the experiment is  $\sim 1.85$  for  $^{98}\text{Cd}$ , and Ag isotopes (the same reduction was found in our calculations for  $^{104-108}\text{Sn}$  [4]); 2.5 for  $^{103,104}\text{In}$  (the same as in  $^{105,107}\text{Sn}$  [4]);  $\sim 3$  for  $^{105-107}\text{In}$ . Note that 8 to 16% of the total strength is located above the Q-window.

The calculated total GT strength within the  $Q_{\beta}$ -window is therefore higher than the observed one. This may lead to some over prediction of the  $\bar{\nu}$ -A capture rates.

**Table 1**

**Experimental Gamow-Teller strength  $B(GT)_{exp}$  within the  $Q_{\beta}$ -window compared with the theoretical values summed within the  $Q_{\beta}$ -window -  $B(GT)_{th}$ , and summed up to 50 MeV -  $B_f(GT)_{th}$ . Here,  $G_A/G_V=1$ ;  $\eta$  is the ratio of  $B(GT)_{th}/B(GT)_{exp}$  and C is the amount of the strength outside the  $Q_{\beta}$ -window**

Nucleus	<sup>97</sup> Ag	<sup>98</sup> Ag	<sup>99</sup> Ag	<sup>98</sup> Cd
$B(GT)_{exp}$	3.0(0.4)	2.7(0.4)	-	3.5(0.8)
$B(GT)_{th}/B_f(GT)_{th}$	5.39/5.84	5.02/5.60	4.47/5.06	6.55/7.17
$\eta$	1.80	1.85	-	1.87
C,%	7.8	10.4	11.7	8.6

Nucleus	<sup>103</sup> In	<sup>104</sup> In	<sup>105</sup> In	<sup>106</sup> In
$B(GT)_{exp}$	2.47(0.25)	1.9(0.3)	1.4(2)	1.4(3)
$B(GT)_{th}/B_f(GT)_{th}$	5.56/6.43	5.40/6.02	4.80/5.62	4.56/5.45
$\eta$	2.25	2.84	3.38	3.25
C,%	13.5	14	14	16

### Supernova electron anti-neutrino capture rates

The neutrinos decoupling in neutron-rich matter leads to a well known temperature hierarchy  $T_{\nu x} > T_{\bar{\nu}} > T_{\nu}$ . The neutrino energy spectra can be approximated as a zero-chemical-potential Fermi-Dirac distribution [5] with the neutrino temperatures  $\sim 8$  MeV, 5 MeV, and 3.5 MeV and average neutrino energies  $\sim 25$  MeV, 16 MeV, and 11 MeV respectively. Due to low average energy of anti-neutrinos, the allowed transition approximation for the energy-dependent  $\bar{\nu}$ -A cross section is used. Anti-neutrino spectrum-averaged cross section is very sensitive to the GT strength distribution given by specific nuclear model.

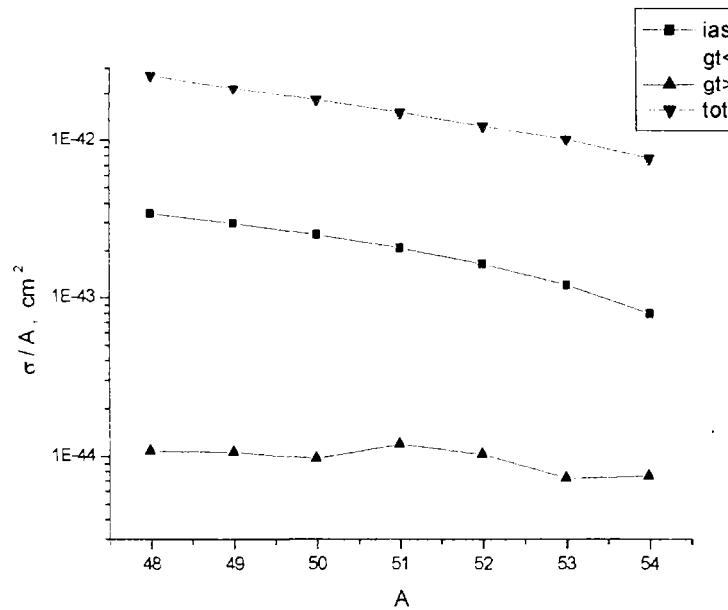


Fig. 1.

The spectrum-averaged anti-neutrino capture cross sections are shown for Ni isotopic chain in Fig.1. In unstable nuclei at decreasing N-Z the total cross section has a rather smooth behavior. The main contribution to the cross section comes from the deexcitation GT component ( $gt_{<}$ ) and IAS. The GT excitation component contribution is in agreement with the calculations of the  $\beta^-$ -decay GT strength above the Q-value (see Table 1).

The author is grateful to Prof. E. Roeckl for stimulating discussions and sending the GSI experimental data prior to publication. The work was supported in part by FNRS, Belgium.

### References

1. Z. Hu, L. Batist, J. Agramunt et al., Phys. Rev., C62 (2000) 064315
2. Y. Aboussir, J. M. Pearson, A.K. Dutta, F. Tondeur, At. Data Nucl. Data Tables 61 (1995) 127; I.N. Borzov, S. Goriely, and J.M. Pearson, Nucl. Phys. A621 (1997) 307c.
3. I.N. Borzov, S. Goriely, Phys.Rev. C62, (2000) 035501.
4. Bobyk, W.A. Kaminski, I.N. Borzov, Acta Phys.Polonica (2000)
5. D.S. Miller, J.R. Wilson, R.W. Mayle Astroph. J. 415, 1993, 278.

# Direct Neutron Capture in a Microscopic Model

*I.N. Borzov, A.V. Avdeenkov, B. Grun<sup>1</sup>, H. Oberhammer<sup>1</sup>*

*<sup>1</sup>Institute of Nuclear Physics, Vienna Univ. of Technology,  
Wiedner Hauptstr. 8-10, A-1040, Vienna, Austria*

Approximately half of all stable nuclei with  $A > 60$  observed in nature were produced during the so-called r-process which is believed to occur in extreme neutron density environments of type II supernova explosions multiple neutron captures lead into the regions of very neutron-rich nuclei. The location of the r-process paths far-off stability influence the nuclear abundances predicted by astrophysical models. An important signature of the r-process is the increased yield peaks located near the neutron closed shells of  $N=50, 82,$  and  $126$ . As the cross sections for most of unstable nuclei involved cannot be derived experimentally, theoretical predictions are of value. The nuclei far-off stability as well as nuclei near shell closures have a very low level density. For that reason statistical Hauser-Feshbach calculations of neutron capture employing the compound nucleus (CN) mechanism fail, and the direct capture (DC) mechanism may dominate the cross section.

The studies of the CN and DC mechanisms related to applicability of the statistical description have been given elsewhere [1]. In Ref. [2] a detailed comparison of DC cross sections calculated using an input from different microscopic theories was performed: a HFB model with the Skyrme force SkP [3], a relativistic mean field theory [4] and the microscopic-macroscopic finite-range droplet model [5]. In the present work we study a possible impact on the DC cross section produced by dependence of spectroscopic factors of the final states on their excitation energy.

## Direct capture cross sections

The DC mechanism implies that the partial cross section  $\sigma_i^{DC}$  is determined by the overlap of the scattering wave function in the entrance channel, the wave function of the bound neutron, and the multipole operator for a specific transition. The non-resonant cross section  $\sigma^{th}$  can be obtained by summing over the fragmentation components  $j$  of all possible final states  $i$  [6]

$$\sigma^{th} = \sum_{ij} C_i^2 S_{ij} \sigma_i^{DC}. \quad (1)$$

Here  $C_i$  and  $S_{ij}$  stand for the isospin Clebsch-Gordan coefficients and spectroscopic factors, respectively. The nucleon-nucleus optical potential is found by folding of the nuclear target density  $\rho_T$  with an energy and density dependent effective NN-interaction [7] including an antisymmetrization correction. The optical potential has a correct behavior in the nuclear exterior. At the low energies relevant for the r-process the imaginary parts of the optical potential are small. For the computation of the DC cross section the direct capture code TEDCA [6] was used only including E1 transitions. The energy dependence of the spectroscopic factors in nuclei with pairing is described by non-linear Dyson equation for normal and abnormal Green's functions [8-10]. The corresponding mass operators contain both the instant and retarded parts responsible for configuration mixing and coupling to collective states. The input single-particle energies, neutron thresholds and phonon strengths have been taken from the experiment when available or calculated self-consistently with the DF3 density functional [11].

We have calculated the distributions of neutron single-particle strengths for low-spin states with  $J < 7/2$  for  $^{125}\text{Sn}$ ,  $^{209}\text{Pb}$ ,  $^{133}\text{Sn}$ , and  $^{233}\text{Pb}$  nuclei. The fragmentation has been found quite pronounced for and  $^{125}\text{Sn}$ ,  $^{209}\text{Pb}$ . As an example, illustrated at Fig.1 in  $^{125}\text{Sn}$  the state with  $J^\pi=4p3/2$  has 16 fragmentation components, 10 of them with energies less than  $S_n=5.73$  MeV. The main component has an energy of  $E_x=3.02$  MeV and a spectroscopic factor  $S_{ij}=0.49$ . The partial DC cross sections have been calculated for fragmented low-spin final states within the  $S_n$ -window. The total DC cross sections given in Eq. (1) at  $E_n=30$  keV are given in Table 1.

The DC cross sections are mostly affected by the reaction Q-value and the spin/parity of the levels located below  $S_n$ . For the residual nucleus  $^{125}\text{Sn}$  our cross section is by far the highest because the other calculations predict no low-spin states at low excitation energy. (Note that self-consistent DF3 calculation [11] predicts the position for  $3p3/2$  and  $3p1/2$  states in agreements with experiment.) For the target nucleus  $^{132}\text{Sn}$  all calculations give comparable cross sections. For these nuclei the impact of the energy dependence of spectroscopic factors is found to be small ( $<10\%$ ). For  $^{208}\text{Pb}$  the cross section is 25% less than the one calculated for  $S_i=1$  (the bracketed value). The explanation is that the main component of the  $4p1/2$  state in our calculations is located at  $E_x=6.37$  MeV, well above  $S_n=3.93$  MeV. The spectroscopic factor of the only  $4p1/2$  state located in our calculations below  $S_n$  is  $S_i=0.003$  in agreement with the experimental value of  $S_{\text{exp}}=0.0036$  [12]. Thus, ascribing the  $S_i=1$  to the state at  $E_x^{\text{exp}}=2.12$  MeV as done in [2] results in an overestimation of the DC cross section. The use of averaged spectroscopic factors [1] is better in this case. For very neutron-rich nuclei like  $^{233}\text{Pb}$  the fragmentation effects are weak.

In summary, the energy dependence of spectroscopic factors may be of importance when the low-spin states are located closely above the threshold. This is more likely the case for stable near closed-shell nuclei. For nuclei far-off stability, the energies of low-spin modes decrease faster than the neutron separation energies. The fragmentation of these states near the Fermi energy is weaker, as pairing reduces the matrix elements of quasiparticle-phonon interaction. A practical way to include fragmentation to large-scale calculations would be limiting the number of dominant single-particle levels.

**Table 1**

**Non-resonant DC cross sections in mb compared with the results of Ref. [2]**

Nucleus	Cross section, $10^{-1}$ , mb				
	HFB	RMFT	FRDM	Present work	Exp.
$^{124}\text{Sn}$	$1.0 \cdot 10^{-1}$	0.12	0.28	2.5	-
$^{132}\text{Sn}$	0.8	2.0	1.0	1.5	-
$^{208}\text{Pb}$	0.1	0.3	0.5	0.5 (0.65)	1.4(4)

## References

1. S. Goriely, Phys. Lett. B436 (1998) 10.
2. T. Rauscher, R. Bieber, H. Oberhummer, K.-L. Kratz, J. Dobaczewski, P. Moeller, M.M. Sharma Phys. Rev. C58 (1998) 2031.
3. J. Dobaczewski, I. Hamamoto, W. Nazarewicz, J.A. Sheikh, Phys. Rev. Lett. 72 (1994) 981.
4. M.M. Sharma, G.A. Lalazisis, and P.Ring, Phys. Lett. B317 (1993) 9.
5. P. Moeller and J.R. Nix, Nucl. Phys. A361 (1981) 117.
6. K. Grün and H. Oberhummer, TU Wien, code TEDCA, 1995, unpublished.
7. A.M. Kobos et al., Nucl. Phys. A425 (1984) 205.
8. S.G. Kadmeňsky and P.A. Lukyanovich, Yad. Fiz. 49 (1989) 384.
9. Y. Dewulf et al., Phys. Lett. B396 (1997) 7.
10. A.V. Avdeenkov and S.P. Kamerdhziev, Phys. At. Nucl. 62 (1999) 563.
11. I.N. Borzov, S.A. Fayans, E. Kroemer, and D. Zawischa, Z. Phys. A335 (1996) 127.
12. ENSDF

# On the Extended Theory of Finite Fermi Systems

*S.P. Kamerdzhev, E.V. Litvinova*

The well-known Theory of Finite Fermi Systems (TFFS) [1] developed by A.B.Migdal and his coworkers takes into account mainly simple configurations. In other words, for even-even nuclei it is the known random phase approximation (magic nuclei) or the quasiparticle random phase approximation (non-magic nuclei) formulated within present many-body theory in the Green function language. However, the latter turned out to be very important for further development of a consistent microscopic theory of Fermi systems, including first of all nuclei.

In the article [2] a realistic and simplest variant of generalization of the TFFS to take explicitly into account some complex configurations with phonons has been discussed. Using general relations for nuclei with pairing (non-magic nuclei) secular equations have been obtained. They describe fragmentation of simple states in odd and even-even nuclei over complex configurations of the quasiparticle $\otimes$ phonon $\otimes$ phonon and 2quasiparticles $\otimes$ phonon kind, correspondingly, which are of great interest at present. The equations contain the effects which were not considered earlier, in fact, and can be studied in experiment. These are ground state correlations, caused by complex configurations, and an additional, i.e. the quasiparticle-phonon, mechanism of nuclear superfluidity [3].

The equations obtained describe characteristics of nuclear excitations in a broad energy region near nuclear binding energy. They are applicable up to the higher energy region of 30-35 MeV especially for description of giant resonance in even-even nuclei. They can be used for both spherical and deformed nuclei. A further development and application of the ETFFS are in progress.

## References

1. A.B.Migdal, Theory of finite Fermi-systems and application to atomic nuclei. Nauka, Moskow, 1965.
2. S.P.Kamerdzhev, E.V.Litvinova, Phys. At. Nucl. 64, No. 4, 2001.
3. A.V.Avdeenkov, S.P.Kamerdzhev, Phys. Lett. B459 (1999) 423; JETP Lett. 69 (1999) 715.

# Microscopic Description of Total Spectrum in $^{40}\text{Ca}(\alpha,\alpha')$ at $E_\alpha = 240$ MeV

*S. Kamerdzhiev, J. Speth<sup>1)</sup>, G. Tertychny*

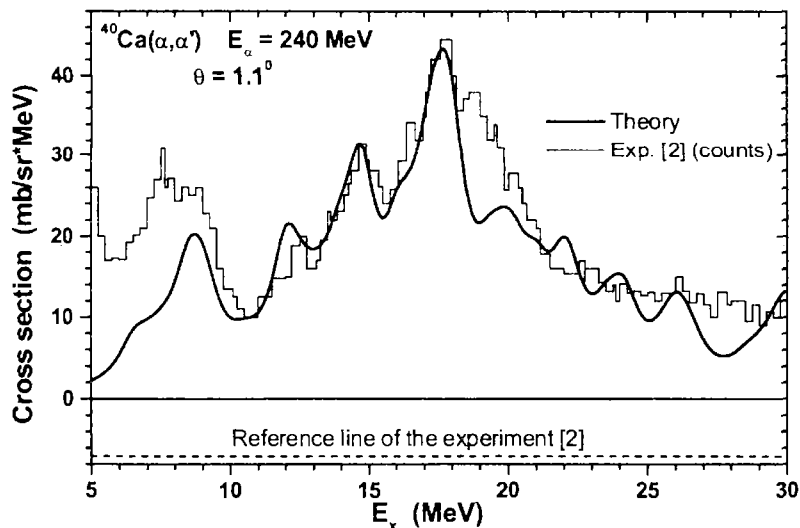
<sup>1)</sup>*Institut für Kernphysik, Forschungszentrum Jülich, 52425 Jülich, Germany*

Here we continue our analysis [1] of the reaction  $^{40}\text{Ca}(\alpha,\alpha')$  at  $E_\alpha=240$  MeV, the excellent experimental results [2] for which give at present a best information about giant resonance region of excitation ( $E_x \cong 5\text{-}30$  MeV) in  $^{40}\text{Ca}$ . This time we calculated total spectrum as sum of contributions of the 6 giant resonances which are possible in the energy region under discussion. In Ref. [1] the contribution of the isoscalar monopole (IS E0) resonance was only considered and compared with the corresponding experimental cross section [1].

The experiment [2] gives a distinct structure of cross sections for both the IS E0 (see [1]) and the summed spectrum, see the figure. This structure is a challenge for any microscopic theory. Our microscopic theory was described in [1].

Because in Fig.2 of [2] there are only counts, the theoretical hystogram was imposed on the theoretical curve in such a way that the maxima of both curves coincided. In this way it was possible to estimate roughly the contribution of the instrumental background as the difference between two horizontal axes shown in the figure. The corresponding integral cross section is about  $7 \cdot 25 = 175$  mb/sr.

We obtained that our microscopic theory which uses known and fixed parameters of the nucleon-nucleon interaction describes reasonably well gross structure of total spectrum, except for the region below 9 MeV which may be connected with the excitations of the  $(\alpha+^{36}\text{Ar})$  system.



## References

1. S. Kamerdzhiev, J. Speth, and G. Tertychny, Eur. Phys. J. A 7, 483 (2000); NPD Annual Report 1999, Obninsk, p. 30.
2. D.H. Youngblood, Y.-W. Lui, and H.L. Clark, Phys. Rev. C 55, 2811 (1997).

# Role of Quasiparticle-Phonon Interaction in Non-Magic Nuclei: A Model Analysis

*S. Kamedzhiev, E. Litvinova, D. Zawischa<sup>1</sup>*

<sup>1)</sup>*Institut für Theoretische Physik, Universität Hannover, Germany*

Using the consistent Green function formalism an approach to describe properties of excited states (first of all, giant resonances) in non-magic even-even nuclei has been formulated in [1]. The approach took into account two kinds of nuclear interaction, namely, the usual (but renormalized) effective particle-hole and particle-particle interactions as well as the quasiparticle-phonon one which induces complex configurations 2quasiparticles $\otimes$ phonon. Ground state correlations due to the complex configurations (GSC<sub>phon</sub>) and a modification of the BCS pairing theory (see [2]) have been included into the approach. These features resulted in a considerable complication of the equations obtained.

Thus, we have to perform a model analysis of the equations. Here the following results have been obtained:

1. For the case of absence of the GSC and within the one-level model (the latter is possible only for nuclei with pairing) we shown that the contribution of the complex configurations is canceled completely.
2. This means that in the one-level approximation only GSC<sub>phon</sub> give a contribution to the complex configuration part. The corresponding equations have been derived which give a possibility to consider a “pure” effect of the GSC<sub>phon</sub>.
3. In order to exclude possible unphysical second order poles of the propagator a simplest method of summation of “dangerous” terms has been applied.
4. In the framework of a two-level model a graphical solution of the secular equation has been obtained which is a generalization of the corresponding QRPA case.

## References

1. S.Kamedzhiev, E.Litvinova, D.Zawischa, submitted to Eur. Phys. Journal A, contribution to the L Meeting on Nuclear Spectroscopy and Nuclear Structure, p.143.
2. A.V.Avdeenkov, S.P.Kamedzhiev, JETP Lett. 69 (1999) 715.

# Spin Dependence of the Nuclear Level Density of $^{165}\text{Er}$ and $^{181}\text{W}$

*B.V. Zhuravlev, N.N. Titarenko, V.I. Trykova*

The spin cut-off parameter of the nuclear level density and effective moment of inertia for nuclei of  $^{165}\text{Er}$  and  $^{181}\text{W}$  have been determined from analysis of the experimental data on level density, average S-wave neutron resonance spacing and spin distribution of low-lying levels. The nuclear level density was determined by us in the excitation energy range of (0-8.5) MeV from the measurements of neutron emission spectra in (p,n) reaction and their analysis in the framework of Hauser-Feshbach statistical theory. The absolute value of the nuclear level density  $\rho(U)$  at the neutron binding energy is related to the average S-wave  $1/2+$  neutron resonance spacing  $\langle D_{1/2+} \rangle$  measured for these nuclei as follows:

$$\rho(U) = 2\sigma^2 / \langle D_{1/2+} \rangle, \quad (1)$$

where:  $\sigma$  - spin cut-off parameter,

$$\sigma^2 = (I_{ef}/h)t, \quad (2)$$

$I_{ef}$  - effective moment of inertia,

$t$  - thermodynamic temperature.

The values of spin cut-off parameter and effective moment of inertia determined according to the relations (1) and (2) are in agreement with their rigid body values.

The spin cut-off parameter at low excitation energy was determined from the approximation of well-identified low-lying level distributions on spin by the statistical distribution. It is shown that the energy dependence of the effective moment of inertia corresponds to the noninteracting fermions model prediction.

This work was supported by RFBR grant 98-02-16026.

## 2.3 NUCLEAR DATA

### Neutron Cross Section Evaluations for $^{238}\text{U}$ up to 150 MeV

*A.V. Ignatyuk, V.P. Lunev, Yu.N. Shubin, E.V. Gai, N.N. Titarenko,  
A.Ventura<sup>1</sup>, W.Gudowski<sup>2</sup>*

<sup>1</sup>*ENEA, Nuclear Data Center and INFN, Bologna Section, 40129 Bologna, Italy*

<sup>2</sup>*Royal Institute of Technology, 100-44 Stockholm, Sweden*

**Abstract:** Investigations aimed at the development of neutron cross section evaluations for  $^{238}\text{U}$  at intermediate energies are briefly described. The coupled-channels optical model is used to calculate the neutron total, elastic and reaction cross sections and the elastic scattering angular distributions. Evaluations of the neutron and charged particle emission cross sections and of the fission cross sections are obtained on the basis of the statistical description that includes direct, pre-equilibrium and equilibrium mechanisms of nuclear reactions. The Kalbach parametrization of angular distributions is used to describe the double-differential cross sections of emitted neutrons and charged particles in ENDF/B-VI format.

#### Introduction

In order to develop main concepts of the accelerator-driven power systems and the corresponding nuclear waste management it is necessary to know nuclear data on spectra and reaction cross sections for structural materials, fissioning actinides and the most important fission products in a very broad energy range. In practice, the energy interval from thermal energies to a few thousand MeV should be covered. The status of available nuclear data differs strongly for the energy regions below and above of 20 MeV. Huge efforts have been made to create libraries of evaluated neutron data (ENDF/B, JENDL, BROND etc.), for the low energy region. In spite of some differences between the evaluations, most data are reasonable enough and their accuracy satisfy requests of major current applications. For energies higher than 20 MeV data are rather scarce and are not systematized yet. A lack of experimental data has to be compensated by the development of reliable calculation methods. The codes based on the intra-nuclear cascade model combined with the evaporation model have been successfully applied for energies above a few hundred MeV. At lower energies, however, nuclear structure effects are so prominent that their description requires more detailed consideration of competitive reaction mechanisms. Therefore, it was decided that the energy region from 20 to 150 MeV requires special consideration and the evaluated data files for this region should be prepared for the most important structural and fissile materials in the same manner as for the energy region below 20 MeV. The list of first priority actinides that can be used in accelerator-driven sub-critical systems, includes isotopes of thorium, uranium and plutonium. The majority of experimental data are available for  $^{238}\text{U}$ . For this reason,  $^{238}\text{U}$  is the best candidate for testing the models developed for nuclear data evaluations at intermediate energies.

The main results of experimental data analysis and calculations recommended for the intermediate energy neutron data file for  $^{238}\text{U}$  are briefly discussed. The corresponding file is in preparation now in the IPPE.

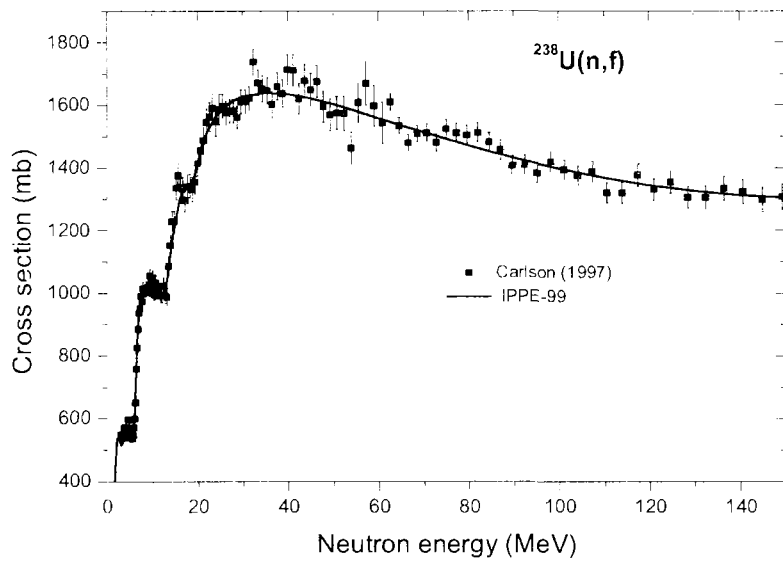


Fig. 1. Evaluated fission cross section in comparison with experimental data [17]

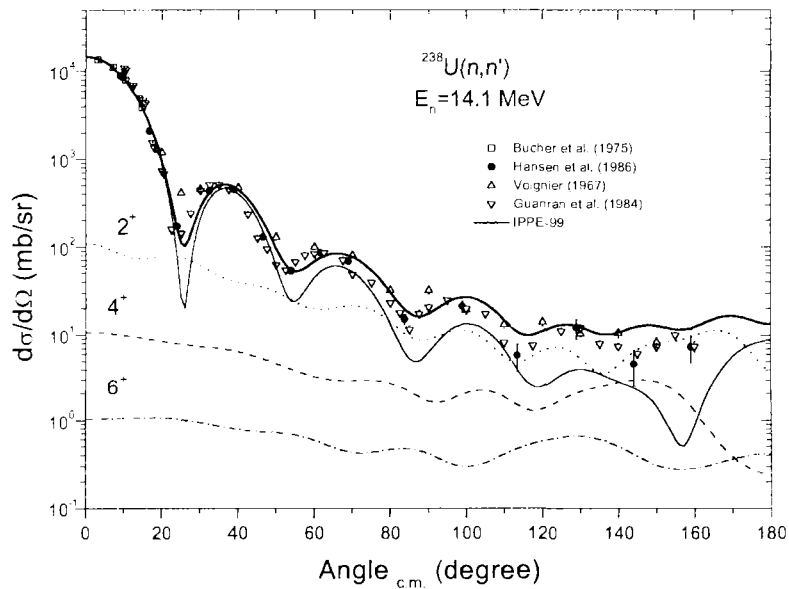


Fig. 2. Comparison of the calculated elastic scattering cross section at 14.1 MeV with experimental data. The scattering cross sections for the ground and collective low-lying levels are shown by solid, dotted, dashed and dot-dashed curves respectively. The thick solid curve is the sum of the cross sections for the ground and collective low-lying levels

Published in *Nuclear Science and Engineering*: 136, 340-356 (2000)

# Neutron and Proton Cross Section Evaluations for $^{232}\text{Th}$ up to 150 MeV

*A.V. Ignatyuk, V. P. Lunev, Yu. N. Shubin, E.V. Gai,  
N.N. Titarenko, W.Gudowski<sup>1</sup>*

<sup>1</sup>*Royal Institute of Technology, 100-44 Stockholm, Sweden*

**Abstract:** Investigations aimed at the development of neutron and proton cross section evaluations for  $^{232}\text{Th}$  at intermediate energies are described. The coupled-channels optical model has been used to calculate the neutron total, elastic and reaction cross sections and the elastic scattering angular distributions. Evaluations of the neutron and charged particle emission cross sections and of the fission cross sections have been obtained on the basis of the statistical description that includes direct, pre-equilibrium and equilibrium mechanisms of nuclear reactions. The Kalbach parametrization of angular distributions has been used to describe the double-differential cross sections of emitted neutrons and charged particles in ENDF/B-VI format.

## Introduction

Recent development of accelerator-driven transmutation systems (ADS) and their relevance for nuclear waste management has created a new interest in high quality nuclear data for fissile isotopes, structural materials and fission products. In practice, the energy interval from thermal energies to a few thousand MeV should be covered in order to properly model ADS [1]. The status of available nuclear data differs strongly for the energy regions below and above of 20 MeV. Huge efforts have been made in the past to create libraries of evaluated neutron data for the low energy region, which met requirements of the conventional nuclear reactors. In spite of some differences between the evaluations, most data in this region satisfies needs of major current applications. In contrary, for energies higher than 20 MeV data are rather scarce and are not yet systematized.

Both neutrons and protons in the energy range between 20 MeV and few hundreds of MeV play non negligible role in accelerator-driven systems and transport of these particles should be simulated with a better precision than allowed by available data today. Various methods are used to get the required data: both systematics with parameters selected from comparison with experimental data and models based on various assumptions. The codes based on the intra-nuclear cascade model combined with the evaporation model have been successfully applied for energies above a few hundred MeV. At lower energies, however, nuclear structure effects are so prominent that their description requires more detailed consideration of competitive reaction mechanisms. Therefore, special attention should be put to this energy region, and the evaluated data files for energies from 20 to 150 MeV should be prepared in the same manner as for the energy region below 20 MeV for the most important structural and fissile materials. Some valuable efforts have been already made by the Los Alamos group and the evaluated data files for more than 40 of the most important structural and shielding materials were extended up to 150 MeV in the ENDF/B-VI library. Also some attempts to prepare similar evaluations for actinides were made by this group, but their evaluations were limited to neutron elastic scattering and neutron production cross sections, mainly for energies below 100 MeV. Fission cross sections, charged particle yields, and fission neutron yields were not included in the files prepared on the basis of

the evaluations. Moreover, these evaluations suffer of some unrealistic fluctuations obtained in the neutron production cross sections.

The renewed interest in the thorium fuel cycle for ADS and advanced conceptual designs of transmutation systems with conventional U-Pu fuels need reliable data at least for the isotopes of thorium, uranium and plutonium. Evaluation of intermediate energy data for all these nuclides is under intensive development now.

The main results of experimental data analysis and evaluations for the intermediate energy neutron and proton data files for  $^{232}\text{Th}$  were discussed.

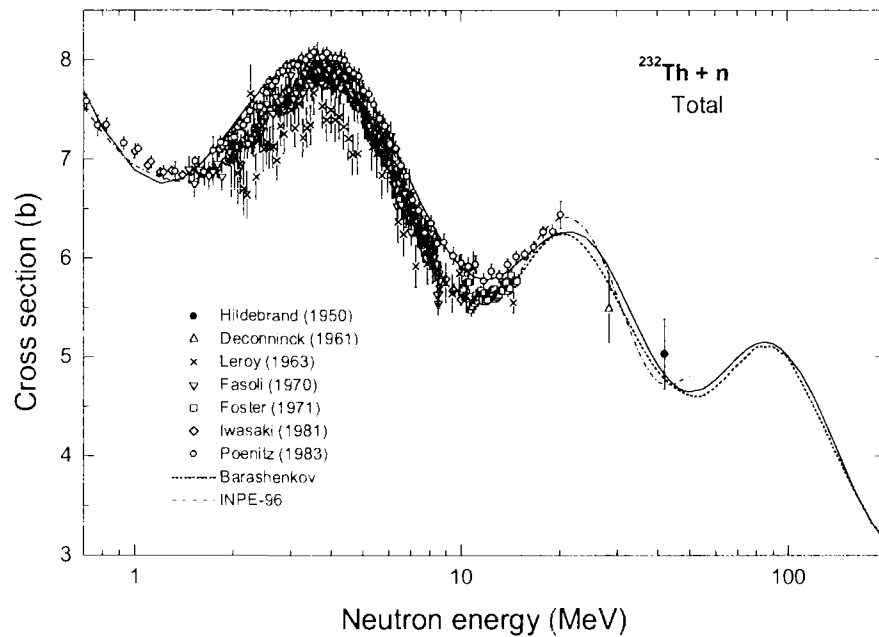


Fig. 1. Comparison of different calculations of the total neutron cross section with experimental data: Hildebrand et al. [17]; Deconninck et al. [18]; Leroy et al. [19]; Fasoli et al. [20], Foster et al. [21], Iwasaky et al. [22], Poenitz et al. [23]

Accepted for publication in *Int J. Nuclear Science and Engineering*

# Model Calculations and Evaluation of Nuclear Data for Medical Radioisotope Production

Yu. N. Shubin

## Summary

A review of recent results on the model calculations and evaluations connected with the development of a reference charged particle cross section database for medical radioisotope production is presented. Nuclear reaction models and codes used in those investigations are briefly outlined, with examples of a few calculation results. The method of statistical optimization of experimental data, based on discrete optimization with rational functions (Pade approximation) is described, and the results of evaluations of excitation functions are presented.

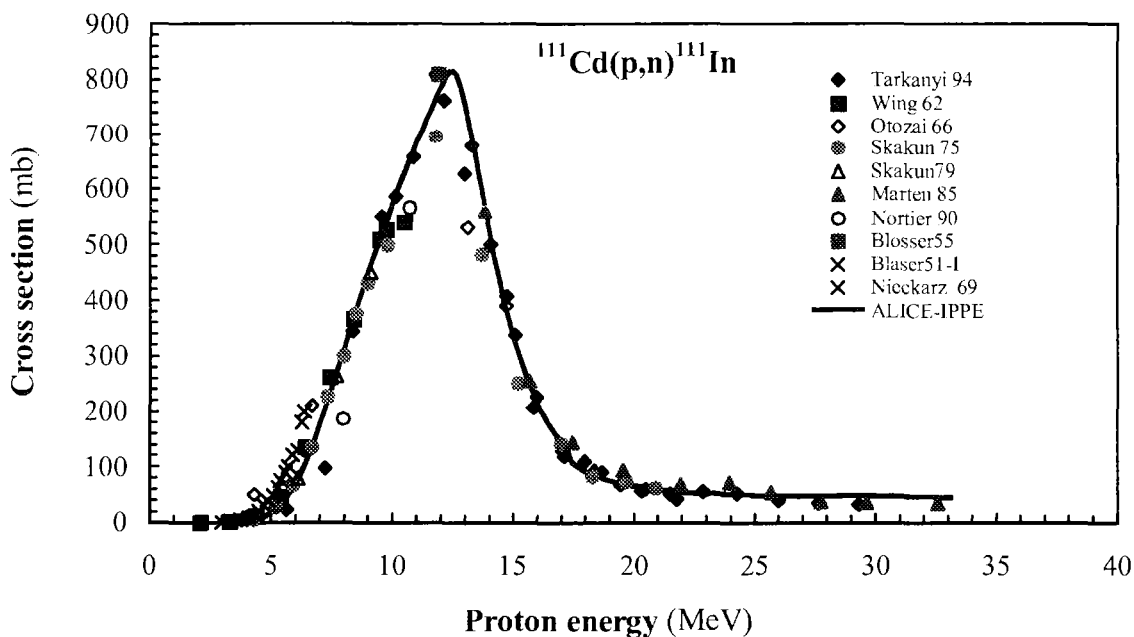


Fig. 1. Excitation function for the  $^{111}\text{Cd}(p,n)^{111}\text{In}$  reaction calculated with the ALICE-IPPE code (solid line). Points are experimental cross sections

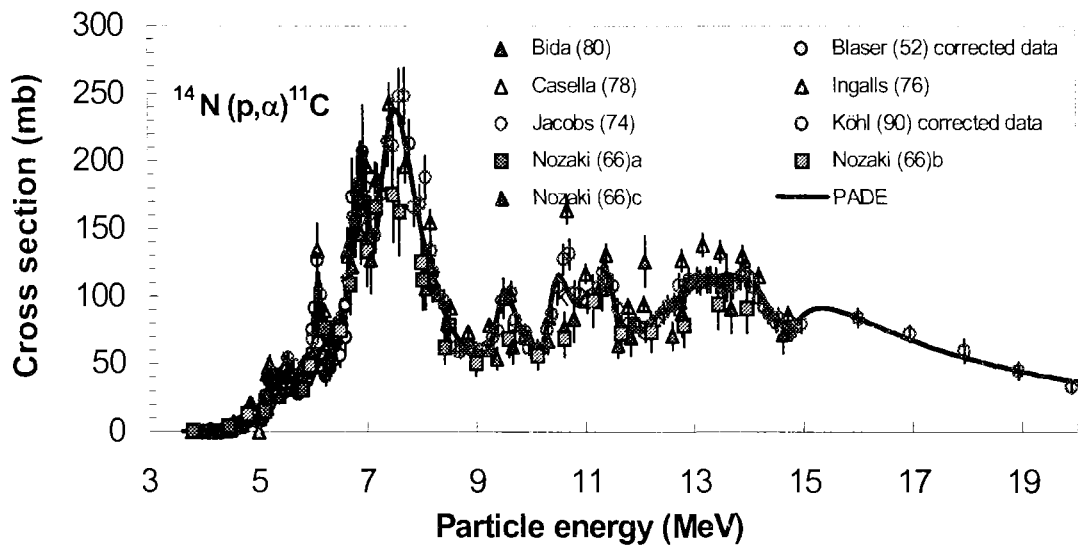


Fig. 2. Excitation function of  $^{14}\text{N}(p,\alpha)^{11}\text{C}$  reaction. Solid line is Pade approximant

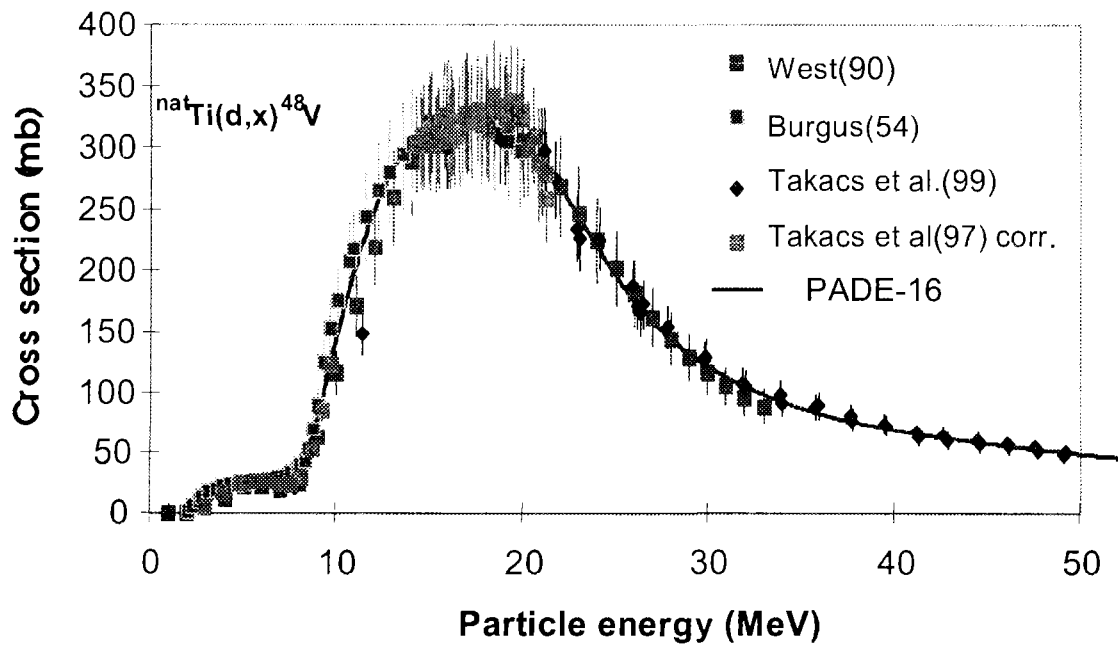


Fig.3. Excitation function of  $^{\text{nat}}\text{Ti}(d,x)^{48}\text{V}$  reaction. Solid line is Pade approximation

Accepted for publication in *Int. J. Radiochimica Acta*.

# Semi-empirical Systematics for $(n,np)$ Reaction Cross-Sections at the Energy of 14.5 MeV

A.I. Dityuk, A.Yu. Konobeyev<sup>1</sup>, V.P. Lunev, Yu.N. Shubin

<sup>1</sup> Institute of Nuclear Power Engineering –249020 Obninsk, Russia

**Abstract.** A new semi-empirical formula for the estimation of the sum of the  $(n,np)$  +  $(n,pn)$  +  $(n,d)$  reaction cross sections at the incident neutron energy of 14.5 MeV was suggested. The formula is based on the account for both equilibrium and non-equilibrium reaction mechanisms and the corresponding analytical formulas of the evaporation and pre-equilibrium exciton models. It is shown that the new semi-empirical systematics not only provides better description of the available experimental data as compared with the ones proposed earlier, but enables to obtain more realistic cross section values for the nuclei remote from the stability valley than those predicted by the empirical systematics and model calculations.

Analytical relations based on an analysis of experimental data on the dependence of various physical values on the number of protons and neutrons in nuclei are often used in nuclear physics. For instance mass formulas or formulas for the position of giant resonance can be mentioned.

Investigations of neutron induced threshold reactions at the energies of 14-15 MeV resulted in the accumulation of experimental data on the reaction cross sections. To describe these data several empirical formulas [1-3] were proposed, which can be used also for the estimation of the cross sections, particularly in the cases, when experimental data are not reliable or are not available at all. In many cases such formulas for cross section prediction are the most simple and reliable means because of the difficulties in performing the measurements and the uncertainty of results obtained using theoretical calculation methods.

There are many experimental data on the  $(n,np)$  reaction cross sections in the energy region 14-15 MeV [4,5] (Hereafter we denote as  $(n,np)$  the sum of the  $(n,np)$ ,  $(n,pn)$  and  $(n,d)$  reactions). The library of the reaction cross sections has been worked out in [6] on the basis of the analysis of experimental data. The results of measurements of the  $(n,np)$  reaction cross sections obtained by different authors for the same nuclei differ considerably in some cases. In the cross section evaluation the preference was given to the measurements performed with modern detectors. The necessary extrapolation of experimental data from the JENDL -3 [7], ENDF/B - VI [8], BROND - 2 [9], MENDL - 2 [10] libraries have been made to define the reaction cross sections at the energy of 14.5 MeV. Some data have been re-normalised [6] using the more reliable values for the monitor reaction cross sections. The library includes data for 49 nuclei from <sup>40</sup>Ar to <sup>201</sup>Hg.

Several analytical relations for the description of the sum of the  $(n,np)$ ,  $(n,pn)$ ,  $(n,d)$  reaction cross sections at the energy of 14.5 MeV were proposed earlier [1,2,3]. These systematics are purely empirical and contain the exponential dependence of the cross sections on the nuclear characteristics only. It can be shown that the exponential dependence is due to the equilibrium, evaporation mechanisms of nuclear reactions. Here the new semi-empirical formula is presented, which has been worked out using the simple idea based on the account of both equilibrium and non-equilibrium reaction mechanisms and the corresponding analytical formulas of the pre-equilibrium exciton

model. The systematics provides better description of the available experimental data as compared with the ones proposed earlier. This simple consideration has allowed already to work out the systematics for the  $(n, \alpha)$  [11] and  $(n, t)$  [12] reactions.

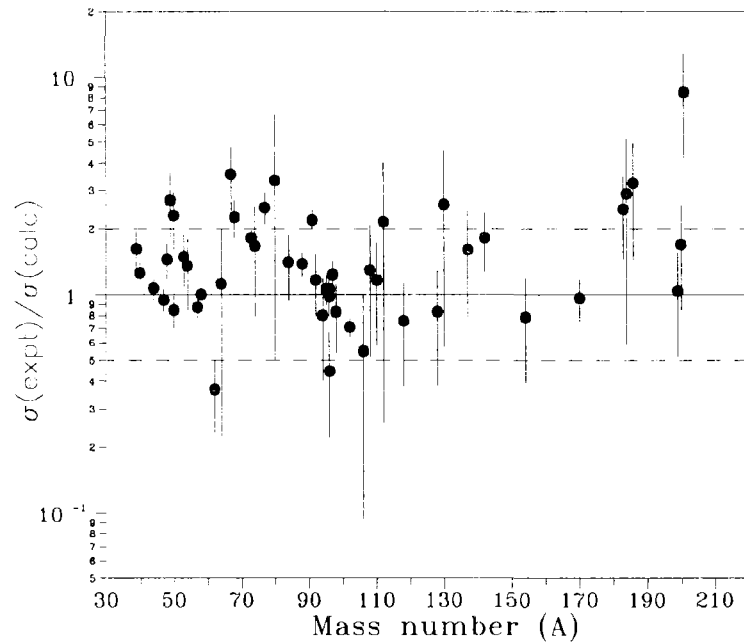


Fig. 1. The ratios of the experimental and calculated cross sections

## References

1. R.A. Forrest, Report AERE-R12419, Harwell Laboratory, 1986.
2. Y. Ikeda et al., Proceeding of the International Conference on Nuclear Data for Science and Technology, Mito, 1988, edited by .
3. S.M. Qaim, Nucl. Phys. A382, 255 (1982).
4. CINDA - A (1935 - 1987), IAEA, Vienna (1990).
5. CINDA 92 (1988 - 1992), IAEA, Vienna (1992).
6. A.I. Dityuk et al., Preprint IPPE-2492, 1996
7. Report IAEA-NDS-110, JENDL - 3.2, Rev. 5, August (1994).
8. Report IAEA-NDS-100, ENDF/B - 6, Rev. 4 (1992).
9. Report IAEA-NDS-90, BROND-2, Rev. 6, August (1992). A.I.Blokhin et al., VANT, Yadernye Konstanty, Obninsk reports 2-3 (1991).
10. Yu.N. Shubin et al., Report IAEA-INDC(CCP)-385 (1995).
11. A.Yu. Konobeyev et al., Nucl. Instr. Meth. B108, 233 (1996).
12. A.Yu. Konobeyev et al., Nuovo Cimemnto A111, 445 (1998)

Submitted to *European Physical Journal A*.

# Calculation and Evaluation of Cross Sections and Neutron Yields for U-238 and Th-232 Fission by Protons with Energies 20-150 MeV

*E.V. Gai, A.V. Ignatyuk, V.P. Lunev, N.N. Titarenko, Yu.N. Shubin*

The investigations on the creation of the evaluated proton file for Th-232 and U-238 at incident proton energies up to 150 MeV are described. Coupled channel optical model calculations are used to obtain the total, elastic and reaction cross sections and the elastic scattering angular distributions. The optimal nucleon optical potential parameters are found on the base of existing experimental data analysis. The evaluations of inelastic and fission cross sections are based on the Hauser-Feshbach statistical theory including direct reactions and pre-equilibrium processes and benchmarking with experimental data. The systematics by Kalbach-Mann are used to describe the angular distributions for all continuum particles. Approximation with rational functions is used for the analysis an evaluation of fission cross sections. The semiempirical formula is proposed for the description of prompt fission neutron number dependence on energy. The investigations resulted in the creation of recommended nuclear data files.

IPPE-REPORT № 10537, Obninsk 2000.

## New Experimental Data, Compilation and Evaluation for the $^{nat}\text{Cu}(\alpha, X)^{66}\text{Ga}$ , $^{nat}\text{Cu}(\alpha, X)^{67}\text{Ga}$ and $^{nat}\text{Cu}(\alpha, X)^{65}\text{Zn}$ Monitor Reactions

*F. Tarkanyi<sup>1</sup>, F. Szelecsenyi<sup>1</sup>, S. Takacs<sup>1</sup>, A. Hermanne<sup>2</sup>, M. Sonck<sup>2</sup>, A. Thielemans<sup>2</sup>  
M. G. Mustafa<sup>3</sup>, Yu. Shubin, and Zhuang Youxiang<sup>4</sup>*

<sup>1</sup>*Institute of Nuclear Research, Cyclotron Department, Debrecen, Hungary*

<sup>2</sup>*Vrije Universiteit Brussel, Cyclotron Department, Belgium*

<sup>3</sup>*Lawrence Livermore National Laboratory, Livermore, USA*

<sup>4</sup>*China Nuclear Data Centre, China Institute of Atomic Energy, Beijing, China*

**Abstract:** In the frame of a systematic investigation of monitor reactions for charged particle beams a detailed compilation and critical comparison of the earlier published data for the  $^{nat}\text{Cu}(\alpha, X)^{66}\text{Ga}$ ,  $^{nat}\text{Cu}(\alpha, X)^{67}\text{Ga}$  and  $^{nat}\text{Cu}(\alpha, X)^{65}\text{Zn}$  reactions has been performed. To solve the surprisingly large discrepancies found in literature we also performed a new series of cross section measurements up to 40 MeV for the above mentioned reactions to understand the reasons of the contradictions and supplying reliable numerical values for a recommended database. The new experimental values and selected, reliable literature data were compared with the predictions of different model calculations. The selected experimental data sets were fitted using different methods to obtain recommended values.

Accepted for publication in *Nuclear Instruments and Methods in Physical Research*

# Investigation of $^3\text{He}$ -induced Reactions on Natural Ti for Nuclear Analytical and Radionuclide Production Purposes

*F. Ditrói<sup>1</sup>, F. Tárkányi<sup>1</sup>, M.A. Ali<sup>2</sup>, L. Andó<sup>1</sup>, S.-J. Heselius<sup>3</sup>, Yu. Shubin  
Zhuang Youxiang<sup>4</sup>, M. G. Mustafa<sup>5</sup>*

<sup>1</sup> *Institute of Nuclear Research, Hung. Acad. of Sci. Debrecen, Hungary*

<sup>2</sup> *AEA Nuclear Research Center, Cairo, Egypt*

<sup>3</sup> *Turku PET Centre, Åbo Akademi University, Turku, Finland*

<sup>4</sup> *China Nuclear Data Centre, China Institute of Atomic Energy, Beijing, China*

<sup>5</sup> *Lawrence Livermore National Laboratory, Livermore, USA*

## Abstract

Excitation functions of  $^3\text{He}$ -induced nuclear reactions producing  $^{43,44m,46,47,48}\text{Sc}$ ,  $^{48}\text{V}$ ,  $^{48,49,51}\text{Cr}$  were measured up to 36 MeV bombarding energy by using the stacked-foil technique on different medium-energy accelerators. The results were compared with the data (cross-section, thick-target yield, activity-distribution functions, ...) from the literature, model calculations and other measurements. Earlier measurements at higher energies up to 135 MeV are also plotted to complete the database for  $^3\text{He}$ -reactions on natural Ti. The new experimental and literature data were compared with the predictions of different model calculations for the  $^{48}\text{V}$  producing reactions. The selected experimental data sets were fitted using different methods to obtain recommended values. The measurements and compilation proved, that the  $^3\text{He}$  induced reactions on natural titanium, especially those leading to  $^{48}\text{V}$  and  $^{48}\text{Cr}$  are especially useful for monitoring, for activation analysis and for Thin Layer Activation (TLA) purposes. Production of  $^{48}\text{V}$  as a radiotracer is also recommended.

Accepted for publication in *Nuclear Instruments and Methods in Physical Research*

# New Cross Sections and Intercomparison of Deuteron Monitor Reactions on Al, Ti, Fe, Ni and Cu

*S. Takács<sup>1</sup>, F. Szelecsényi<sup>1</sup>, F. Tárkányi<sup>1</sup>, M. Sonck<sup>2</sup>, A. Hermanne<sup>2</sup>, Yu. Shubin, A. Dityuk, M. G. Mustafa<sup>3</sup> and Zhuang Youxiang<sup>4</sup>*

<sup>1</sup>*Institute of Nuclear Research, Cyclotron Department, Debrecen, Hungary*

<sup>2</sup>*Vrije Universiteit Brussel, Cyclotron Department, Brussels, Belgium*

<sup>3</sup>*Lawrence Livermore National Laboratory, Livermore, USA*

<sup>4</sup>*China Nuclear Data Centre, China Institute of Atomic Energy, Beijing, People's Republic of China*

## Abstract

The  $^{27}\text{Al}(d,x)^{22,24}\text{Na}$  reactions are frequently used to monitor deuteron beams above 20 MeV. To extend possible monitoring energy region toward lower energies new monitor reactions are proposed and experimental cross-section are measured for the processes  $^{27}\text{Al}(d,x)^{22,24}\text{Na}$ ,  $^{\text{nat}}\text{Ti}(d,x)^{48}\text{V}$ ,  $^{\text{nat}}\text{Fe}(d,x)^{56}\text{Co}$ ,  $^{\text{nat}}\text{Ni}(d,x)^{61}\text{Cu}$  and  $^{\text{nat}}\text{Cu}(d,x)^{65}\text{Zn}$ . The excitation functions were studied using the activation method on stacks of thin metallic foil targets with natural isotopic composition. The data sets of the six processes were cross-checked with each other to provide reliable numerical cross-sections. Detailed literature compilation and critical comparison was made on the available data sets for the studied reactions. Predictions of model calculations were compared with the new experimental data. After establishing selection criteria, consistent data sets were chosen for each of the processes, which were then fitted with a spline or Padé method to provide recommended cross-sections.

Accepted for publication in *Nuclear Instruments and Methods in Physical Research*

## **ACT-1000 – Group Activation Cross Section Library for VVER-1000 Type Reactor**

*K.I. Zolotarev, A.B. Pashchenko*

On basis of evaluated microscopic cross section data files the problem-oriented ACT-1000 library of group-averaged activation cross sections for VVER-1000 type reactor was generated. The ACT-1000 data library was designed for calculation of induced activity for main dose-generated nuclides, which are contained in VVER-1000 structural materials. In preparation of ACT-1000 library the 47 group-averaged cross section data for  $10^{-9}$ -17,33 MeV energy range were used for calculation of space-energy neutron flux distribution.

# Evaluation of $^{54}\text{Fe}(n,2n)^{53\text{m}+g}\text{Fe}$ Reaction Cross Sections for High Energy Dosimetry Applications

*K.I. Zolotarev, A.B. Pashchenko*

The new evaluation of excitation function for the high energy threshold  $^{54}\text{Fe}(n,2n)^{53\text{m}+g}\text{Fe}$  dosimetry reaction in the energy range from the threshold to 20 MeV is briefly described. The cross section uncertainties and the covariance matrix were estimated simultaneously from the analysis. The adopted curve is compared to the available processed experimental data and the existing FEI-93, ENDF/B-VI and JENDL-3.2 evaluations. The ENDF-6 formatted data file is available from the Web site of the Russian Nuclear Data Center (RNDC) online (<http://www.rndc.ippe.obninsk.ru>).

## Introduction

Several threshold neutron activation reactions/detectors have been proposed to measure the higher than 16 MeV neutron flux including  $^{54}\text{Fe}(n,2n)^{53\text{m}+g}\text{Fe}$  reaction as candidate. The accuracy requested is about 20%. The energy range is from threshold to 20 MeV. The lack of reliable evaluations for this reaction in national data bases stimulated effort to construct a new excitation function for inclusion to the Russian Reactor Dosimetry File (RRDF-98). This RRDF-98 evaluation supersedes previous preliminary FEI-93 evaluation performed by authors in 1993 for the following reasons. First and foremost, in the course of previous evaluation, the cross section data for  $^{27}\text{Al}(n,p)^{27}\text{Mg}$  monitor reaction have been taken according to the obsolete recommendation. Consequently, it was necessary to make corrections of experimental data measured relative to  $^{27}\text{Al}(n,p)^{27}\text{Mg}$  reaction. Furthermore, the previous evaluated curve FEI-93 did not take into account experimental data measured by Andreev&Serov. Moreover, high precision measurements covering wide energy ranges from 15.2 to 18.3 MeV and from 16.07 to 20.36 MeV have been reported recently by Fessler.

## Analysis and processing of experimental data

The threshold of  $^{54}\text{Fe}(n,2n)^{53\text{m}+g}\text{Fe}$  is 13.626 MeV. In the energy range from threshold to 16.63 MeV  $^{54}\text{Fe}(n,2n)$  reaction leads to the  $^{53}\text{Fe}$  formation in the ground state. At neutron energies exceeding 16.63 MeV the 3.04 MeV isomer level of the  $^{53}\text{Fe}$  ( $J=19/2^-$ ,  $T_{1/2}=2.58$  min) is excited. The transition from isomer level to ground state is realized with a probability of 100%.

The  $^{54}\text{Fe}(n,2n)^{53\text{m}+g}\text{Fe}$  reaction cross-section measurements cover range from the threshold to 20.36 MeV. All used the activation technique. The original experimental data are shown in Fig.1. The original experimental data have been renormalized, if necessary, to the up-to-dated recommended standard cross-sections, quantum and positron yields.

After considering and processing all experimental data a smooth curve was drawn through these data points as calculated using the generalized least square method. The evaluated group cross-sections are given in the Table 1. Uncertainties given in the Table were calculated for confidence level  $P=0.95$  ( $2\sigma$ ).

As expected and illustrated in the Table 1, the greatest uncertainties of evaluated cross sections for the  $^{54}\text{Fe}(n,2n)^{53\text{m}+g}\text{Fe}$  reaction were estimated for the nearthreshold energy range 13.7-14.5 MeV and varies from about 50 to 15%. Because of importance -

of  $^{54}\text{Fe}(n,2n)^{53\text{m}}\text{Fe}$  reaction for high energy dosimetry applications, we feel that additional precise measurements from 13.7 to 14.5 MeV are required.

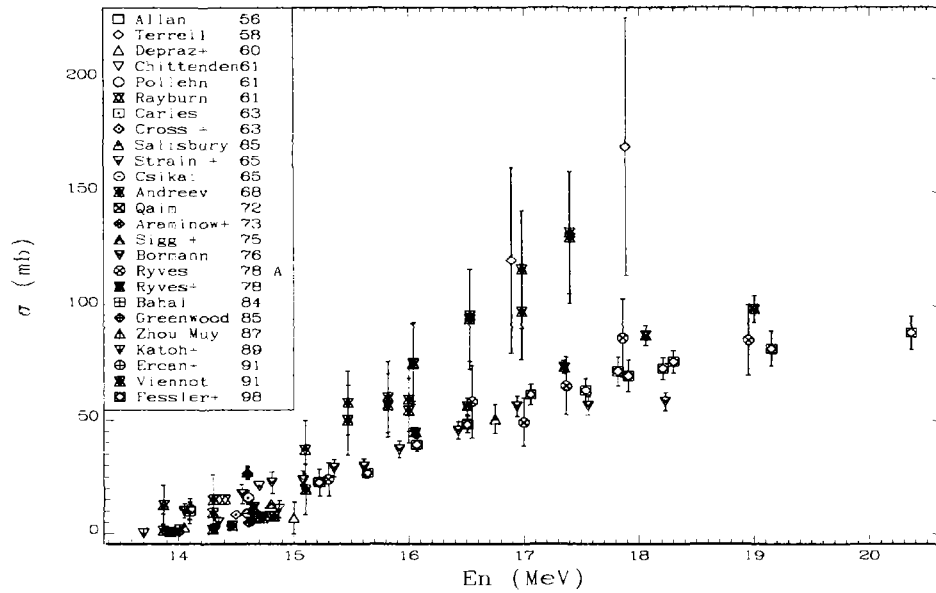


Fig. 1. The original experimental data for the  $^{54}\text{Fe}(n,2n)^{53\text{m}+g}\text{Fe}$  reaction excitation function in the energy range from threshold to 20 MeV

Table 1

**Group cross-sections and their uncertainties for the reaction  $^{54}\text{Fe}(n,2n)^{53\text{m}+g}\text{Fe}$**

Energy group [MeV] to [MeV]	Group number	Cross-section [mb]	Error [mb]	Error [%]
13.700 - 13.900	1	0.41	0.21	52.28
13.900 - 14.100	2	1.11	0.32	28.84
14.100 - 14.300	3	2.30	0.46	20.00
14.300 - 14.500	4	4.02	0.61	15.12
14.500 - 14.700	5	6.28	0.77	12.33
14.700 - 14.900	6	9.08	0.96	10.60
14.900 - 15.100	7	12.41	1.16	9.38
15.100 - 15.300	8	16.21	1.36	8.40
15.300 - 15.500	9	20.43	1.55	7.58
15.500 - 16.000	10	28.60	1.84	6.42
16.000 - 16.500	11	40.90	2.27	5.55
16.500 - 17.000	12	52.77	2.72	5.15
17.000 - 17.500	13	63.19	3.04	4.80
17.500 - 18.000	14	71.69	3.20	4.47
18.000 - 19.000	15	80.69	3.65	4.52
19.000 - 20.000	16	87.81	5.51	6.27
20.000 - 21.000	17	91.15	8.06	8.84

## 2.4 TRANSMUTATION

### Radiological Aspects of Heavy Metal Liquid Targets for Accelerator-Driven Systems as Intense Neutron Sources

*E.V. Gai, A.V. Ignatyuk, V.P. Lunev, Yu.N. Shubin*

**Abstract.** General problems arising in development of intense neutron sources as a part of accelerator-driven systems and first experience accumulated in IPPE during last several years are briefly discussed. The calculation and analysis of nuclear-physical properties of the targets, such as the accumulation of spallation reaction products, activity and heat release for various versions of heavy liquid metal targets were performed in IPPE. The sensitivity of the results of calculations to the various sets of nuclear data was considered. The main radiology characteristics of the lead-bismuth target are briefly described. The production of short-lived nuclides was estimated, the total activity and volatile nuclide accumulation, residual heat release, the energies of various decay modes were analysed.

#### Introduction

Various properties of hybrid electro-nuclear systems, which can be used for scientific investigations or energy production, to utilize plutonium or to transmute long-lived radioactive waste, in a large degree depend on target characteristics: safety, lifetime and productivity as neutron source. First concepts of ADS supposed the use of accelerator having proton energy about 1-2 GeV and current 100-300 mA to have necessary intensity of neutrons. To provide the effective heat removal it was proposed that in the targets liquid heavy metal should be used. Reliable estimations of radiological properties of targets are necessary to design electronuclear facility, which secures all safety requirements.

#### The analysis of long-lived radioactivity

The results of calculations of the total activity and activities of some most important nuclides for the lead target are shown in Fig1. One can see that various isotopes of Pt, Au, Hg, Tl, Pb and Bi make more significant contribution to the long-lived ( $T_{1/2} > 100$  d) activity than  $^{210}\text{Po}$  isotope for both targets [1,2]. The nuclides making main contributions to the total activity of the targets after different cooling times were identified. The isotope  $^{195}\text{Au}$  (half-life  $T_{1/2} = 186$  d) provides main contribution in the cooling time range 10 days 1 year together with the isotope  $^{204}\text{Tl}$  ( $T_{1/2} = 3.78$  years, begins to dominate after 3 years). The  $^{193}\text{Pt}$  contribution becomes significant later. For lead target the  $^{210}\text{Po}$  contribution is by a few orders of magnitude lower than the contribution of those isotopes. Alternative isotopes dominate also in lead-bismuth target activity for the same range of cooling times. The  $^{210}\text{Po}$  activity is only 2.5 times lower than the activity of  $^{195}\text{Au}$ . After three years the total activity is determined by  $^{207}\text{Bi}$  nuclide ( $T_{1/2} = 32.2$  years). The comparison of the activities of lead and lead-bismuth targets irradiated by 800 MeV protons for one year demonstrates that the total activities of the targets begin to differ significantly only after one year. This is due to the formation of long-lived bismuth isotopes in the  $(n, 2n)$  and  $(n, 3n)$  reactions in lead-bismuth target ( $^{207}\text{Bi}$  and, for longer times,  $^{208}\text{Bi}$ ).

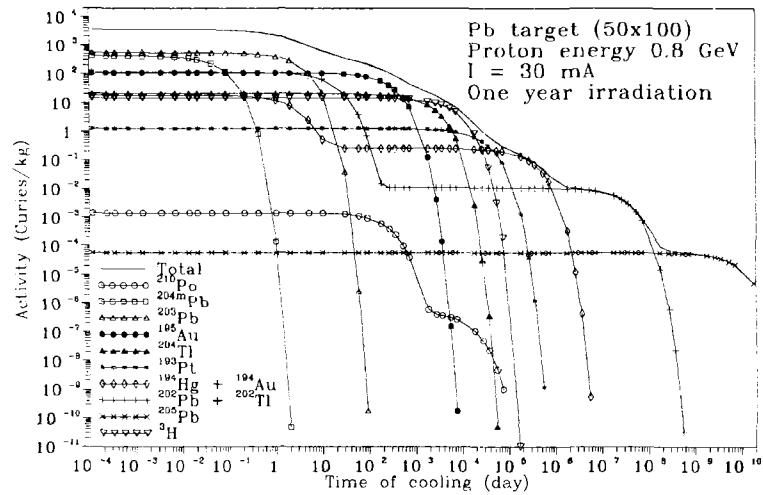


Fig. 1. Total and partial activities of lead target as a function of cooling time

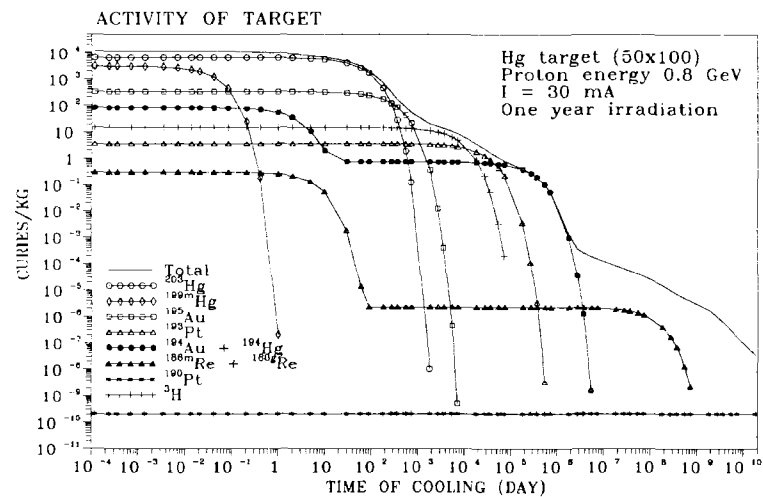


Fig. 2: Total and partial activities of mercury target as a function of cooling time

The calculations and analysis of the mercury target activity for the same irradiation conditions were carried out (Fig. 2). One can see that there is some difference in the list of the main contributing nuclides to the long-lived activity in comparison with lead or lead-bismuth targets. The other feature of mercury target is the determining contribution of fission products to the long-lived activity at very large cooling times. To evaluate correctly the possible uncertainties of the calculations and the effect of cross section data errors on the results it is necessary to analyse the spectral contributions of neutrons and protons to the accumulating activities. These results indicate that the dominating long-lived activities determined by platinum, gold, mercury and thallium isotopes are formed by hard components of proton and neutron spectra with the energies above 20 MeV.

The component of neutron spectrum with the energies below 20 MeV corresponding to 96.6 % of the total neutron flux makes some  $10^3$ - $10^4$  times lower contribution to the total long-lived activity ( $T_{1/2} > 1000$  d) than protons and neutrons from the high energy part of the spectra comprising less than 4 % of the total flux of the particles.

It must be pointed out however that the accumulation of long-lived isotopes  $^{207}\text{Bi}$  ( $T_{1/2}= 1.39 \cdot 10^4$  d),  $^{208}\text{Bi}$  ( $T_{1/2}=1.34 \cdot 10^8$  d) and  $^{210}\text{Po}$  ( $T_{1/2}=138$  d) is due to the  $(n,2n)$ ,  $(n,3n)$  and  $(n,\gamma)$  reaction on soft neutrons. The total activity of those isotopes is more than 1000 times lower than that of gold, mercury and thallium for lead and lead-bismuth targets for cooling times longer than 1 year.

Our analysis demonstrates that the uncertainties of the results of calculations of the long-lived activity of the targets are determined by the errors of the cross sections of the threshold reactions at intermediate energies of protons and neutrons.

The results obtained for the lead-bismuth target under construction in IPPE now in the frame of ISTC Project No. 559 are shown in Fig.3.

### Activity of volatile nuclides

The activity of volatile radionuclides at the moment of the accelerator shutdown was calculated. In contrast to the task of the accumulation of the total activity in this case the considerable contribution give short-lived radionuclides. Their quantities in the target are determined by the relation between the production rate and decay rate. For this purpose the decay chains have been analyzed for all isotopes, the number of the decay chains differs from three (for Br) to nine (for cesium, xenon and iodine). One can see that the contribution of mercury to the activity of volatile nuclides comprises at the moment more than 75%.

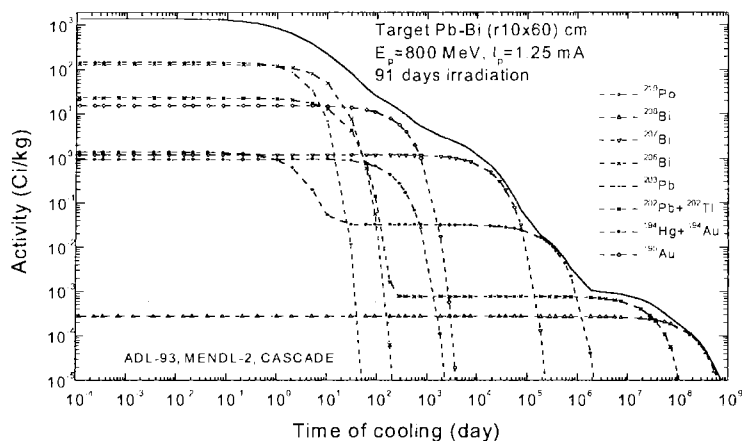


Fig. 3. Total and partial activities of lead-bismuth target after three month irradiation

The radiology characteristics have been estimated for all main components of the system [3].

### Conclusion

The obtained results showed that long-lived radioactivity accumulates mainly due to primary nuclear reactions. Secondary reactions are responsible for the production of small number of long-lived isotopes Bi-207, Po-210 and some others, being generated by radiative capture of low energy neutrons. It is possible to make a conclusion that neutrons in the energy range 20 - 800 MeV and protons with energy above 100 MeV give main contribution to the total activity generation although these parts of spectra inside the target give comparatively small contribution to the total flux.

The correct consideration of short-lived nuclides contribution is the main problem in the analysis of the target properties in the case of short accelerator shutdowns. They make the determining contribution to the both activity and the heat release at the first moments after the accelerator shutdown, creating the intermediate links and additional channels for the long-lived nuclides accumulation chains. The strong dependence of calculated concentrations of short-lived nuclides on the choice of the cross section data library for the determining of the reaction rates was noted, particularly for volatile nuclides.

The most dangerous are gaseous and volatile radionuclides, which are produced due to thermal diffusion and evaporation from the lead-bismuth mirror of volume compensator into protective gas system (helium). Among them there are noble gases krypton and xenon, radionuclides of polonium, mercury, cesium, iodine, bromine, and rubidium.

### References

1. Shubin Yu. N., Ignatyuk A. V., Konobeyev A. Yu., Lunev V. P. and Kulikov E. V. Analysis of energy release, beam attenuation, radiation damage, gas production and accumulation of long-lived activity in pb and pb-bi targets. In *Proc. 2d Int. Conf. On Accelerator-Driven Technologies and Applications, June 3-7, 1996, Kalmar, Sweden*, Ed. by H. Conde (Gotab, Stockholm, 1997), pp.953-959.
2. Gai E. V., Ignatyuk A. V., Lunev V. P. and Shubin Yu. N., Safety Aspects of Targets for ADS. In *Proc. 3d Int. Conf. ADTT'99, 3-7 June 1999, Praha, Chekhia* (CD-edition).
3. Efimov E. I., Ignatiev S. V., Levanov V. I., Pankratov D. V. and Shubin Yu. N., Radiological Properties of Heavy Liquid Metal Targets of Accelerator Driven Systems. *Ibid.*

Accepted for publication in *World Scientific*

## **Evaluation and Analysis of Neutron Emission from Target Materials of ITEP Electro-Nuclear Neutron Generator**

*Yu.N. Shubin, A.V. Ignatyuk, N.T. Kulagin, Z.V. Rudneva*

The results of evaluation and analysis of neutron spectra and angular distributions from the materials proposed as a target materials ( $^9\text{Be}$ ,  $^{238}\text{U}$ ) irradiated by proton beam of various energies (36, 100 and 200 MeV) are discussed. Reaction cross sections were calculated using various computer codes: ALICE-IPPE, LAHET, CASCADO, SHIELD. Available activation libraries of nuclear data, existing experimental data and evaluations in the intermediate energy region, performed in various laboratories, were analyzed. The recommendations for the spectra and angular distributions of neutrons in the target of electro-nuclear neutron generator being under construction in ITEP on the base of the heavy-water reactor TWR and the linear proton accelerator ISTR-36 have been worked out.

The investigations performed earlier for various materials, which can be used as the neutron generator target, have shown that:

- Neutron yield per proton increases with the thickness of the target, when the thickness is less than proton free path, and is practically constant for the larger thickness (complete absorption).
- Neutron yield per proton increases with incident proton energy for all materials investigated.
- Neutron yield increases with mass number increase. The only exception is  $^9\text{Be}$ , which has neutron yield at low energies ( $\approx 40$  MeV) comparable with ones for heavy nuclei (Pb).
- Between the materials investigated the maximum yield has  $^8\text{U}$ .

To increase the effectiveness of the target as a neutron source of the electro-nuclear neutron generator at the energy of 36 MeV the combined target can be suggested basing on the following. At small energies about 20 MeV the reaction cross section for U is small (this is approximately a third of a free path). At the same time the yield for Be is considerably higher than for the other elements. Thus the suggested combination of U and Be (1 mm U + 3 mm Be) could increase the target effectiveness even in the comparison with the target made of U only.

The knowledge of the spectra and angular distributions is needed to estimate the radiological conditions and the safe operation of the whole system. Therefore we analyzed available experimental data, existing calculations and evaluations, and performed the new calculations of the spectra and angular distributions of neutrons produced in these materials. The results of the work are presented as a recommendations, which can be used as for designing and operation of electro-nuclear generator of ITEP, and also for the estimation of the properties of the more powerful accelerator-driven systems.

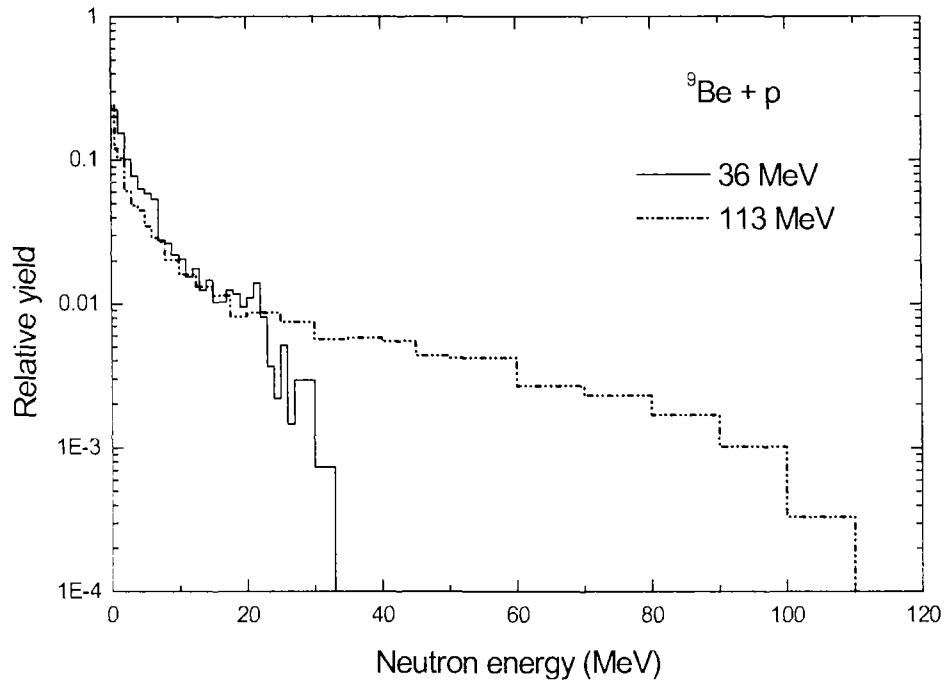


Fig. 1. Neutron spectra from the thick Be target at the energy of 36 and 113 MeV, calculated with the LAHET code, normalized to 1.0

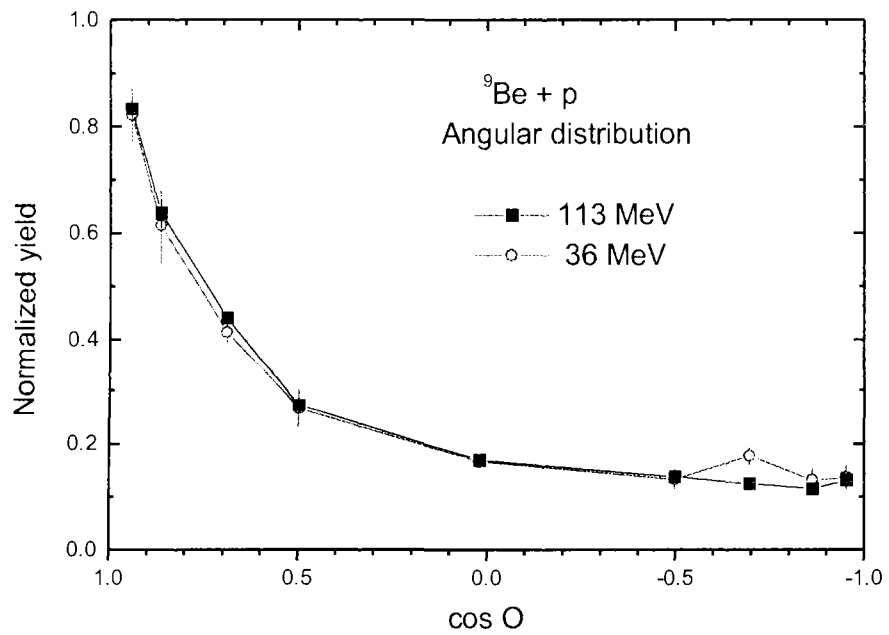


Fig. 2. Angular distributions from thick Be target calculated with the LAHET code normalized to 1.0.

*Report IPPE-10410, Obninsk (2000).*

# Incineration of Transuranics in Hard Neutron Spectra

*G.L. Khorasanov, A.I. Blokhin, V.V. Sinitsa*

The purpose of the paper is to estimate the possibility of transuranics (TRU) burning in a hard neutron spectrum via nuclear fission. Corresponding neutron cross section data are taken from the new Russian data set ABBN-93 [1] operated with 28 neutron energy groups. These data are compared with the national evaluated nuclear data libraries BROND-2, ENDF/B-VI, JEF-2.2 and JENDL-3.2.

Calculated mean values of neutron multiplication coefficient for TRUs immersed in acting neutron spectra are called as a criterion for fission ability. As it known, the coefficient of neutron multiplication  $k$  for the act of nuclear fission is expressed by the following formula:

$$k = \frac{\bar{\nu}}{1 + \bar{\alpha}} \quad (1)$$

where  $\bar{\nu}$  is the mean value of prompt neutrons per the act of fission:

$$\bar{\nu} = \sum_g \nu_g f(E_g) \quad (2)$$

$g$  - is a group number,

$f(E_g)$  - is an acting neutron spectrum in the 28 group approximation.

The second coefficient  $\bar{\alpha}$ , coming in (1), is delivered as the following expressions:

$$\bar{\alpha} = \sum_g \left( \frac{\sigma_c}{\sigma_f} \right)_g f(E_g) \quad (3)$$

where  $\sigma_c$  and  $\sigma_f$  - are the cross section of neutron capture and fission, correspondingly. We consider here only the process of neutron capture via radiation ( $n, \gamma$ ) reaction.

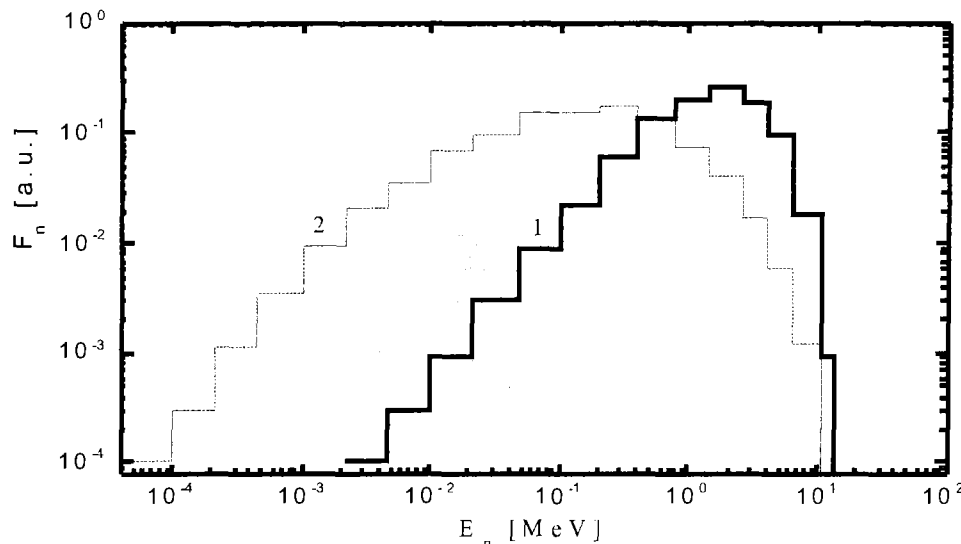


Fig.1. Spectra of fission neutrons (1) and core neutrons of fast reactors with lead coolant (2)

Calculations of k were performed for the following nuclides: uranium U-235, -238, neptunium Np-237, plutonium Pu-238, -239, -240, -241, -242, americium Am-241, -243, curium Cm-242, -244, -246, -248.

The spectrum of fission neutrons (SFN) is considered here as the most possible hard spectrum. The other examined here spectrum is the one calculated for fast reactors(FR) with a lead coolant. Both of these spectra are given in Fig.1.

In the Table 1 the values of calculated coefficients of neutron multiplication for TRUs immersed in SFN are given.

Table 1

**Coefficients of neutron multiplication for TRUs averaged over SFN**

Nuclide	Coefficient of neutron multiplication				
	ABBN-93	BROND-2	ENDF/B-VI	JEF-2	JENDL-3
Cm-242	3.24621	3.14970	1.45172	3.18454	3.24727
Pu-241	3.08349	3.08928	3.02882	2.82128	3.00457
Pu-239	3.04998	3.03997	3.08220	3.03031	3.04988
Pu-238	2.99277	2.92354	2.86231	3.18510	2.95095
Cm-246	2.47907		0.38123	0.38123	2.56148
U-235	2.46280	2.47356	2.46273	2.45492	2.43418
Cm-244		2.05346	2.14511	2.35853	2.27251
Cm-248	2.42919		2.97279	2.97279	2.59760
Pu-240	2.37716	2.42817	2.35240	2.25599	2.24415
Pu-242	1.27237	2.41149	1.57361	1.52313	1.54149
Np-237	0.76978	0.75066	0.59875	0.58049	0.85192
Am-241	0.57113	0.53582	0.52247	0.44695	0.59493
Am-243	0.95606	0.42117	0.47491	0.24284	0.34344
U-238	0.02882	0.00056	0.00005	0.00005	0.00005

Table 2

**Coefficients of neutron multiplication for TRUs averaged over core neutron spectrum of FR with lead coolant**

Nuclide	Coefficients of neutron multiplication				
	ABBN-93	BROND-2	ENDF/B-VI	JEF-2	JENDL-3
Pu-241	2.6604	2.6609	2.6442	2.4781	2.5810
Pu-239	2.4375	2.4084	2.4508	2.4282	2.4371
U-235	2.0155	2.0162	2.0153	2.0212	1.9797
Pu-238	1.9143	2.0397	1.7035	2.9459	1.8058
Cm-242	1.4689	1.6161		0.9142	1.5143
Pu-240	0.5810	0.7254	0.5175	0.4802	0.4641
Cm-244		0.4703	0.3089	0.4168	0.4267
Cm-246	0.3921		0.0193	0.0193	0.5091
Cm-248	0.3585		0.5377	0.5377	0.5748
Pu-242	0.0787	1.1755	0.1156	0.0928	0.0894
Np-237	0.0316	0.0459	0.0254	0.0241	0.0540
Am-241	0.0541	0.0435	0.0452	0.0404	0.0467
Am-243	0.0085	0.0353	0.0383	0.0142	0.0238
U-238	0.0050	0.0001	0.0001	0.0001	0.0001

In Table 2 the same coefficients calculated for core neutron spectrum of FR with lead coolant are represented.

From these calculations it follows that such TRU isotopes as Pu-238, -239, -241 and Cm-242 are perfectly fissionable in the FR spectrum ( $k > 1$ ). Other TRU isotopes, such as Pu-240, Cm-244, -246, -248 have less coefficients of neutron multiplication,  $0.3 < k < 0.7$ , but they can be considered as a sufficiently fissionable nuclei in FR spectrum. As concerns neptunium Np-237, americium Am-241, Am-243 and plutonium Pu-242, their coefficients of neutron multiplication in FR spectrum are sufficiently low ( $k = 0.008 - 0.08$ ), much less than  $k$  values for SFN ( $k = 0.6 - 1.3$ ).

The results obtained indicate that minor actinides, Np-237, Am-241, Am-243, and plutonium higher isotope, Pu-242, can not be successfully burned in neutron spectrum of FR core with lead coolant via nuclear fission.

Meanwhile, the efficiency of MA and Pu-242 burning in FRs can be increased in the case of neutron spectrum hardening by well known techniques [2] or by the choice of low-moderating lead coolant based on lead enriched with isotope Pb-208 [3].

## References

1. G.N.Manturov, M.N.Nikolaev, A.M.Tsibuliya. ABBN-93 group nuclear data set. VANT, Ser.: Yadernye constanty, 1996, №1, p.59-98, (in Russian).
2. S.S.Pavlenko, S.G.Usynina, V.A.Chirkov. Influence of the acting spectrum of neutrons in FBR on plutonium utilization in U-free fuel elements. Communication of Higher Schools. Yadernaya energetica, 1997, №2, p.67-70 (in Russian).
3. G.L.Khorasanov, A.P.Ivanov, V.V.Korobeinikov, A.I.Blokhin, A.L.Shimkevich. Lead Coolant for Fast Reactor-Burner with Hard Neutron Spectrum. Ibid, 1999, №1, p. 80-84 (in Russian).

## High Enriched Lead-206 for Small Nuclear Power Plants

*G.L. Khorasanov, A.P. Ivanov, A.I. Blokhin, V.N. Prusakov<sup>1</sup>, A.N. Tcheltsov<sup>1</sup>*

<sup>1</sup> *RRC «Kurchatov Institute» - Institute of Molecular Physics, Russia*

Now the same attention is given to the development of small nuclear engineering based on nuclear reactors with the power up to 300 MW [1]. For example, the policy of the Ministry of Russian Federation for Atomic Energy in the field of nuclear engineering [2] includes the creation of small nuclear power installations (NPI) for remote regions of Russia in 2001-2010 years. IAEA elaborates a development program of small nuclear engineering for developing countries. According to this program the need for small NPI will be 70-80 units for the next decade, and after 2015 the annual need for them will be up to 10-50 units [3].

In modern projects of perspective NPI the preference is given to fast reactors (FR) with heavy liquid metal coolants. Internal self-hardening, absence of poisoning effects, compensation of uranium fuel burn-out by produced plutonium fuel and other positive features of FR will enable in future to lengthen operating campaign of the reactor till 10-12 years, and service life of FR - till 30-60 years [4,5].

As it known, the coolant, circulating through the core of FR, is activated and accumulates long-lived radionuclides. Taking in account the masses of coolant materials in considered FR ( 20-200 tons ) and the scales of introduction of small NPI in the future, we can have problems with handling completed coolant after FR removal from exploitation and during repair and emergency works. So it is desirable to have a low-activation coolant with low content of long-lived radionuclides - products of nuclear reactions. In paper [6], presented at the ICONE-8 conference, it is offered to use lead enriched with isotope Pb-206 as a low-activation coolant for FRs. Its content in a natural mixture of lead isotopes is 24 %, and the demanded enrichment of isotope does not exceed 95-98 %. However, usage of coolant of enriched lead can result in increasing the price of power, owing to what NPI can become noncompetitive in relation to other power sources.

The purpose of this paper is to point out the interval of the prices of the product lead-206, at which it can be demanded for nuclear engineering in large volumes. We also consider possible ways to decrease the costs of obtaining the product lead-206 for the need of small nuclear engineering.

By the present time a number of the projects of small NPIs with a lead-bismuth coolant for remote regions of Russia is designed. There are reactor installations (RI) such as ANGSTROM, SVBR-75, BRUS-150 and others, designed in SSC RF IPPE, Obninsk, and EDO "Gidropress", Podolsk, Russia. Their basic power and cost characteristics, and also specific coolant demands are listed in table 1.

Table 1

### Basic Power and Cost Characteristics of the Small NPIs

The naming of NPI Basic characteristics of NPI	ANGSTRO M modular arrangement [7]	SVBR-75 modular arrangement [8]	SVBR-75 monoblock [8]	BRUS - 150 monoblock [7]
Thermal capacity, MW	30	265	265	500
Thermal supply capacity, MW	14			
Electric capacity, MW	6	90	90	170
Coolant weight, tons	40	80	190	350
Specific demand for coolant, tons/MW (therm.)	1.3	0.3	0.7	0.7
NPI cost oriented, million of dollars USA	20	180	200	340
Coolant cost limited, million of dollars USA	4	36	40	68
Enriched lead-206 price limited, USD/kg	100	450	210	200

From the Table 1 follows, that the specific costs for creation of NPI are 2 million dollars USA for 1 MW (el.), and the approximate cost of single (100 MW<sub>el</sub>) small NPI is not less than 200 million dollars. In the reviewed projects we used the lead-bismuth coolant having good thermal and physical properties and low melting point (125°C). However the lead-bismuth coolant is characterized by the high induced radioactivity, which leads to the losses of valuable non-ferrous metal after RI removal from exploitation [9]. Besides, for reliable localization of radioactive coolant, in some projects of small NPIs the additional intermediate circuit with heavy metal coolant is envisioned. Usage of low-activation enriched lead-206 in the NPI will allow to avoid problems connected with the induced activity of the coolant. However, the fact, that the cost of such coolant should not exceed 20 % from overall costs of NPI, bounds the possibility of using enriched lead-206 in NPI. As follows from the Table 1, the maximal acceptable price of lead-206 should not be higher than 200 USD/kg, then NPI will be able to compete to other sources of electric power and heat. At the favorable scenario of development of nuclear engineering and the annual creation of 10 units of small NPIs, the general demands for lead-206 with enrichment C=95% can be about 1-2 thousand tons per year after 2015.

Large-scale stable isotope separation has become practicable after an appropriate up-to-date gas centrifuge had been devised. This kind of work has been carried out at the RRC «Kurchatov Institute» and detailed information was given in [10]. Stable isotope separation by the method of centrifuge separation of gaseous components of different chemical elements is based on several considerations. The initial compound must have the vapor pressure of about 5 mm Hg and higher at the moderate temperatures. The structure of the gas centrifuge meets the requirements for the optimal ability to separate isotopes of certain mass. In [10] some of the chemical compounds are listed that are being used in the commercial stable isotope separation. Methyl derivatives of tin, lead, zinc and cadmium were synthesized and used for the separation of corresponding

isotopes on centrifuges.  $\text{Sn}(\text{CH}_3)_4$ ,  $\text{Pb}(\text{CH}_3)_4$ ,  $\text{Zn}(\text{CH}_3)_2$  and  $\text{Cd}(\text{CH}_3)_2$  have a high volatility and thermal stability.

Lead has no volatile fluorides, and the most suitable for centrifugation is an organometallic compound, tetramethyl lead - $\text{Pb}(\text{CH}_3)_4$ . Tetramethyl lead first, has sufficient vapour pressure at room temperature, which can provide necessary gas-filling of centrifuge and acceptable flows in the cascade stages; second, the chemical activity and thermal stability of this compound are within the limits permitting the stationary mode of cascade performance to be reached.

The tetramethyl lead properties have been studied so much that it is possible to state that this compound is not unique. The experimental results we obtained in studying tetramethyl lead synthesized for the work agree with the available data with an accuracy to a measurement error. It should be noted that the substance under investigation must be preliminary cleaned from impurities since the latter affect significantly the results obtained

Examples of enriched lead isotopes  $^{206}\text{Pb}$ ,  $^{207}\text{Pb}$ ,  $^{208}\text{Pb}$  ( $C > 95\%$ ) were produced at the RRC «Kurchatov Institute» by a gas centrifuge technology [11].

The cost of enriched lead-206 is determined by the price of initial actuating substance and costs of the enriching process. Thus the consumptions on purchasing tetramethyl lead are essential. The current price of tetramethyl lead is close to 1000 dollars/kg while the price of natural lead only ~1 dollar/kg. The costs of lead enrichment with isotope Pb-206 are reduced due to the high content of lead-206 in natural lead and demanded final level of enrichment ( $C \approx 95\%$ ).

In the future, the price of the product lead-206 can be decreased at the expense of the following factors:

- reaching an industrial level with production of several tons of enriched lead-206 per year,
- developing the cheap know-how of obtaining the actuating substance - tetramethyl lead,
- usage of initial actuating substance and separating power for attendant obtaining other stable lead isotopes, for example Pb-208, which is also demanded for nuclear technology in large volumes [12].

## References

1. A.V.Zrodnikov. Power Engineering Based on Small Nuclear Reactors. "Atompressa", 2000, N2 (379), p.1, Moscow: the Ministry of RF for Atomic Energy (in Russian).
2. The Development Strategy of Nuclear Engineering in Russia in the First Half of the XXI Century. Bulletin TSOI, 2000, N6, p. 4-7, Moscow :TSNIIatominform (in Russian).
3. Introduction of Small and Medium Reactors in Developing Countries. Proc. of Advisory Group Meetings, Tunis, Tunisia, 3-6 September 1996.
4. B.F.Gromov, O.G.Grigoriev, A.V.Dedoul et al. Use of Russian Technology of Naval Reactors with Lead-Bismuth Coolant in Civil Nuclear Power. In: Heavy Liquid Metal Coolants in Nuclear Technology, Obninsk: SSC RF IPPE, 1999, vol.1, p. 41 - 48.
5. E.Greenspan, D.C.Wade. Encapsulated Nuclear Reactor Heat Source Module. Transactions of the American Nucl. Society, 1999, v.80, p. 197-198.

6. G.L.Khorasanov, A.P.Ivanov, A.I.Blokhin et al. Molten Lead Enriched with Isotope Pb-206 as a Low-Activation Coolant for Emerging Nuclear Power Systems. In: the Book of Abstracts and CD-ROM Proceedings of the ICONE-8, Baltimore, Maryland, USA, April 2-6, 2000, Paper # ICONE-8385.
7. B.F.Gromov, Yu.S.Belomytsev, V.A.Gubarev et al. Reactor Inherently Safe Cooling with Alloy Lead-Bismuth. *Atomnaya energiya*, 1994, vol.76, N4, p. 332-339 (in Russian).
8. O.G.Grigoriev, G.I.Toshinsky, S.K.Legunencko. Demands in Bismuth for Commercial Usage of SVBR-75 Reactor Installations for Solving Different Tasks. In: *Heavy Liquid Metal Coolants in Nuclear Technology*, Obninsk: SSC RF IPPE, 1999, vol.2, p. 558-563.
9. V.I.Usanov, D.V.Pankratov, E.P.Popov et al. Long-Lived Radionuclides of Sodium, Lead-Bismuth and Lead Coolants in Fast Reactors. *Atomnaya energiya*, 1999, vol.87, N3, p. 204-210 (in Russian).
10. V.N.Prusakov and A.A.Sazykin. Progress in Isotope Separation. In: *Proc. of the 5th Int. Symp. on Synthesis and Application of Isotopes and Isotopically Labeled Compounds*, June 20-24, 1994, Strasbourg, France.
11. I.A.Suvorov and A.N.Tcheltsov. Stable Enriched Isotopes and the Use of Isotope Targets for Radioisotope Productions. *Nucl. Instr. and Methods in Phys. Research*, 1989, v. A282, p.286-289.
12. G.L.Khorasanov, A.P.Ivanov, V.V.Korobeinikov et al. Lead Coolant for Fast Reactor-Burner with Hard Neutron Spectrum. *Communications of Higher Schools. Nuclear Power Engineering*, 1999, N1, p. 80-84 (in Russian). In: *CD-ROM Proceedings of the GLOBAL'99*, Jacson Hole, Wyoming, USA, August 29 – September 3, 1999, Paper # 344.

## 2.5 CONDENSED MATTER PHYSICS

### Neutron Scattering Microscopic Investigation of Liquid Lead and Lead-Potassium Eutectic Alloy

*N.M. Blagoveshchenskii, V.A. Morozov, A.G. Novikov,  
V.V. Savostin, A.L. Shimkevich*

Liquid lead, being assumed as a coolant for fast nuclear reactors of next generation, has a number of safety eligibility. Along with that, there are considerable technological difficulties for using this coolant. The most complex one arises from high oxygen solubility in liquid lead at working temperatures, which in its turn entails intense corrosion of structural materials. One way to solve this problem is doping of lead with impurities decreasing oxygen solubility. Pb-K system is represented as an especial interest in this aspect.

Lead and potassium melts are studied earlier and staying up to date the matter of multiple microscopic investigations: by neutron diffraction [1], reverse Monte-Carlo method [2] and molecular dynamics simulation [3]. A singular interest to these melts results from Zintl's clusters which exist in liquid Pb-K ( $\geq 25\%$  at.) system in form of quasi-molecular groups of  $(\text{Pb}_4)^-\text{K}^+$  with tetrahedral packing of atoms. However, there are no data on that for Pb-K alloys with potassium concentration lower than 25% at. An estimate depicts that Pb-K (9% at. K) eutectic alloy can have optimal properties as a heavy coolant. The present work task is to investigate liquid lead and Pb-K (9% at.) eutectic alloy by neutron diffraction and inelastic scattering to obtain information of its atomic structure and microdynamics.

The DIN-2PI time-of-flight spectrometer [4] is used in experiments. It is located at one of neutron beams of the IBR-2 pulsed reactor (Frank Laboratory of Neutron Physics, JINR, Dubna). In neutron diffraction experiments main chopper was extracted from the spectrometer, so the full spectrum of thermal neutrons was incoming into the sample. An especial collimator is installed in place of the chopper to remove an excess neutron intensity without changing the beam geometry. The range of neutron wave-vector transfer  $Q$  has amounted to  $0.3 < Q < 22 \text{ \AA}^{-1}$  in the diffraction experiments.

The metal sample is made as a cylindrical layer with 4 mm in thickness, 100 mm in diameter, and 150 mm in height. It is cased in 0.2 mm thick foil of Armco-iron. The early experiments have shown that this material appreciably decreases elastic neutron scattering.

The neutron scattering experiments on pure lead and Pb-K eutectic alloy are carried out at 630 and 870 K (the meltinpoint is 600 K for lead and 545 K for Pb-K eutectics). Thus, information for pure solvent and potassium solution is obtained in the same experimental conditions and it enables to do direct comparison of data.

Furnace with two heaters has been used. They are arranged up and down the sample beyond the neutron beam and screened of neutrons by absorbing sheets from Ti + 10% at. Gd. The overall heaters capacity is of about 2 kW. The furnace construction enables to get a sample temperature up to 900 K at vacuum chamber of  $10^{-3}$  mm Hg. To avoid container damage while melting or cooling the sample, the possibility for separating a switch of heaters is provided. The sample is warmed with upper heater and only after its melting, the lower one is switched on also. The temperature is controlled by Eurotherm system with  $\pm 0.1$  K accuracy.

An experimental static structure factor  $S(Q)$  is obtained by neutron diffraction for identifying the liquid-matrix structure. It is shown narrowly in Fig. 1 for low  $Q$  range which represents an especial interest due to Pb-K alloys of potassium concentration more than 25 % at. have a pre-peak in this range [1]. It is concerned with appearance of Zintl's clusters in the melt. One can see that the Zintl's pre-peak is absent in the Pb-K eutectic alloy. It is evidenced an absence of clusterisation and micro-inhomogenities in the Pb-K (9% at.) system.

Along with that, some increasing of the alloy scattering intensity for low  $Q$  indicates to inflexibility of liquid alloy matrix as to lead melt.

In spite of lead melt has been investigated repeatedly [1–3], its microdynamics is uncertain yet. According to known data, the ability of liquid lead to sustain existence of collective modes lies between liquid inert gases (Van-der-Vaals liquids) and liquid alkali metals. In this connection, another task of our neutron experiment is in measuring inelastic scattering spectra to observe the modes of collective atomic excitations for studying its characteristics.

The inelastic neutron scattering spectra of liquid lead are represented in Fig. 2. The characteristic peak of collective modes is clearly visible. The detailed analysis of these data is performed now.

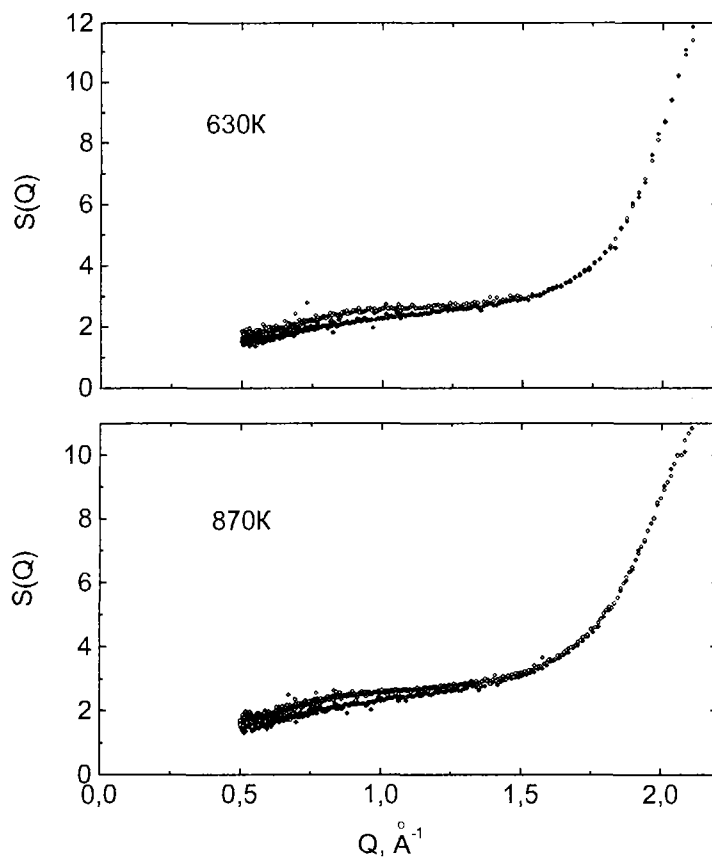


Fig. 1. The static structure factor of liquid lead (full circles) and Pb-K (9% at.) eutectic alloy (open circles) at two temperatures

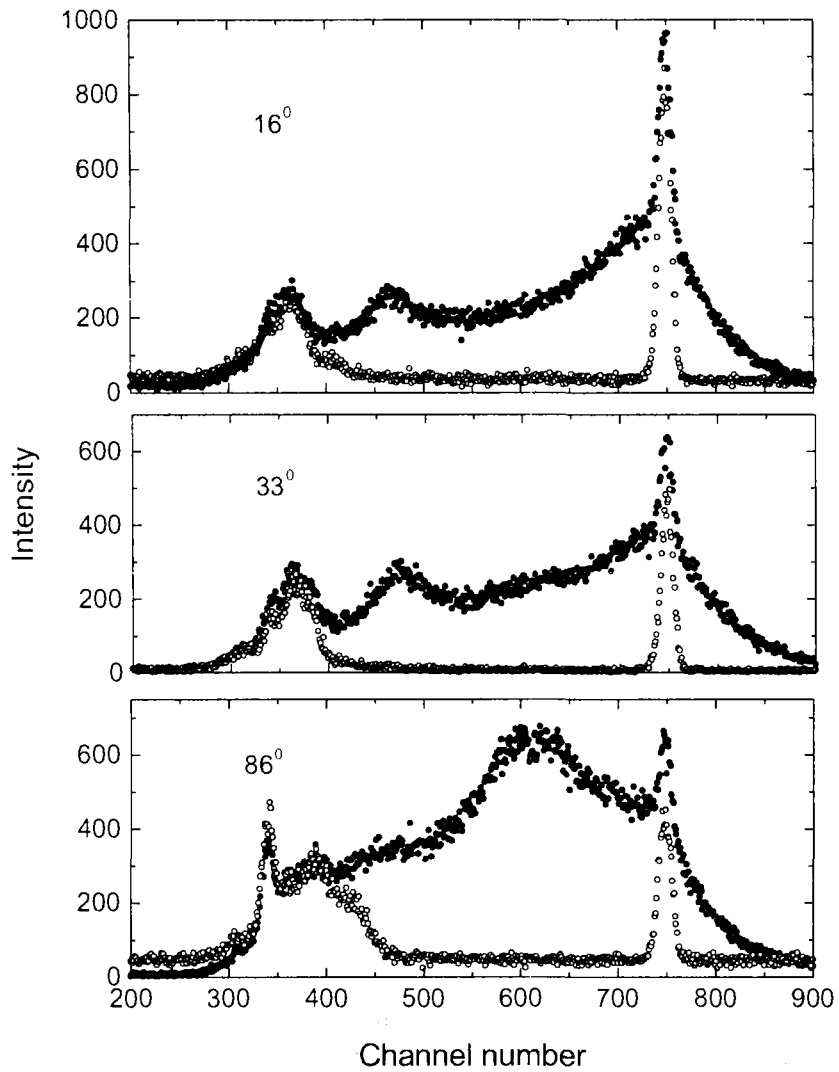


Fig. 2. The spectra of inelastic neutron scattering on liquid lead sample in container (full circles) and empty container (open circles) for three scattering angles at 630 K. The incident neutron energy is 3 meV

#### References

1. H.T.J. Reijers, W. van der Lugt, C. van Dijk, M-L. Saboungi, *J. Phys.: Condens. Matter* 1 (1989) 5229.
2. M.A. Howe, R.L. McGreevy, *J. Phys.: Condens. Matter* 3 (1991) 577.
3. M. Stolz, R. Winter, W.S. Howells, R.L. McGreevy, *J. Phys.: Condens. Matter* 7 (1995) 5733.
4. V.V. Sikolenko, ed., *User Guide. Neutron Experimental Facilities for Condensed Matter Investigations at FLNP JINR (JINR, Dubna, 1997)*, p. 25.

# Surface Excitations in Thin Helium Film in Silica Aerogels

*I.V. Bogoyavlenskii, A.V. Puchkov, H.J. Lauter<sup>1</sup>, A. Skomorokhov*

<sup>1</sup>*Institute Laue Langevin, F-38042, Grenoble Cedex 9, France*

Liquid helium attracts the attention of experimentalists and theorists nowadays even more than as previously. The long term studies of the excitation spectrum of bulk liquid helium on DIN-1M, DIN-2PR, and DIN-2PI spectrometers (IBR-30 and IBR-2 reactors) brought interesting results [1] in parallel with the investigations at other neutron centres. During the last years the interest in this field widened from bulk helium to helium in confined geometries. So properties of helium in porous media like exfoliated or powdered graphite, zeolites, sponge, vycor glass, aerogels, and xerogels were explored. It turns out that liquid helium properties in porous media differ from those of bulk helium and depend on geometrical parameters and type of porous media [2]. It appears that the surface properties of the media have great influence on the helium adjacent to the confinement. Neutron scattering studies of thin liquid helium films on different substrates are started now to get an understanding of these properties

Neutron scattering data, taken from helium films on graphite show the existence of the ripples at the liquid-gas interface of the film and of excitation, which have the character of 2-dimensional rotons at the solid-liquid interface of the film, called layered-phonon-roton modes [3]. In very thin films only these two excitations may exist, whereas in the example of a 4-monolayer film parts of the bulk phonon-roton curve are visible.

The interest to study the excitations in a <sup>4</sup>He film adsorbed on silica aerogel is, that <sup>4</sup>He films in the aerogel shows a different behavior compared to films on other substrates as e.g. graphite. Apart from this, bulk helium in aerogel, graphite or vycor shows a different exponent for the temperature dependence of the superfluid component near the lambda-transition. This may be related again to the different interface properties of the helium film excitations on the fractal aerogel surface.

The results presented here are the first attempt of the investigation of liquid helium films on the DIN-2PI spectrometer.

The incident neutron energy was 2.58 meV. The range of scattering angles and of momentum transfers was 11° - 133° and 0.2-2.0Å<sup>-1</sup>, respectively. The aerogel sample had been annealed at 600C under a pressure of ~10<sup>-4</sup> torr during 3 days. The MAX ORANGE cryostat has been used together with the special sample-stick for the filling of the aerogel sample with helium gas under pressure-temperature control. The measurement was carried out at a sample temperature of T=1.55K. Three different coverages have been tested: corresponding to a monolayer (20 l of normal pressure helium gas), a 2-3 layer film (58 l), and a filling of 68 l, a coverage at which the signal from the bulk roton is just appearing. It should be mentioned that the first layered part of the helium film adjacent to the aerogel substrate is amorphous and is added to the aerogel substrate.

Fig. 1 shows the experimental dynamic structure factor of aerogel+helium at constant angle at T=1.55K. No background was subtracted. The scattered intensity at the angle of 133° picks up the signal from the roton region near the momentum transfer of Q=1.9Å<sup>-1</sup>. At T=1.55K the energy of the bulk roton (BR) and the layer roton (LR) are

very close. Perhaps the influence of the bulk roton appears already at the 58 l-coverage due to its high intensity.

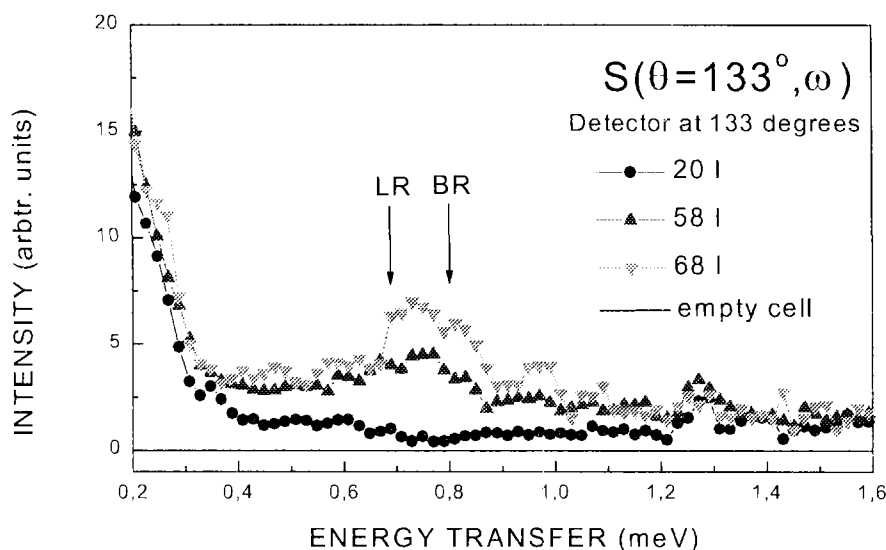


Fig.1. Experimental dynamic structure of a thin  $^4\text{He}$  film adsorbed on silica aerogel for three coverages at  $T=1.55\text{K}$ . No difference between the 20 l-coverage spectrum and the empty cell spectrum was found. The scattering angle corresponds to a momentum transfer near the "roton minimum". No background was subtracted. Arrows mark the values of the bulk roton (BR) energy [3] and the layer roton (LR) energy [3].

The first experiment on the DIN -2PI spectrometer with thin helium films shows the good performance of this spectrometer even without cold source. In particular the very low background is an absolute necessary feature to observe the very small signals.

## References

1. I.V.Bogoyavlenskii, A.V.Puchkov and A.Skomorokhov, «The association between temperature dependence of liquid  $^4\text{He}$  scattering law and the phenomena of the Bose condensation», *Physica*, B276 -278, 2000, p.465.
2. M.Chan, N.Mulders and J.Reppy, *Physics Today*, August 1996, p.30.
3. B.Clements, H.Godfrin, E.Krotscheck, H.J.Lauter, P.Leiderer, V.Passiouk, "Excitations in a thin liquid  $^4\text{He}$  film from inelastic neutron scattering", *Phys. Rev.*, B53, 1996, p.12242.
4. I.V.Bogoyavlenskii, A.V.Puchkov, A.N.Skomorokhov and S.V.Poupko, "Neutron scattering study of  $^4\text{He}$   $S(Q,\omega)$  at the phonon -maxon region", *Physica*, B234 -236, 1997, p.324.

# Quasielastic Scattering Investigation of Liquid Phosphorus Oxychloride POCl<sub>3</sub>

*A.G. Novikov, O.V. Sobolev<sup>1</sup>*

<sup>1</sup>*Frank Laboratory of Neutron Physics, Joint Institute for Nuclear Research, 141980, Dubna,  
Moscow Reg., Russia*

In the frame of neutron scattering experiments on liquid POCl<sub>3</sub> [1] we have measured and analysed the quasielastic component of its common double-differential scattering cross section (DDSCS). The detail description of the procedure and results of analysis will be published [2]. Now we give short information, concerning with these questions.

For separation of quasielastic component from the total DDSCS and its subsequent analysis the following procedures were performed:

- time-of-flight DDSCS were transformed into energy scale and then by interpolation into the form  $S(Q, \varepsilon)$  at  $Q = \text{const}$ , where  $S(Q, \varepsilon)$  is the scattering law (or dynamic scattering function) and  $\varepsilon$  - energy transfer;
- from the total DDSCS the inelastic contribution was removed; it was shown by calculations and practically [3,4], that for  $S(Q, \varepsilon)$  in the vicinity of quasielastic peak the inelastic contribution can be considered as a flattened background with relatively small amplitude, so the approximation appropriate for  $S(Q, \varepsilon)$  can be written:

$$S(Q, \varepsilon) = \{S_q(Q, \varepsilon) + [a + b\varepsilon]\} \otimes R(Q, \varepsilon) \quad (1)$$

where the expression in square brackets represents inelastic scattering effects and sign  $\otimes$  means the convolution of natural scattering law with resolution of spectrometer  $R(Q, \varepsilon)$ , measured by special vanadium sample.

The shapes and halfwidths (full width at halfmaximum, FWHM) of quasielastic peaks arise from a number of effects, including coherent and incoherent scattering, translation and rotation components of diffusion motions (the detail expressions for DDSCS of quasielastic scattering on molecular liquids with mixed (coherent and incoherent) scattering are given in [5,6]). It turned out, that in our case some alleviation takes place, because according to results of [7] on peak widening of Rayleigh scattering effects of rotation diffusion in liquid POCl<sub>3</sub> are expected to be negligible. This conclusion can be conformed by the estimation of rotation diffusion coefficient in liquid POCl<sub>3</sub> on the basis of Einstein – Stokes law for rotation motion [8]:

$$D = kT/8\pi\eta R^3 \quad (2)$$

Substituting in (2) viscosity (for room temperature  $\eta = 1.06$  cP [9]) and effective radius of POCl<sub>3</sub> molecule ( $R_{\text{eff}} \approx 3$  Å), we find:  $D_{\text{rot}} \approx 1.3 \cdot 10^{10} \text{ c}^{-1}$  and

$$\Delta E_{\text{rot}} = 2D_{\text{rot}} \cdot h \sim 0.02 \text{ meV}.$$

Keeping in mind the resolution of our spectrometer for elastic scattering ( $\Delta E_0 \sim 0.1 \div 0.13$  meV), we are led to conclusion, that these effects can not be observed under our experimental conditions. So, the later analysis of experimental quasielastic DDSCS will be performed under assumption, that we deal only with effects of translation

diffusion. In so doing, we have supposed, the quasielastic peaks are superposition of two components, hypotically corresponding to coherent and incoherent contributions:

$$S_q(Q, \varepsilon) = \{1/\pi \sum_{i=1,2} c_i(Q) \Delta E_i(Q) / (\varepsilon^2 + \Delta E_i^2)\} \otimes R(Q, \varepsilon), \quad (3)$$

with their own Q-depended weights and halfwidths  $c_i(Q)$ ,  $\Delta E_i(Q)$ , which are shown on Fig. 1 and 2. The common integral intensity of quasielastic scattering (the sum of coherent and incoherent contributions:  $c_1(Q) + c_2(Q) = \int_{-\infty}^{\infty} S_q(Q, \varepsilon) d\varepsilon$ ) is not far from diffraction results [1].

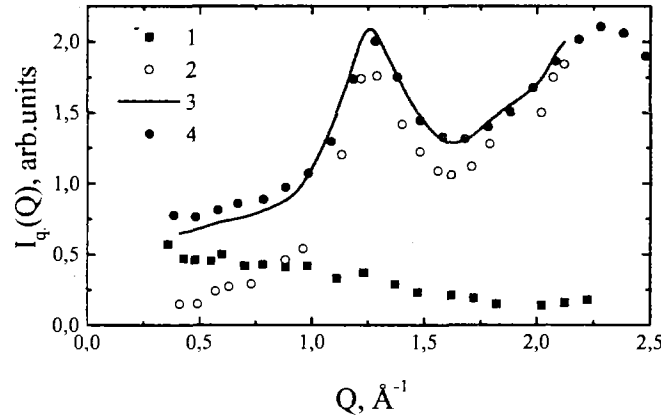


Fig. 1. Integral intensity of quasielastic scattering.

1 – incoherent component; 2 – coherent component; 3 – sum of coherent and incoherent components; 4 – angular differential scattering cross section (diffraction experiment, see [1])

The curve 1 of Fig.1 gives the integral intensity of incoherent quasielastic scattering, which can be expressed as [10]:

$$S_q(Q) \sim \sum_s / 4\pi \exp\{-u^2 Q^2\}, \quad (4)$$

where  $W = u^2 Q^2$  is Debye - Waller factor and  $u^2$  - mean - square amplitude of molecular vibration, inferred from analysis of this curve, is  $(u^2)^{1/2} = (0.55 \pm 0.05) \text{ \AA}$ .

Now draw our attention to Fig. 2. Curve 1 corresponds to the common halfwidth of quasielastic peak (in one-Lorentzian representation). The main contribution in the intensity of this peak arises from coherent scattering, so, its halfwidth demonstrates some evidence of oscillatory behaviour, being distinctive feature of coherently scattering liquids [11] (its first minimum coincides with the position of the first structure factor maximum,  $Q \sim (1.2 - 1.3) \text{ \AA}^{-1}$ , see [1]). We did not try to describe this curve by Scold model [12], because it contains a remarkable portion of incoherent scattering. Curve 2 of Fig.2 shows the halfwidth of incoherent quasielastic peak (two-Lorentzian representation). In small Q-region curves 1 and 2 are near each other (coherent effects are weak), but then they come apart, and curve 2 tends to flatten, what is commonly understood, as an evidence of jump diffusion process, which is distinctive for highly associated liquids. Fitting curve 2 by mixed diffusion model [13], assuming the diffusion process to be superposition of two mechanisms: continuous and jump ones, we get parameters of model: common selfdiffusion coefficient  $D$ , coefficient of collective

diffusion (diffusion of particle together with nearest surrounding)  $D_0$  and the residence time of molecule at the temporary equilibrium position  $\tau_0$ :

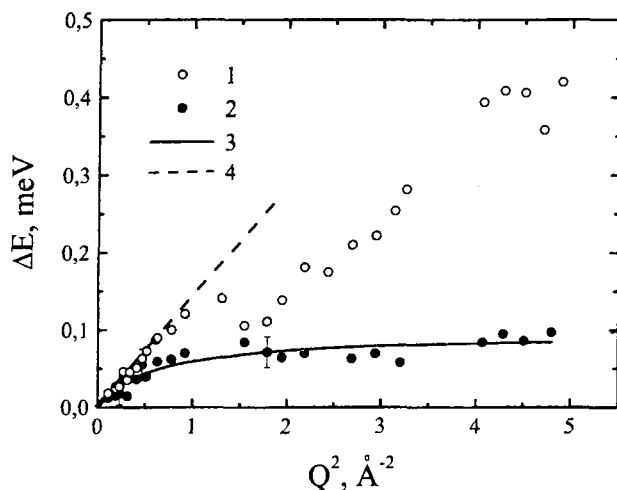


Fig. 2. Halfwidths of quasielastic peaks.

1 – common halfwidth of quasielastic peak (one – Lorentzian description); 2 – halfwidth of incoherent component of quasielastic peak; 3 – description of incoherent quasielastic peak halfwidth with the model of mixed diffusion.

$$D = (2.3 \pm 0.8) \text{ cm}^2/\text{c};$$

$$D_0 \sim 0.02 \text{ cm}^2/\text{c};$$

$$\tau_0 = (7 \pm 1) \cdot 10^{-12} \text{ c.}$$

The work was performed under financial support of Russian Federation Program “Actual Directions in Condensed Matter Physics”, project “Neutron studies”.

## References

1. A.Novikov, D.Seliverstov, O.Sobolev. Annual Reportn of FLNP, JINR, Dubna, 1999, p. 89-90.
2. A.Novikov, O.Sobolev. J. of Mol. Liquids. (in press).
3. S.Iskanderov, A.Novikov. Rus. J. Phys. Chem., v.56, 1982, p.1469.
4. A.G.Novikov, M.N.Ivanovskii, V.V.Savostin, A.L.Shimkevich, O.V.Sobolev, M.V.Zaezjev. J. Phys.: Cond. Matter., 8, 1996, p.3525.
5. F.Bermejo, F.Batallant, E.Enciso, R.White, A.Dianoux, W.Howells. J. Phys.: Cond. Matt., 2, 1990, p.1301.
6. F.Bermejo, M.Alvarez, M.Garcia-Hernandez at al. J. Phys.: Cond. Matt., 3, 1991, p.851.
7. R.Pappalardo, A.Lempicki. J. Appl. Phys., v.43, 1972, p.1699.
8. G.Sposito. J. Chem. Phys., v.74, 1981, p.6943.
9. K.C.Krasnov. Molecular constants of inorganic compounds. Leningrad, “Nauka”, 1977, 448 p., (in russian).
10. I.Gurevich, L.Tarasov. Low-energy neutron physics. North-Holland, Amsterdam, 1968, 608 p.
11. J.Copley, S.Lovesey. The Dynamic Properties of Monatomic Liquids. Rep. Prog. Phys., v.38, 1985, p.461.
12. K.Skold. Phys. Rev. Lett., v.19, 1967, p.1023.
13. V.Oskotskii. Sov. Phys. Solid State. 5 (1963) 789.

# Inelastic Neutron Scattering and Hydration Kinetics in Aqueous Solutions

*A.G. Novikov, M.N. Rodnikova<sup>1</sup>, O.V. Sobolev<sup>2</sup>*

<sup>1</sup>*Kurnakov Institute of General and Inorganic Chemistry RAS, 117907, Moscow, Russia*

<sup>2</sup>*Frank Laboratory of Neutron Physics, JINR, 141980, Dubna, Moscow reg., Russia*

It is well known, that slow neutron scattering is an effective and adequate instrument for investigation of molecular structure and microdynamics in aqueous solutions. Last years we have performed a number of inelastic (including quasielastic) neutron scattering experiments, aimed to clarify an influence of solutes on microdynamics of water molecules in ionic (LiCl, CsCl, [1]) and hydrophobic ((CH<sub>3</sub>)<sub>4</sub>NCl, (C<sub>4</sub>H<sub>9</sub>)<sub>4</sub>NCl, (C<sub>6</sub>H<sub>5</sub>)<sub>4</sub>PCl, [2,3]) aqueous solutions. From results of these experiments the information about diffusion processes (coefficients of self- and collective diffusion, residence times of molecules, static and dynamic hydration numbers) and vibration-rotation dynamics (in the form of generalized frequency distribution, GFD) for water molecules, incorporated in hydration shells was extracted. Basing on these data the comparative analysis of ionic and hydrophobic hydration effects was performed with the conclusion, that the ionic hydration destroys the hydrogen bond network in surrounding water, and conversely hydrophobic one retains it to be untouched.

The dynamical information, above mentioned, corresponds to the equilibrium state of solutions under study. But for chemical kinetics it is more important to understand a way, which proceed transition processes in solutions, when a disturbance of equilibrium takes place, for example, by instant appearance of a charge on one of solute and to be able to describe the time-space picture of transition from old equilibrium state of a solution to new one. This problem, known in contemporary literature as “fast hydration dynamics” (FHD) takes last decade much attention and is under intensive investigation experimentally [4], theoretically [5] and by molecular dynamics (MD) simulation [6]. The frequently used characteristic for description of the transition processes mentioned is called as time correlation function of hydration energy  $S(t)$ . At present there are some theories, dealing with FHD, which give the relation between  $S(t)$  and GFD  $g(\omega)$  of hydration water molecules. In particular (see [5]):

$$S(t) = 1 - kT \langle (\delta V)^2 \rangle^{-1} \int \frac{d\omega g(\omega)(1 - \cos(\omega t))}{\omega^2} \quad (1)$$

where  $(\delta V)^2 = kT(1-1/\epsilon)/a$  – mean-square fluctuations of interaction potential and  $a$  – radius of sphere beyond which ranges the solution can be considered as structureless continuum with dielectric constant  $\epsilon$ .

Our first attempt to use this relation in combination with GFD for water molecules, obtained by us, demonstrates the qualitative agreement between experimental and calculated (by MD and theory)  $S(t)$  curves (see fig. 1). So, there are grounds to believe, the inelastic neutron scattering method among with information about the equilibrium microdynamics of aqueous solutions can be applied for investigation of transition processes, associated with fast hydration dynamics.

The work was performed under financial support of Russian Federation Program “Actual Directions in Condensed Matter Physics”, project “Neutron studies”.

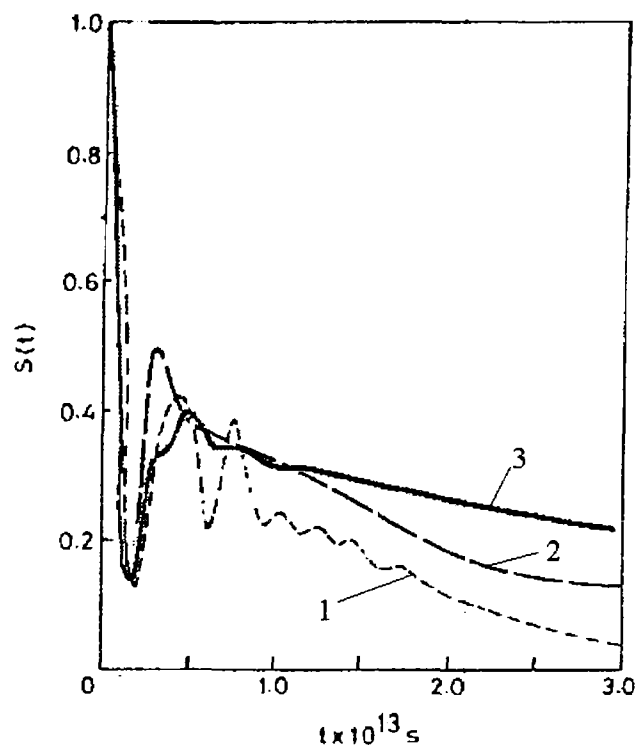


Fig.1. Time correlation function of hydration energy  $S(t)$ :

- 1 – MD simulation [6];
- 2 – theoretical calculation [5];
- 3 – calculation by equation (1) with the use of the experimental  $g(\omega)$

#### References

1. A.Novikov, M.Rodnikova, O.Sobolev. *J. Mol. Liquids.* 82, 83, (1999).
2. A.G.Novikov, M.N.Rodnikova, V.V.Savostin, O.V.Sobolev. *Chem. Phys. Letters.* 259, 391, (1996)
3. A.Novikov, M.Rodnikova, J.Barthel, O.Sjbolev. *J. Mol. Liquids.* 79, 203, (1999).
4. S.Rosenthal, X.Xie, M.Du, G.Fleming. *J. Chem. Phys.* 95, 4715, (1991).
5. R. Stratt, M.Cho. *J. Chem. Phys.* 100, 6700, (1994).
6. M.Maroncelli, G.Fleming. *J.Chem. Phys.* 89, 5044, (1988).

# Phonons in Coarse Grained and Plastically Deformed Vanadium

*S. Danilkin, M. Jung<sup>1</sup>, H. Wipf<sup>1</sup>*

<sup>1</sup> *Technische Universitat Darmstadt, D-64289 Darmstadt, Germany*

Aim of the study was to observe changes in the vibrational density of states ( $g(\varepsilon)$ ) of vanadium due to deviations from perfect crystalline order. We investigated differences in the  $g(\varepsilon)$  between plastically deformed and well-annealed vanadium. Vanadium is most suitable material for measurements of  $g(\varepsilon)$  because it scatters neutrons nearly exclusively incoherently.

The measurements were done with DIN-2PI spectrometer at incident energy of neutrons 10 meV in scattering angle range of  $70 \div 130^\circ$ . Samples were vanadium plate of 1 mm thickness and the same material after the cold deformation (90 %). The second sample consisted of 10 plates to have the same total thickness as the annealed vanadium sample. The time-of-flight spectra of two vanadium samples normalised by the area of the elastic peak are shown in Fig. 1. The spectrum of the deformed vanadium has higher intensity in the low energy region at  $\varepsilon \approx 4$  meV.

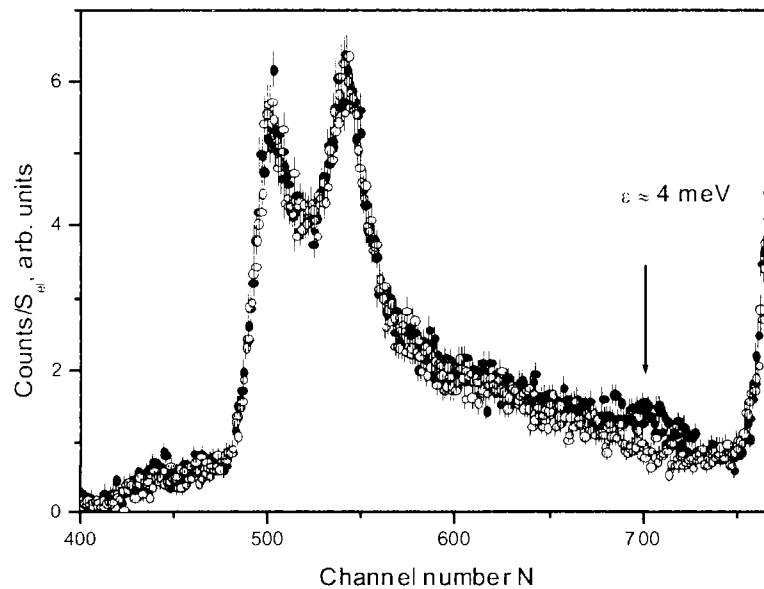


Fig. 1. INS spectrum of deformed (●) and annealed (○) vanadium

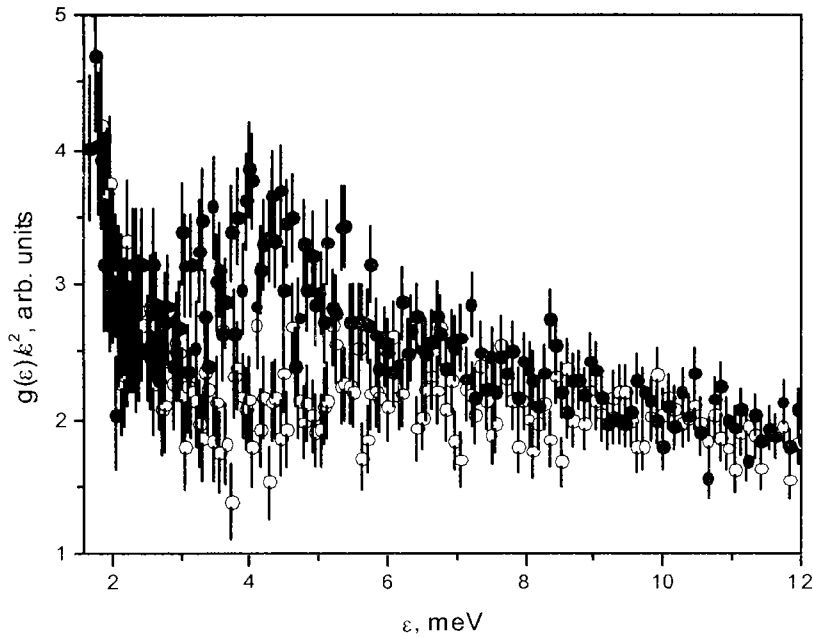


Fig. 2. Function  $g(\varepsilon)/\varepsilon$  of deformed (●) and annealed (?) vanadium

These additional modes are also seen in the  $g(\varepsilon)$  of deformed vanadium, but they are less pronounced there. To observe the deviation of  $g(\varepsilon)$  from the Debye spectrum the function  $g(\varepsilon)/\varepsilon^2$  was calculated for both samples (Fig. 2). This function for the annealed vanadium has a nearly linear behaviour in the energy range 2 ÷ 12 meV while that of deformed vanadium has a pronounced peak at  $\varepsilon \approx 4$  meV. At frequencies lower than 2 meV the increase of intensity is connected with contribution from the elastic line. The similar excess soft modes designated as the “boson peak” were observed earlier in different glasses and amorphous alloys [1]. INS study of austenitic steels showed that an enhancement of the low-frequency VDOS may also be induced by cold plastic deformation - the distinct increase of the VDOS in the low-frequency range between 8 and 16 meV was observed after cold plastic deformation (70%) in Fe-18Cr-10Mn-16Ni-0.5N alloy [2]. Also these changes are in fact very similar to those found for nanocrystalline materials [3, 4] demonstrated recently that the low-frequency increase of the  $g(\varepsilon)$  results predominantly from atoms in or at grain boundaries or surfaces.

### References

1. A. Meyer, J. Wuttke et al., Phys. Rev. B, 53, 12107 (1996).
2. S. Danilkin, V. Minaev, V. Sumin: Preprint No. FEI -2371, 1994, IPPE, Obninsk, Russia.
3. U. Stuhr, H. Wipf, K.H. Andersen, H. Hahn, Phys. Rev. Lett. 81, 1449 (1998).
4. A. Kara, T. Rahman, Phys. Rev. Lett. 81, 1453 (1998).

# Nonlinear Breather Vibrations of Crystals in Vicinity of Defect Generation Threshold

*O.A. Dubovsky, A.V. Orlov, V.A. Semenov*

Dynamics of nonlinear vibrations with high amplitude is investigated in present article for crystals of di-iron phosphide  $\text{Fe}_2\text{P}$  type in vicinity of defect generation threshold. A projection of unit cell of crystal  $\text{Fe}_2\text{P}$  with a space group  $P\bar{6}2m$  on a base plane  $ab$  is shown in Fig.1a [1]. Three nearest strongly interacting atoms Fe (big dark circles) in a base plane form trimer. Fe atoms in a neighboured planes (little dark circles), interacting with Fe in base plane, leads in a specific sense only to modification of mass for atoms in base plane. The existence of solitons of special type – so called intrinsic mode – was found earlier in Ref [2-9] for anharmonic crystals. In present work the analytic solution was found for system of nonlinear dynamic equations for crystallite with energy of vibrations intermediate between low energy vibrations of investigated by DIN spectrometer and that of defect migration investigated in material technology with using heuristic parameters like diffusion coefficient. It was found, that nonlinear resonance periodic vibrations (NRPV) in such crystallite, like FRIM solitons on interface [10-12], are of breather type with oscillating module  $\rho(\tau)$  and oscillating phase  $\varphi(\tau)$  of a system. NRPV of a breather type with closed multyrotational trajectory exist only with rational fractional changing of phase on a period of module vibration. Time dependence of phase  $\varphi(\tau)$  is shown in Fig. 1b

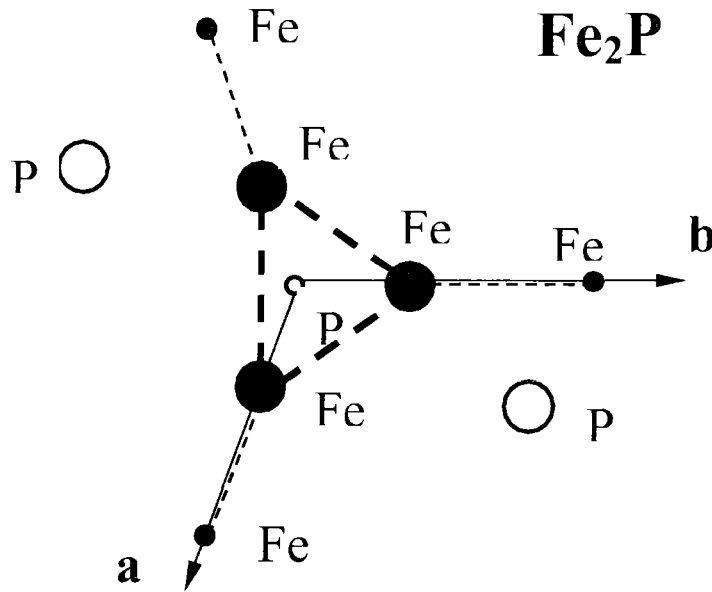


Fig.1a. A projection of unit cell of crystal  $\text{Fe}_2\text{P}$  on a base plane  $ab$ .

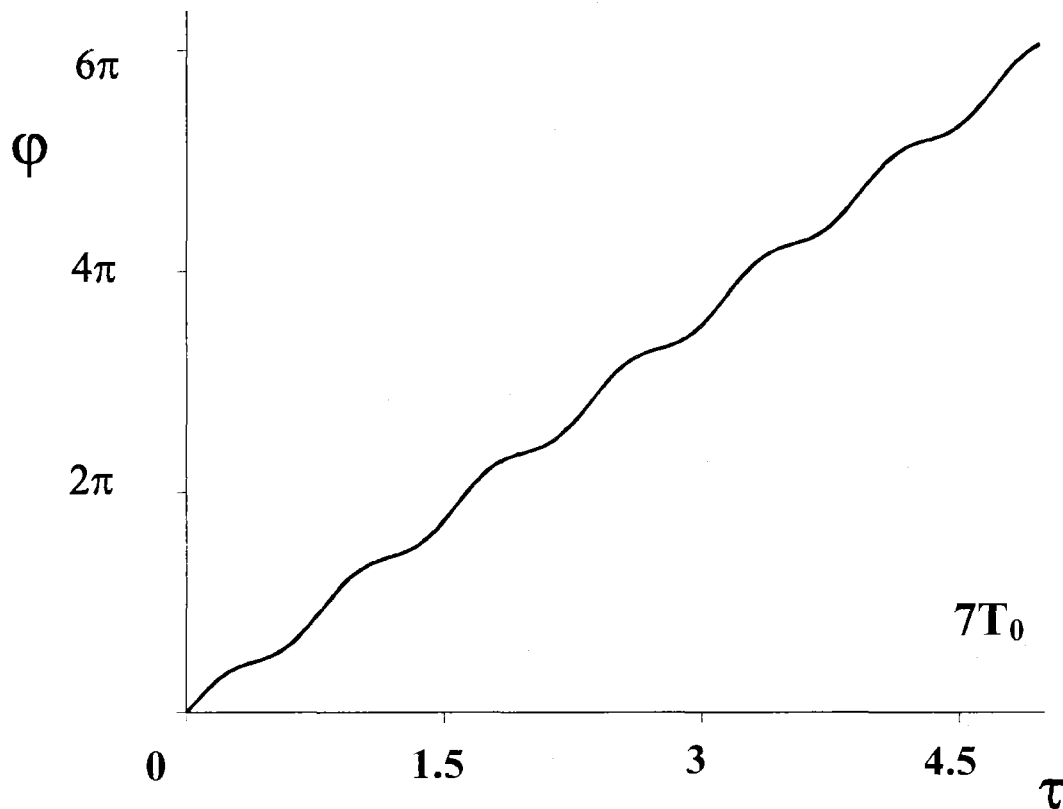


Fig.1b. Time dependence of phase  $\varphi(\tau)$

#### References

1. B.G.Hyde, S.Andersen. Inorganic crystal structure. A Willey -interscience publication, 1989.
2. A.M.Kosevich, A.S.Kovalev. JETP 67, 5(11), 1713 (1974).
3. A.J.Sievers, S.Takeno. Phys. Rev. Lett . 61, 8, 970 (1988).
4. S.Takeno, K.Kisoda, A.J.Sievers. Progr. Theor. Phys. Suppl . 94, 242, (1988).
5. V.M.Burlakov, S.A.Kiselev, V.N.Pyrkov. Phys. Rev . B42, 8, 4291 (1990).
6. V.M.Burlakov, S.A.Kiselev. JETP 99, 5, 1526 (1991).
7. J.B.Page. Phys. Rev. B41, 11, 7835 (1990).
8. A.S.Kovalev, O.V.Usatenko, O.A.Chubykalo. Fizika Tverdogo Tela 35, 3, 693 (1993).
9. O.A.Dubovsky, A.V.Orlov. Fizika Tverdogo Tela 36, 10, 3131 (1994).
10. O.A.Dubovsky, A.V.Orlov. Fizika Tverdogo Tela 38 , 4, 1221 (1996).
11. O.A.Dubovsky, A.V.Orlov. Fizika Tverdogo Tela 38 , 6, 1931 (1996).
12. O.A.Dubovsky. Fizika Tverdogo Tela 42 , 4, 665 (2000).

# Gap Kinematic Frenkel Biexcitons

*O.A. Dubovsky*

The aim of this article is search of possible position for Frenkel biexcitons in the region of two particle excitations and revealing of spectral peculiarities, allowing to identify experimentally these states. It was shown in Ref [1], that formation of bound kinematic Frenkel biexciton (BKFB) is possible in a crystals with few molecules in the unit cell due to Pauli type of Frenkel excitons. The dispersion equation for wave dependence of energy was received for BKFB in crystals of arbitrary symmetry [2]. The solution of this dispersion equation for crystals of specific symmetry reveals existence of gap kinematic Frenkel biexcitons (GKFB). The isolated terms of these biexcitons are found in the gap between components of Davydov multiplet for two-exciton unbound states. In the crystals with two monomers in unit cell these terms are in a gap between two low-frequency components of Davydov triplet. They have not resonance with central component band, that took place for previously investigated crystals of higher symmetry [1]. The found biexcitons, in contrast to previously investigated ones [1,3], have finite, nonzero dispersion. It is shown, that sign of effective mass of GKFB is oppose to sign of effective mass of one-particle states.

## References

1. O.A.Dubovsky. Fizika Tverdogo Tela 41, 3, 423 (1999).
2. O.A.Dubovsky. Fizika Tverdogo Tela 42, 3, 440 (2000).
3. V.M.Agranovich, O.A.Dubovsky, D.M.Basko, G.C.La Rocca, F.Bassani. Appl. Phys. Lett. (2000), in press.

# Breather Solitons of New Type at Fermi Resonance of Optic Vibrations in Crystals

*O.A. Dubovsky*

The nonlinear soliton excitations of principle new type are found [1]. This excitations exist at Fermi resonance of optical vibration in crystal in addition to found before solitons – multiexciton bound complexes of peak, crater and dark types with one base frequency, amplitude and envelope [2,3]. Found excitations have slow oscillating amplitude in some interval for base high frequency vibration. The frequency of this oscillating is multiple to frequency of high frequency vibration. The extent of oscillating determines in correspondence with multiplicity the series of main frequencies that condensate to base frequency of optical vibration. It is found space dependence of two envelopes for new solitons of peak type. The slope of space envelopes for soliton decreases with increased multiplicity. The radius of localization for excitations in soliton increases accordingly. The some distinctive features of new type solitons are noted.

## References

1. O.A.Dubovsky. Fizika Tverdogo Tela 42, 4, 665 (2000).
2. O.A.Dubovsky, A.V.Orlov. Fizika Tverdogo Tela 38, 4, 1221 (1996).
3. O.A.Dubovsky, A.V.Orlov. Fizika Tverdogo Tela 38, 6, 1931 (1996).
4. O.A.Dubovsky, A.V.Orlov. Fizika Tverdogo Tela 41, 4, 712 (1999).
5. O.A.Dubovsky, A.V.Orlov. Fizika Tverdogo Tela 36, 10, 3131 (1994).
6. V.M.Agranovich, J.J.Lalov. Uspehi Fizicheskikh Nauk, 146, 2, 267 (1985).
7. V.M.Agranovich, O.A.Dubovsky. Chem.Phys.Lett., 210, 4-6, 458 (1993).
8. V.M.Agranovich, O.A.Dubovsky, A.M.Kamchatnov. J.Phys.Chem. 98, 51, 13(1994)

## 2.6 MATHEMATICAL MODELING

### Numerical Simulation of Anomalous Doping Effect in *Ge* Single Crystals Grown by *FZ*-Technique Aboard the Space Crafts

*V.K. Artemiev, V.P. Ginkin, V.I. Folomeev,  
A.V. Kartavykh<sup>1</sup>, M.G. Milvidskii<sup>1</sup>, V.V. Rakov<sup>1</sup>*

<sup>1</sup>*The Institute for Chemical Problems in Microelectronics*

The goal of the present work was to develop a mathematical model and a numerical algorithm to solve the problem of convective heat-mass transfer under the influence of the surface tension force on the free surface of the melt. Using the developed model, an analysis was performed to study the interaction of the thermocapillar and concentrational convection in growing crystals of germanium by the floating zone technique under the space conditions.

On the basis of the proposed model, it appeared to be possible to explain the mechanism of suppression of thermocapillar convection through the development of concentrational-capillar convection resulting from the transfer of the impurity driven out of the crystal in the crystallization process. In case of low concentrations of the impurity, this suppression is not complete, as a result a strong radial nonuniformity in the distribution of the impurity is observed. In case of high doping levels, the effect of suppression reveals itself much more explicitly, which leads to the development of single vortex flow in the melt region, so the radial nonuniformity in the impurity distribution is reduced considerably.

The calculations showed that using a constant value of viscosity, it was impossible to explain the anomalous effect in the distribution of the impurity observed in the experiments on the growth of single crystals by the floating zone technique aboard the spacecrafts "FOTON" [1], [2]. It is only inclusion into the model of a temperature dependence of viscosity of the melt, which has an anomalous character near the crystallization temperature, that enabled us to reproduce in our calculations the observed anomalous effect not only qualitatively, but quantitatively.

0

#### References

1. A.V.Kartavykh, E.S.Kopeliovich, M.G.Mil'vidskii, V.V.Rakov // *J.Cryst.Growth*. 1999. V205. No4. P497.
2. A.V.Kartavykh, E.S.Kopeliovich, M.G.Mil'vidskii, V.V.Rakov // *Microgravity sci. & technol.* 1999. V12. No1. P16.

## **Development and Calibration of a Three-Dimensional Regional Hydrogeologic Model for the Mayak Site**

*C.R. Cole, K.A. Hoover, M.G. Foley, L.H. Gerhardstein,  
M.D. Williams, S.K. Wurstner,  
E.G. Drozhko, L.M. Samsonova, N.A. Vasil'kova, A.I. Zinin, G.A. Zinina*

This paper discusses a hydrogeologic model being developed through a joint Russian and U.S. study to quantify the hydrogeology of the Mayak territory, located in the southern Urals. Nuclear fuel cycle activities at the Mayak Site resulted in the contamination of soils and groundwater with chemical and radioactive wastes. A three-dimensional hydrogeologic model of the Mayak territory is being developed to investigate groundwater flow and contaminant transport to help address waste management issues and for subsequent use in forecasting and evaluating environmental restoration measures. Groundwater flow through the region was quantified using Coupled Fluid, Energy, and Solute Transport (CFEST) code, developed in the Pacific Northwest National Laboratory. Modeling results indicate that groundwater flow directions are controlled by rivers, lakes, and reservoirs, while flow velocities are more sensitive to spatial changes in hydraulic conductivity as a result of differential fracturing of the rocks.

# Crystallization Rate and Boundary Conditions Role for the Zone Method

*N.V. Gusev*

The floating zone method for crystal growth is considered numerically. For Ge crystal being pulled through a toroidal heater, the roles of phase change heat, boundary conditions, crystal's length to diameter ratio, heater's axial temperatures gradients are analyzed. Distributions along the crystal's axis of temperature, of liquid zone size and of its position relative to the heater are calculated for various parameters, using one dimensional conduction-radiation model and are compared with the stationary solution. Calculations show that for widely used growing rates less than 50mm/hour the process is practically stationary in the middle part of the crystal and is not influenced by butts cooling. On the contrary, the melt zone length temperatures and phase front position depend on the butts cooling- the effect observed experimentally and easily ascribed to the stopping of the heater at butts. Analyzed results show the possibilities of such approach for optimization of crystal growth process.

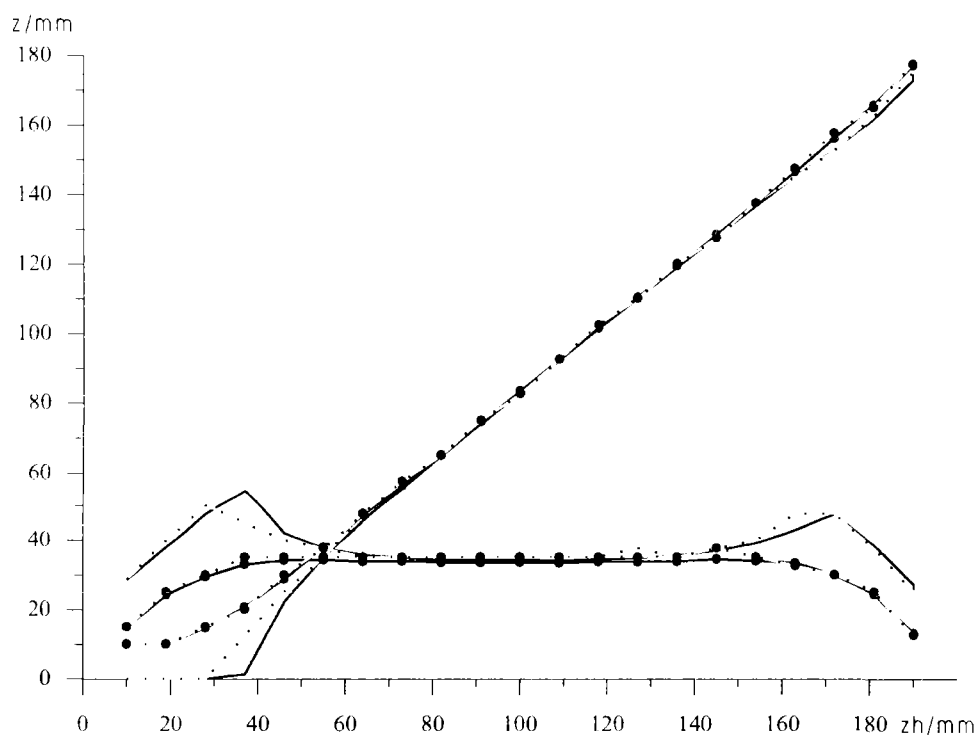


Fig. 1. The melt zone length and phase front place(diagonal curves) for various positions of the heater center. Crystal length  $L=200$ mm , Temperature gradient  $grTh=150$ K/cm, heater temperature  $Th=1450$ K, solid lines for rate of crystal movement  $V=18$  mm/hour, dotted lines for  $V=0$ , marked lines are for the five times increased butts cooling

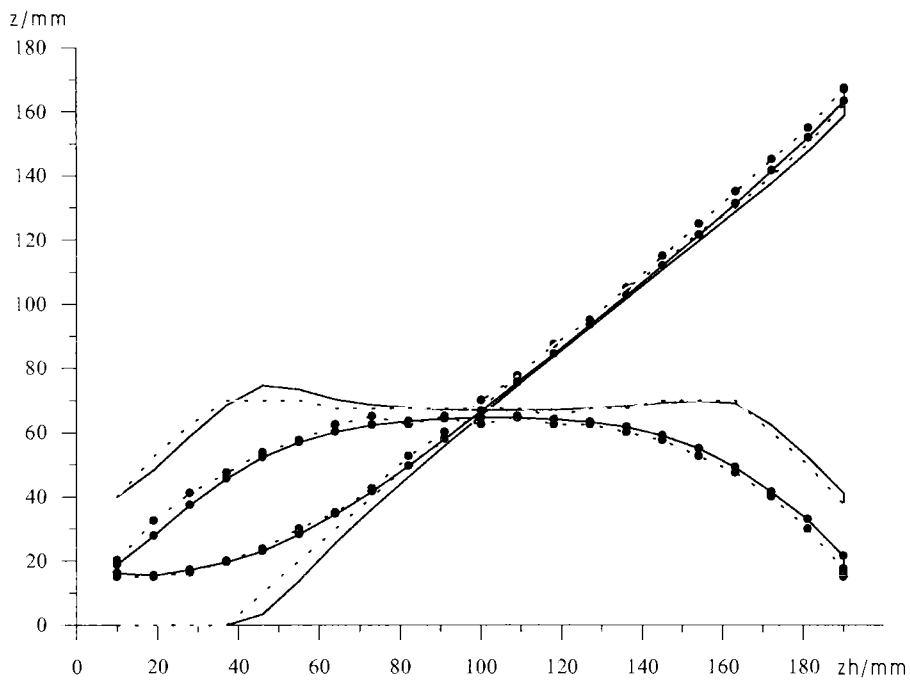


Fig. 2. The same parameters as in Fig. 1, but  $grTh=50K/cm$  and  $Th=1350K$

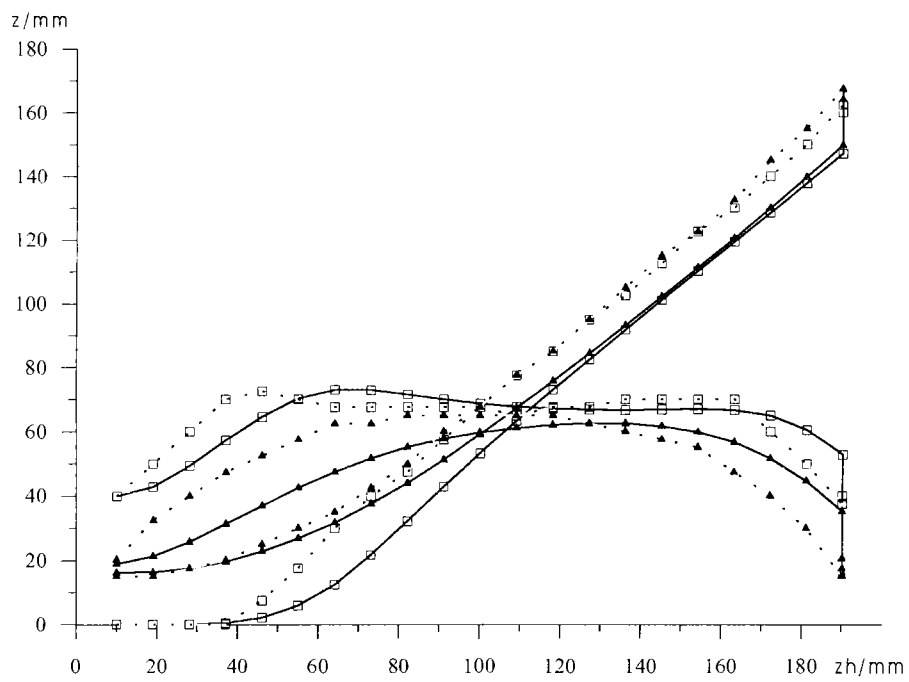


Fig. 3. Increased pulling rate  $V=90mm/hour$ ,  $L=200$   $grTh=50$   $Th=1350K$

### References

1. Физические величины. Справочник под ред. И.С.Григорьева и Е.З.Мейлихова. Москва: Энергоатомиздат, 1991.

# Molecular–Dynamics Studying the Cooperative Motion of Potassium Atoms in Liquid Mixture with Oxygen

*A.L. Shimkevich, I.Yu. Shimkevich*

The molecular–dynamics simulation is performed in the frame of NVE ensemble for investigating a cooperative motion of atoms in liquid potassium at the temperature of 550 K and oxygen effect on this motion in potassium melt.

Liquid potassium with oxygen is considered as the ternary system  $K+K^++O^{2-}$  when for neutrally potassium–oxygen system, only part of potassium particles are ionized in 2/1 ratio of oxygen anions in mixture.

The simulation runs are fulfilled on the same model used in calculation for liquid potassium [1–3] and potassium–oxygen alloy [4, 5] with MDMC code [3] in PC – PENTIUM and workstation “SUN – ULTRA”.

The MD–simulation is conducted on the model of 2000 particles in a cubic cell with periodic boundary conditions. The cube edge length for potassium,  $L = 55.08 \text{ \AA}$  and  $N_K = 2000$ ., For potassium–oxygen system,  $L = 54.004 \text{ \AA}$ , we have  $N_K = 1490$ ,  $N_{K^+} = 340$  and  $N_{O^{2-}} = 170$ , according to the oxide mass density,  $\rho_{K_2O} = 2320 \text{ kg}\cdot\text{m}^{-3}$ , at the given oxygen concentration of 8.5% at for unsaturated solution at 550 K [6] and the mass density of liquid potassium,  $\rho_K = 777 \text{ kg}\cdot\text{m}^{-3}$ . The motion equations are solved on Verlet’s algorithm with the time step of  $\Delta t = 1.0 \cdot 10^{-15} \text{ s}$ .

Pair potentials for describing the interaction between atoms are selected the same as in paper [5]. The potentials for neutral potassium atoms (K,K), the neutral atom and an ion (K,K<sup>+</sup>) are evaluated for treating the electron–ion coupling in the frame of the pseudo–potential concept with  $R_c = 1.1854 \text{ \AA}$  and  $\nu = 1.8253 / 4$ . Born–Mayer’s potential without dispersion terms is used for describing (K<sup>+</sup>,K<sup>+</sup>), (K<sup>+</sup>,O<sup>-</sup>), (O<sup>-</sup>,O<sup>-</sup>) and (K,O<sup>-</sup>) interaction with ion charges:  $Z_{O^{2-}} = -2$ ,  $Z_{K^+} = 1$ .

The minimum cut-off for all the potentials is  $R_{min} = 0.82 \text{ \AA}$ . The upper one is  $R_{max} = 10 \text{ \AA}$  for the potentials of  $U_{KK}$ ,  $U_{KK^+}$  and  $R_{max} = 6 \text{ \AA}$  for the potential of  $U_{KO^{2-}}$ . For  $U_{K^+O^{2-}}$ ,  $U_{K^+K^+}$ , and  $U_{O^{2-}O^{2-}}$ ,  $R_{max}$  is chosen equal to the half of cube edge,  $R_{max} = 25 \text{ \AA}$ .

For each particle, its geometrical neighbours into Verlet’s sphere (of the radius equal to  $R_{max} + 1 \text{ \AA}$ ) are recalculated over 10 time steps.

The potassium–oxygen system is simulated in the condition of charge exchange between each potassium ion and a nearest potassium atom in given time step /5/. The realizing the charge exchange, the system is relaxed to equilibrium. Then for studying the cooperation of atom motion, such the characteristics as a mean–square atoms displacement,  $\langle [r_\alpha(t)]^2 \rangle$ , a velocity auto–correlation function,  $Z_{\alpha\beta}(t)$ , self–diffusion coefficients,  $D_{\alpha\beta}$ , and a density autocorrelation function van Hove,  $G_d^{\alpha\beta}(\vec{r}, t)$ , are calculated. The auto–correlation velocity function,  $Z_{\alpha\beta}(t)$ , is calculated in the time interval of  $\Delta T = 10 \text{ ps}$  for clean potassium and  $\Delta T = 2 \text{ ps}$  for its alloy with oxygen.

In table followed, the mean–square asymptotic is  $6Dt + C$ , which is over 0.35 ps for clean potassium and its alloy with oxygen. It is confirmed by the values of self–diffusion coefficients (see Table).

**Comparison of potassium characteristics in two systems ( $T = 550$  K)**

Melt		Clean potassium	potassium–oxygen
Correlation functions		KK	KK
Time of damping the first coordination sphere, ps		3.0	5.0
Asymptotic of $\langle r^2(t) \rangle$ , ps		$> 0.35$	$> 0.35$
The time of sign changing of function $Z(t)$ , ps		0.21	0.24
Self-diffusion	$D_{Z(t)}$	13.8	12.3
$D, 10^{-5} \cdot \text{cm}^2/\text{s}$	$D_{\langle r^2(t) \rangle}$	12.5	11.6

The configuration of nearest potassium neighbours almost disappears in time,  $t \approx 3$  ps, for clean potassium, but it is placed in the alloy with oxygen for the first coordination sphere (see Figure). Van Hove function for system with oxygen demonstrate more long space cooperation of atomic configurations.

It reflects the clusters character of diffusion migration of potassium atoms, when chaotic particle displacement accomplish together with their nearest surrounding.

Thus, we can conclude that oxygen impurity in potassium too much influenced at the space correlation of cooperation motion of metal atoms.

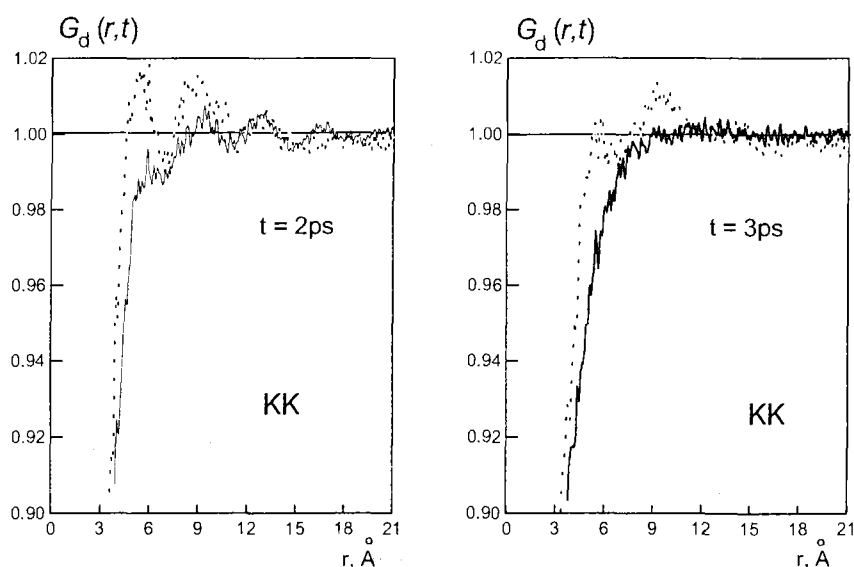


Fig. Van Hove function of clean potassium (solid line) and potassium in potassium–oxygen system (dashed line) in  $t = 2$  ps and 3 ps

### References

1. V.V.Kuzin, V.A.Morozov, A.L.Shimkevich, I.Yu.Shimkevich. // Preprint IPPE – 2415, Obninsk, 1994.
2. I.Yu.Shimkevich, A.G.Novikov, V.V.Savostin, A.L.Shimkevich. Structure and Dynamic Properties of MD-model of Liquid Potassium // Preprint IPPE – 2437, Obninsk, 1995.
3. I.Yu.Shimkevich, A.L.Shimkevich. MDMC (Molecular -Dynamics and Monte -Carlo) Software to Study Crystalline and Irregular Systems // Preprint IPPE – 2524, Obninsk, 1996.

4. I.Yu.Shimkevich, A.L.Shimkevich, V.V.Kuzin. Molecular Dynamics Study of Ternary System,  $K+K^q+O^{-2q}$  // Condensed Matter Physics, 1999, Vol.2, No.2(18), P.329-337.
5. I.Yu.Shimkevich, V.V.Kuzin, A.L. Shimkevich. Dynamic Structure of Oxygen in Liquid Potassium Studied by MD Method and Statistical Geometry // Journal of Non-Crystalline Solids, 1999, Vol.250-252, P.129-134.
6. M.N.Ivanovsky, A.G.Novikov, V.V.Savostin, A.L.Shimkevich, M.V.Zaezjev. High Temperature, Vol.32, No.5, 1994, P.701.

# The Eutectic–Alloy PbK (9% at.) Microstructure and Atomic–Dynamics Studied by Methods of Molecular Dynamics and Statistical Geometry

*A.L. Shimkevich, I.Yu. Shimkevich*

Results of molecular–dynamics studying the influence of potassium in liquid lead at temperature of 870 K are presented [1]. The investigation of structural and dynamic characteristics of  $Pb_{0.91}K_{0.09}$  is carried out on the model when a part of lead particles is ionized in putting potassium ions in mixture. Molecular–dynamics simulation is performed in frame of NVE ensemble in the cubic cell with periodic boundary conditions. MD–simulation of liquid lead at 870 K is fulfilled on the model of  $N = 2048$  particles in the cube cell with an edge length,  $L = 40.847 \text{ \AA}$ , according to the mass density,  $\rho_{Pb} = 10339 \text{ kg}\cdot\text{m}^{-3}$ . MD–simulation of system  $Pb_{0.91}K_{0.09}$  is fulfilled on the model of  $N = 2251$  particles including neutral lead atoms of  $N_{Pb} = 1845$  and the number of lead anion equal to the number of potassium cations,  $N_{Pb^-} = N_{K^+} = 203$ . The MD–cell of system  $Pb_{0.91}K_{0.09}$  with an edge length,  $L = 44.776 \text{ \AA}$  ( $N = 2251$ ), is selected according to the eutectic–alloy mass density,  $\rho_{PbK(9\%)} = 9189.9 \text{ kg}\cdot\text{m}^{-3}$ .

Such the characteristics as a partial radial distribution functions,  $g_{\alpha\beta}(r)$ , a static structure factors,  $S_{\alpha\beta}(q)$ , a mean–square atoms displacement,  $\langle [r_{\alpha}(t)]^2 \rangle$ , a velocity auto-correlation functions,  $Z_{\alpha}(t)$ , a frequency spectrum,  $Z_{\alpha}(\omega)$ , and self–diffusion coefficients,  $D_{\alpha\beta}$ , are examined in comparison with clean lead and its alloy with potassium.

The additional analysis of an atomic alloy configuration is performed upon the basic of Voronoi–Delaunay division of space into polyhedral.

The numerical experiments are fulfilled with MDMC code [2] in the same concept for exchanging the charges of ions as is used for simulating potassium alloy with oxygen [3] in PC – PENTIUM and workstation “SUN – ULTRA”.

The potentials for neutral lead atoms (Pb,Pb), neutral atom and ion (Pb,Pb<sup>+</sup>) are evaluated as [4]. Born-Mayer-Huggin’s potential without dispersion terms [3,5] is used for describing (Pb<sup>-</sup>,Pb<sup>-</sup>), (K<sup>+</sup>,K<sup>+</sup>), (Pb<sup>-</sup>,K<sup>+</sup>) and (Pb,K<sup>+</sup>) interaction with ion charges:  $Z_{Pb^-} = -1$ ,  $Z_{K^+} = 1$ . The parameters of that potentials are the same as recommended for system PbK [5]. The upper cut-off for the potentials is  $R_{max} = 15.5 \text{ \AA}$  for the potentials of  $U_{PbPb}$ ,  $U_{PbPb^-}$  and  $R_{max} = 7 \text{ \AA}$  for the potential,  $U_{PbK^+}$ . For  $U_{Pb^-Pb^-}$ ,  $U_{K^+K^+}$ , and  $U_{Pb^-K^+}$ ,  $R_{max}$  is chosen equal to the half of cube edge,  $R_{max} = L/2 \text{ \AA}$ .

The data of height and position of two peaks, and the first minimum of pair correlation functions are given in Table1, the data of self–diffusion coefficients are in Table 2. One can see that inclusion of potassium atoms in liquid lead does not change the liquid structure but has strength effect on motion of lead atoms.

Table 1

**Height, position of two peaks and first minimum of RDF,  
coordination numbers for models**

<i>RDF</i>	N	<i>t</i> , пс	$g_{\max_1}$	$r_{\max_1}$ , Å	$r_{\min_1}$ , Å	$g_{\max_2}$	$r_{\max_2}$ , Å	$N_z$
<b>Clean lead</b>	2048	65	2.69	3.30	4.80	1.23	6.40	13.4
Eutectic-alloy <i>Pb</i> <sub>0.91</sub> <i>K</i> <sub>0.09</sub>	2251	134						
PbPb			3.26	3.25	4.70	1.28	6.25	10.9
PbPb <sup>-</sup>			1.89	3.30	4.65	1.09	6.35	0.80
PbK <sup>+</sup>			2.11	4.00	5.35	1.27	6.80	1.29
Pb <sup>-</sup> K <sup>+</sup>			14.0	3.60	5.30	1.50	7.35	3.83
K <sup>+</sup> K <sup>+</sup>			2.17	4.00	5.75	2.40	6.90	2.94
Pb <sup>-</sup> Pb <sup>-</sup>			2.91	5.60	8.20	1.21	10.70	6.98

Table 2

**Coefficient of self-diffusion  $D$ ,  $10^{-5}$ , cm<sup>2</sup>/s and position of  
the maximum normalized spectrum  $Z_a^n(\varepsilon)$**

<i>Clean Pb</i>	$D_{\langle r^2(t) \rangle}$	$D_{Z(\omega=0)}$	$D_{Z(t)}$	<i>Clean Pb</i>	$\varepsilon_{\max}$ [meV]
$D_{Pb^{\cdot}}$	3.457	3.357	3.359		2.274
<i>Pb</i> <sub>0.91</sub> <i>K</i> <sub>0.09</sub>				<i>Pb</i> <sub>0.91</sub> <i>K</i> <sub>0.09</sub>	
$D_{Pb}$	1.589	1.677	1.584	$\varepsilon_{\max}^{Pb}$	4.342
$D_{Pb^-}$	0.284	0.431	0.333	$\varepsilon_{\max}^{Pb^-}$	6.409
$D_{K^+}$	0.314	0.297	-0.073	$\varepsilon_{\max}^{K^+}$	22.12

### References

1. V.A.Blokhin, M.N.Ivanovsky, T.A.Kuvshinchikova, V.V.Kuzin, N.I.Loginov, V.A.Morozov, A.G.Novikov, S.S.Pletenets, V.V.Savostin, A.L.Shimkevich, I.Yu.Shimkevich, B.A.Shmatko. Structure, Atomic Dynamics, Thermodynamics, and Impurity Condition of Lead and Bismuth Melts // Moskow, CRI Atominform, IPPE-0290, 1999, p.1-77 (in Russian).
2. I.Yu.Shimkevich, A.L.Shimkevich. MDMC (Molecular-Dynamics and Monte-Carlo) Software to Study Crystalline and Irregular Systems // Preprint IPPE-2524, Obninsk, 1996.
3. I.Yu.Shimkevich, V.V.Kuzin, A.L.Shimkevich. Dynamic Structure of Oxygen in Liquid Potassium Studied by MD Method and Statistical Geometry // Journal of Non-Crystalline Solids, 1999, v.250-252, p.129-134.
4. M.Dzugutov, K.-E.Larsson, I.Ebbsjö. Pair Potential in Liquid Lead // Phys. Rev. A, 1988, v.38, No.7, p.3609-3617.
5. H.T.J.Reijers, W. van der Lugt, Marie-Louise Saboungi. Molecular-dynamics study of liquid NaPb, KPb, RbPb, and CsPb alloys // Phys. Rev. B, 1990-II, v.42, No.6, p.3395-3405.

# **Development of the 1D Drift Flux Model of Non-Equilibrium Two-Phase Flow in Simple and Sub-Channel Geometry for Accident Analysis of NPP Regimes**

*Y.N. Kornienko*

One dimensional mathematical models are extensively used in thermohydraulics assessment of Nuclear Power Plant (NPP) accident conditions. Because, specifically 1D system of the conservation laws allow to significantly reduce needed computer time and space, especially for "best estimate" code calculations. On the example of drift flux model it is proposed the closure strategy of 1D models of conservation laws and closure relationships for NPP two-phase thermohydraulics needed for development and verification of the best estimated codes.

This approach is generalization of the known Zuber-Findley and Hancox-Nicoll methods for two-phase flow distribution parameters  $C_s$  with taking into account of the non-monotone void fraction distribution in transversal direction in the terms of two superimposed monotone profiles. It is very useful for assessment of the saddle-shape void fraction profile effects. The two-phase flow distribution parameters  $C_s$  were developed as for simple (circular and flat) pipe) and sub-channel geometry. The basic assumptions were power-mode approximations for describing of the profiles local volume flux density, phase velocity and temperature. The general analytical (quadrature) relationships for  $C_s$  were obtained and their 3D illustrations were done.

Also, there were proposed the generalized formulation and simple approach for construction of the friction factor, heat and mass transfer coefficients within the gradient hypothesis and boundary layer assumptions. The contribution of momentum, heat and mass transfer as well as their sources (and sinks) in the channel cross-section were taken into account. These friction factor, heat and mass transfer coefficients with taking into account of transversal and azimuthal variations were obtained for subchannel geometry as well.

## 2.7 APPLIED RESEARCH

### Features of Gas Flow Through Porous Structure of Reactor Track Membranes

*A.A. Tumanov, S.A. Kosarev*

Feature of a reactor way of effecting track membranes is the stability and reliable control of conditions of irradiation of a film by the fission fragments. Therefore value of density of pores for membranes is known with good accuracy. Thus, there is a capability, measuring stream of air through TM, to determine value of diameter of pores. However realization of measurements  $dV/dt$  at pressure about 1 atmosphere is suitable for definition only of small values of diameters ( $d < 0.1$  microns). Definition of pore size in more broad interval demands realization of measurements of passing of air through TM on the plant working at pressure, smaller atmospheric (under atmospheric attenuation).

The experiments were conducted with PET-film by depth 8 microns, irradiated by the fission fragments on the reactor with a fluence  $1.6 \cdot 10^8 \text{ cm}^{-2}$ . Etching membranes model chosen from all linen of a lot of a film, was conducted in the course of time from 40 to 180 seconds in a working bosh of the technological line, filled solution NaOH 3.6 N,  $75^\circ\text{C}$ . The flow measurements of air  $(dV/dt)_E$  for each time of etching were conducted on several membrane's models and by several times, including at different air pressures. The errors of observed data are within the limits of 10%. The average value of the obtained observed data are showing in the Table 1. The diameters of pores on considered films of "line" were determined by a method of a point of a bubble ( $d_B$ ), beginning with diameter 0.07-0.08 microns. The diameter's value is less than this value (are showing in the table with sprockets) was by a linear extrapolation on time of etching. Besides the measurements of diameters of pores with the help of electronic microscope were conducted and these values also are showing in the Table 1.

The nature of flow of gas through channels can be sectioned into three types, using for ratings of a flow regime by value of parameter of Knudsen ( $L/r$ ):

- 1)  $(L/r) < 10^{-2}$ , a viscous flow regime (v), ( $d = 2r > 13$  microns).
- 2)  $(L/r) > 1$ , a molecular mode (m), ( $d < 0,13$  microns).
- 3)  $10^{-2} < (L/r) < 1$ , a combination drive of flow (c).

Where:  $L$  a free length of a molecule of air,  $r$  - radius of a channel. At normal conditions for air  $L \approx 0.067$  microns, ratings of diameters of channels indicated in brackets for each type of a flow regime of air from here are made also.

By the obtained experimental results of an air flow by conformity to model of a molecular flow regime the values of diameters of pores  $d_p$  were counted, which one also are showing in Table 1 and in Fig.1. As it is visible from the Table 1, excepting the smallest pores, the calculation diameters of pores approximately in 1.5 times exceed their true values. Examined the obtained relations of diameters of pores from time of etching, it is possible to state a well-marked linear dependence with time of "swelling" about 30 seconds (Fig.1). It is visible, that the calculation values of diameters of pores essentially exceed the data of a bubble and electronic microscope. Higher values of calculated diameters of pores or the smaller productivity received from  $d_{\Pi}$  and  $d_{\Sigma M}$  is indicated on large ability to handle of membranes. Which is connected that the porous structure of reactor's TM is a composite system of

intersected pores, instead of it is simple by combination (sum) separately of missing channels.

The main conclusion of the conducted measurements can be served the found considerable excess (in 3-4 times at a considered porosity) actual ability to handle of reactor track membranes above its anticipated values.

The work was funded by the Russian Foundation of Fundamental Research and Government of the Kaluga Region (Grant № 01-03-96013).

Table 1

**The results of a series of experiments by measurement of air flow through TM with different diameters of pores**

$t_{ET}$ , s	$(dV/dt)_E$ , ml/s·sm <sup>2</sup> ·atm	$d_B$ , μm	$d_{EM}$ , μm	$d_C$ , μm	$d_C/d_B$
60	0.70	0.06*	0.05	0.07	1.2
80	4.5	0.09	0.09	0.14	1.6
100	12.5	0.13	0.12	0.20	1.5
120	28.6	0.18	0.18	0.26	1.4
140	50	0.21	0.22	0.32	1.5
160	76.9	0.24	-	0.36	1.5
180	167	0.30	0.27	0.46	1.5

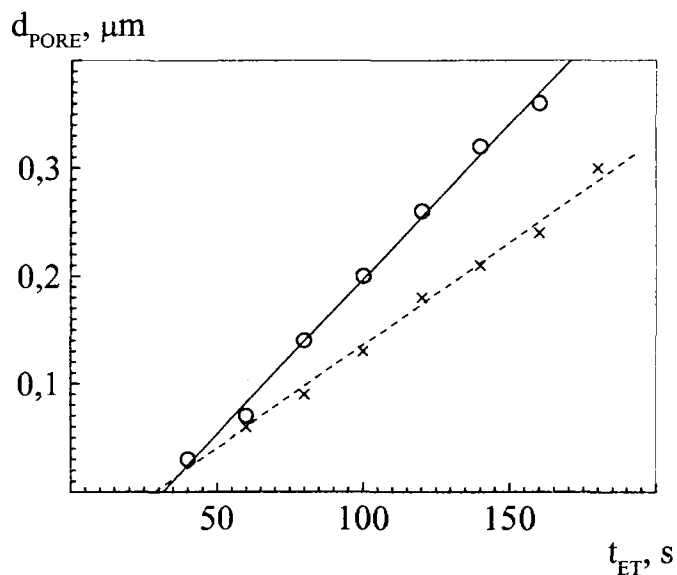


Fig. 1. Matching of relation of diameters of pores from time of etching for an experiment series.  
 × - measurement with the help of a method of a point of a bubble. ○ - calculation of diameters, outgoing from experimental values of an air flow through a membrane

# The Fission Fragments Interaction with Polymeric Compounds and Formation of Latent Track

*A.A. Tumanov, S.A. Kosarev*

The main purpose of the present work is the study of process of interaction of the fission fragments with polymeric materials conducting to formation of latent tracks. The important application of this phenomenon are registration a method of the charged particles and manufacturing of track membranes.

An initial stage of latent tracks formation process is the interaction of heavy ions with substance. We propose, that the basic methods to account of energy losses ( $dE/dx$ ) could be served by the theories Bethe-Bloch and Lindhard. The Bethe formula used for quiet high velocities of an ion ( $V \gg V_0Z$ ) [1]. In the field of low speeds of ions ( $V < V_0Z^{2/3}$ ) when a change of a charge of an ion and the electrons of an ion start to interact with kernels of a target atoms the theory Lindhard has been used. The total losses of energy include electronic ( $d\varepsilon/d\xi_e$ ) and nuclear ( $d\varepsilon/d\xi_n$ ) components [1]. The calculation of a range of an ion in substance is carried out with use of classical dependence on energy losses. Accepting, that the dependence of Bethe and Lindhard should be coordinated, and finding a point of crossing for these dependence [1]. We consider, that the bottom limit of integration procedure should not be zero (at aspiration to zero the integral is missed), but the minimal meaning of average potential of ionization, as a potential of hydrogen atom ionization is ( $I=18.7$  eV).

The presented approach is realized at the code OD-1. With its help calculation of energy losses and range of the fission fragments (see Fig.1) in polyethylene terephthalate (PET) has been carried out.

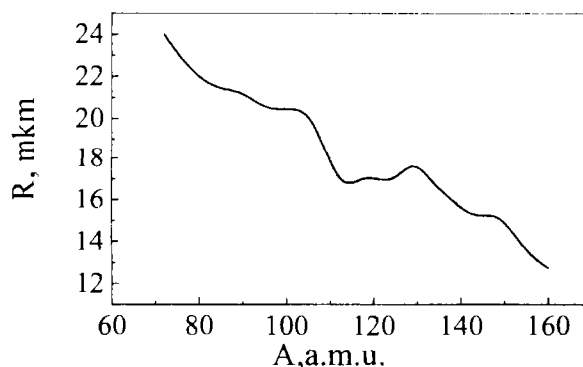


Fig. 1. Dependence of the fission fragments range from the atomic mass

The comparison of accounted results with these codes with experimental data was done. In area of energy (interval from 0.71 to 0.14 MeV/n) for an ions in (reference [2]) the codes do not present the experimental results. There are systematic deviations from 5% to 9% for TRIM-91 from 11% to 20% for SRIM-98.

In energies area from 1 MeV/n to 0.24 MeV/n, the experimental data [3] and calculation dependence of residual energy of the fission fragment on the path length are especially in good agreement. The calculation dependence of residual energy of the

fission fragment on the path length obtained with the use of codes OD-1, TRIM-91 and SRIM-98 lay in the range limited by the experimental error, which equals to 5%.

The importance of the factor of energy losses for formation of a latent track is suggested by the found of his core and halo size [4]. The authors developed a half-empirical dependence of the experimentally certain sizes of latent tracks from values of energy losses. The sizes of tracks are determined indirectly, with the help conductivity cell method, and the additional researches to suppose these conclusions are required. However we consider this approach as successful for the structure of a latent track consideration. In this connection we have lead accounts of values for energy losses, taking dependence from the reference [4] have determined distributions of tracks of the fission fragment on the sizes depending on a way by them in PET. In a work [5] is resulted some other view on the sizes of a track. Approves, that the sizes of a track depend only on speed of a particle and do not depend on a charge and weight. The given statement misses a little to conclusions of work [4] and merits more in-depth consideration. We consider, that, in principal, through electronic microscope it is possible to check up one of the basic statements of that references: the diameter of a track decreases with increase of run distance (see Fig. 2).

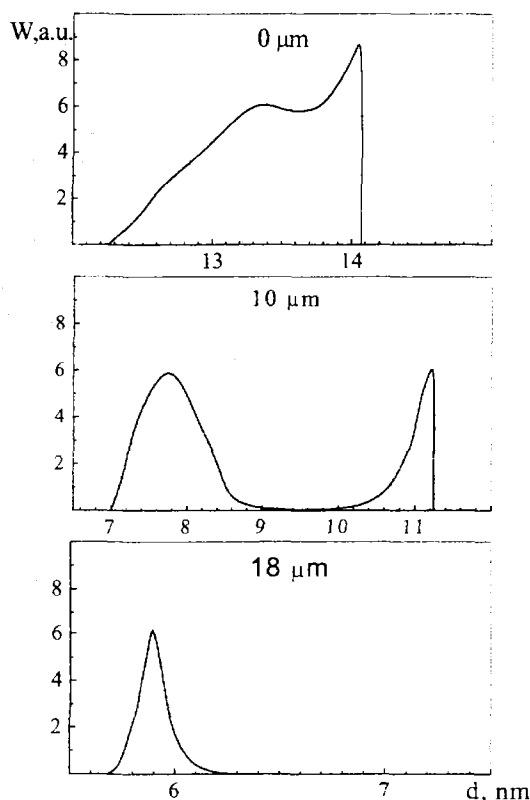


Fig. 2. Distribution of tracks of the fission fragment on the sizes for any thickness

The work was funded by the Russian Foundation of Fundamental Research and Government of the Kaluga Region (Grant № 01-03-96013).

## References

1. G.S.Zhdanov, A.A.Tumanov, S.A.Kosarev et al., The works of regional competition scientific projects in a field of natural sciences. Kaluga. "ADES". 2000. №1. 169-192.
2. Hu Bitao, Qi Zhong, Nucl. Instr. and Meth. B 145 (1998) 288-292.
3. A.V. Khudyakov, Preprint SSC RF IPPE. 1998. P. 14
4. P. Apel et al., Nucl. Instr. and Meth. in Phys. Res. B 146 (1998) 468-474.
5. A.M.Mitrev, Russian chemical journal. 1998. Tom 42. №4. 40-45.

# Physico-mechanical Properties of Thin Polyethylene Terephthalate Films Irradiated by Accelerated Multi-charge Ions and Uranium Fission Fragments

G.S. Zhdanov, N.V. Lomonosova<sup>1</sup>, A.V. Bogacheva<sup>2</sup>, V.K. Milinchuk<sup>2</sup>

<sup>1</sup>*SRC "Karpov Institute of Physical Chemistry", Obninsk, Russia*

<sup>2</sup>*Institute of Nuclear Power Engineering, Obninsk, Russia*

The effect of high-energy radiation on the polymeric materials causes irreversible chemical and structural transformation resulting in significant changes of physico-mechanical properties. Numerous papers describe interaction of the accelerated electrons and  $\gamma$ -radiation with polymers, while the data on the impact of accelerated heavy ions on the polymeric properties are practically absent. At the same time accelerated heavy ions find a wide application in different high-tech processes. To these belong the production of polymeric track membranes, ion lithography, polymer track detectors, plasma treatment of polymers, etc. Therefore, understanding of the mechanisms of heavy ion interaction with polymers is very significant.

Extensive experimental material has been used in the paper to study the influence of accelerated ions and uranium fission fragments on physico-mechanical properties of thin polyethylene terephthalate films. The film samples of about 10-20  $\mu\text{m}$  thickness were cut in three different directions: parallel, at a right and 45° angles to the film orientation direction. The irradiation was made with argon and xenon ions of about 1 MeV/nucleon energy and uranium fission fragments. The fluences varied in the range from  $10^5$  to  $10^{10}$   $\text{cm}^{-2}$ . Mechanical properties (strength, elastic module and elongation-at-break) were determined on the stretching diagrams obtained with the automated instrument UMIV-3. Thermo-mechanical curves and diagrams of isothermal heating were used to evaluate thermo-mechanical characteristics, i.e., the temperature of softening, flow and melting. Molecular orientation was determined by the method of double refraction and isometric heating.

The effect of fission fragments (fluence  $5 \cdot 10^7$   $\text{cm}^{-2}$ ) results in a drastic decrease of the strength and elastic module in the samples cut parallel and at a right angle to the film orientation. In the samples cut at an angle of 45° to the stretching direction, a strength parameter and elastic module of the irradiated film do not differ from similar characteristics of the initial film and exceed the corresponding values in two other directions. At a fluence of about  $5 \cdot 10^8$   $\text{cm}^{-2}$  the strength of samples increases and reaches the value equal to that of the initial film, but then decreases again with increasing fluence. The analysis of thermo-mechanical curves of the film samples cut relative to different orientation directions enables to conclude that the effect of heavy ions on the polymers has an anisotropic character. This proves the fact that heavy ions induce the appearance and propagation of the microshock waves when passing through the polymer.

The work was funded by the Russian Foundation of Fundamental Research and Government of the Kaluga Region (Grant № 01-03-96013).

## Low-rated Wear and Corrosion Monitoring by Thin Layer Activation Technique

*V.V. Sokovikov, I.O. Konstantinov*

In literature there are described many different nuclear measuring methods for very low rates of wear and corrosion in the range of tens and hundreds nm. They are – direct or indirect implantation, recoil and scattering of radioactive products from nuclear reactions, diffusion and some others [1-4].

However modern machinery mainly does not need in such techniques as usual values of surface loss lie within the limits of tens or sometimes unities of  $\mu\text{m}$ . Less values maybe even don't need to be monitored as they provide rather long service life of equipment.

Nevertheless new materials (e.g. hard alloys, ceramics a.o.) and modern processing techniques using lasers, ion beams a.o. allow to obtain very smooth surfaces. Destruction monitoring of such surfaces may call for very precise techniques.

The above listed methods are rather exotic, many of them either change initial surface or are difficult for calibration; all of them are complicated and expensive. Therefore we tried to adapt our traditional thin layer activation (TLA) technique [5] for monitoring low destruction rates .

Of course the best results we gain while measuring the activity of accumulated debris, i.e. the destruction products removed. This version of technique allows to reach the determination limit about tens of nm . The main problem in this version is a correct gathering of debris, what is especially problematic in industrial conditions.

TLA gives quantitative results and has therefore a developed metrological apparatus [6]. Evaluation of metrological parameters provides a grounded approach the precision demands of a client and a reasonable choice of activation and measurement conditions. The low values destruction measuring possibilities are defined by the determination limit.

The decrease of the determination limit of the material removed may be attained by lowering the irradiation energy  $E$  and the beam incidence angle  $\theta$ . The energy is limited by the yield value, very small near the reaction threshold, so the irradiation time will be enormously large. Small incidence angle may result either in a very small beam current (in the case of double slit system providing correct setting of the angle), or in a large error because of rather indefinite angle value. In activation practice the minimum applicable yield should not be lower than  $1 \mu\text{Ci}/\mu\text{Ah}$ , and the beam incident angle less than  $15^\circ - 20^\circ$ . These activation conditions allow to reduce the determination limit down to  $0.3 - 0.5 \mu\text{m}$

Further decreasing of the determination limit may be connected only with specific devices providing a more precise angle adjustment and special methods.

The first example of such devices is presented in Fig.1 and is based on the swinging technique by regular changing beam incidence angle from a certain preset angle (e.g.  $30^\circ$ ) down to  $0^\circ$ . The slope of calibration curve is increased without reducing the activation depth.

These devices are designed for irradiation of cylindrical surfaces and therefore are combined with the possibility of irradiation in the course of rotation. While using these devices the determination limit of material loss was halved.

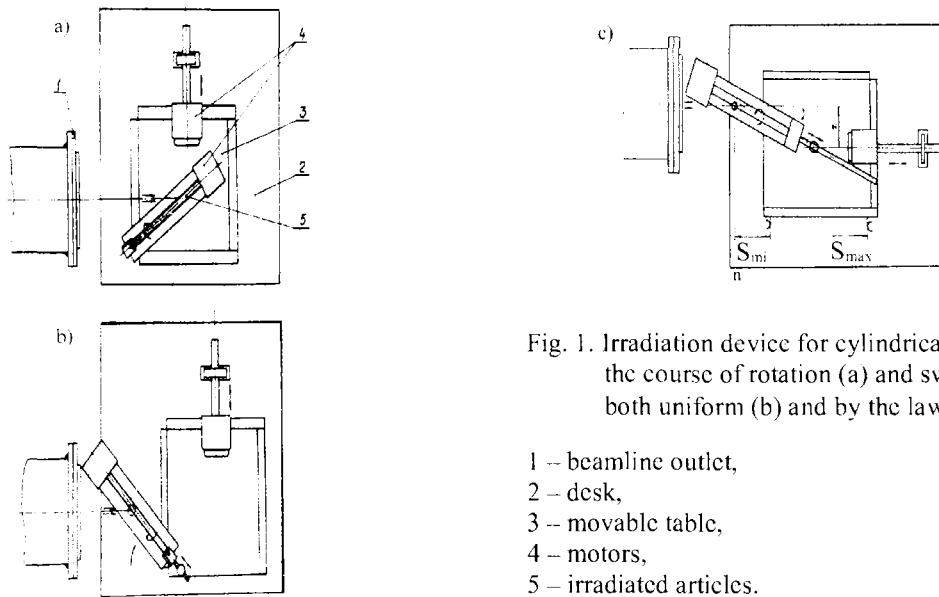


Fig. 1. Irradiation device for cylindrical articles in the course of rotation (a) and swinging, both uniform (b) and by the law  $\theta \sim t^{-1}$  (c)

- 1 – beamline outlet,
- 2 – desk,
- 3 – movable table,
- 4 – motors,
- 5 – irradiated articles.

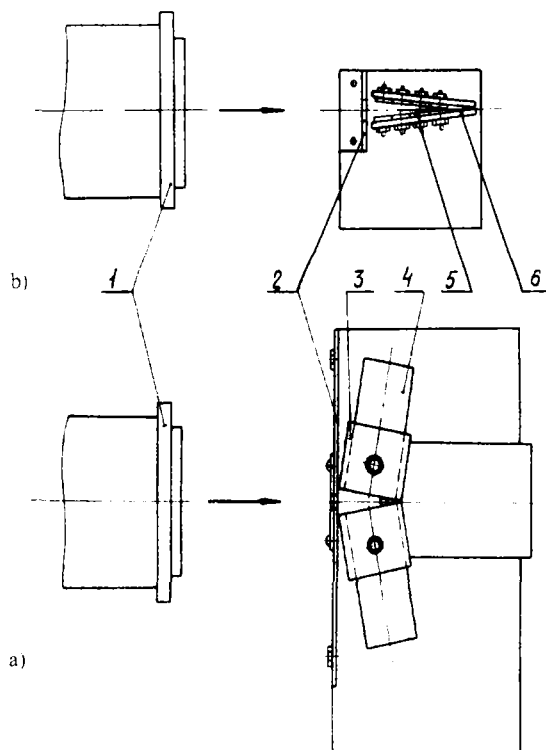


Fig. 2. Irradiation geometry at small incident angles  
a) coupons  
b) cams of internal-combustion engine

- 1 - beam-line;
- 2 - diaphragm;
- 3 - bushes;
- 4 - cams;
- 5 - coupons;
- 6 - screen.

The second version of devices and methods is shown in Fig. 2, presenting the irradiation geometry where similar component parts or samples are installed one to another at a known angle  $\varphi$  (equal to  $12^\circ$ ). The beam is directed into the opening of the angle between irradiating surfaces ( $\varphi = \theta_1 + \theta_2$ ). X- and  $\gamma$ -radiation intensities  $N_x$  and  $N_\gamma$  of the irradiated samples are measured and the ratio  $N_x/N_\gamma$  strongly depends on the label thickness

$$\left(\frac{N_x}{N_\gamma}\right)_1 : \left(\frac{N_x}{N_\gamma}\right)_2 = \frac{\int_0^1 e^{-\mu f(a) \sin \theta_1} da}{\int_0^1 e^{-\mu f(a) \sin \theta_2} da} = \Phi(\theta_1, \theta_2)$$

Here  $f(a)$  is a previously obtained and well-known activity distribution in the same material irradiated at  $\theta = 90^\circ$  and  $\mu$  - X-ray absorbing coefficient for radionuclide under study distributed in the surface by the law  $f(a) \sin \theta$ .

$$\text{Solving a set of equations } \begin{cases} \Phi(\theta_1, \theta_2) = \left(\frac{N_x}{N_\gamma}\right)_1 : \left(\frac{N_x}{N_\gamma}\right)_2 \\ \theta_1 + \theta_2 = \varphi \end{cases}$$

allows to obtain both angles and a sufficiently precise calibration curve.

Estimation of sensitivity  $\left(\frac{d\Phi}{d\theta}\right)^{-1}$  shows that it is maximum at  $\theta_1 = \theta_2$ , therefore the beam axis is to be directed at the bisectrix of angle  $\varphi$ .

Such type of devices was used for irradiation of coupons employed in studying of turbine blade erosion and cams for estimation of motor oils antipitting properties. The label thickness obtained was about 5-6  $\mu\text{m}$  and the determination limit of thickness loss was  $x_b \sim 0,1 \mu\text{m}$ .

In conclusion of this subject it can be stated that traditional TLA technique can successfully provide wear determination with  $x_b \sim 0,1 \mu\text{m}$ .

## References

1. A.S.Khanna, K.G.Prasad, Monitoring of corrosion and wear by nuclear techniques, Report of the Research Co-ordination Meeting of the CRP on Nuclear Methods in Monitoring Wear and Corrosion in Industry, 4-8 June 1996, Debrecen, Hungary
2. I.Mahunka, F.Ditroi, Thin layer activation and wear measurements, *ibid*
3. T.W.Conlon. MeV Ion Recoil Techniques in Research and Technology Nucl.Instr.and Methods, B9 (1985) 311.
4. T.W.Conlon. Indirect Recoil Implantation Following Nuclear Reactions: Theory and Potential Applications. Nucl.Instr.and Methods, 171 (1980) 297.
5. I.O.Konstantinov. Surface activation technique in wear and corrosion monitoring. Izotopy v SSSR, 73 (1988) 5.
6. I.O.Konstantinov, V.V.Sokovikov. Metrological aspects of material activation at the IPPE accelerators. Proc.of XII Intern.Conf. on Electrostatic Accelerators, 25-28 Nov.1997, Obninsk, 1999, pp.142-147.

## Statistical Model of Nuclear Pore Distribution on Track Membrane Surface

V.S.Shorin

Stochastic process of nuclear pore producing on track membrane surface takes to pore overlaps. The forming multiply holes can largely decrease filter selectivity. The analytical approach [1, 2] to overlap problem had made it possible to predict the distribution probability functions  $W_1$  (for single holes) and  $W_2$  (for duplex holes in the case of low porosity  $P < 0.2$ ) only. Now the statistical model of double and triple overlaps for circular pores of unique diameter  $d$  on a planar surface is described for membranes of middle porosity ( $P < 0.5$ ). The ion beam is assumed to be normally incident to membrane surface and to be the Poisson flux with the mean value  $\bar{n} = N_0/L^2$  where  $N_0$  is total number of tracks on the quadratic area of membrane with the side length  $L$ ,  $P = \bar{n}S_1$ ,  $S_1 = \pi d^2/4$ . The model bases on an idea of "guard zone" area  $S_m^G$  for multiply pore of multiplicity  $m$ . The random value  $S_m^G$  is defined as a geometric figure area where none of  $(N_0 - m)$  another pore centres must be found in. It is equal to the area of intersection of  $m$  circles of radius  $d$  around pore centres. The single hole has  $S_1^G = 4S_1$ . There are two configurations for triplex hole with different linear sizes namely "chain" (*ch*), when there are two uncrossing pores, and "full triplet" (*fl*), when all the pores are crossed with each other. Each configuration has its own "guard zone" area  $S_3^G$ . Theoretical evaluations of  $W_m$  were obtained by numerical integration using the formula for differential probabilities [3]

$$dW_2(r_{12}) = \lambda \exp(-\bar{n}S_2^G(r_{12})) dr_{12}^2,$$

$$dW_3(r_{12}, r_{13}, \phi) = \pi^{-1} \lambda^2 \exp(-\bar{n}S_3^G(r_{12}, r_{13}, \phi)) dr_{12}^2 dr_{13}^2 d\phi$$

where  $\lambda = 4P$ ,  $r_{ik}$  is a relative distance between  $i$ - and  $k$ - centers of the multipore (in units of  $d$ ),  $\phi$  is an angle between the vectors  $\vec{r}_{12}$  and  $\vec{r}_{13}$ . The results of calculations were completely confirmed by computer simulation in the range  $P < 0.5$ . The mean of the random value  $S_m^G$  was found to be almost independent on porosity both for duplets and triplets. Its value at  $P=0$  has proved to be an important parameter of the approach which has given approximate values of  $W_m$  in the form of  $W_m^i \cong a_m^i (\lambda)^{m-1} \exp(-\lambda \gamma_m^i)$ , where  $\gamma_m^i = \langle S_{mi}^G \rangle / 4S_1$  and  $a_2=1$ ,  $\gamma_2=(1+3\sqrt{3})/4\pi=1.4135$  ( $\gamma_2=23/16=1.4375$  for quadratic holes),  $\gamma_3^{ch}=1.92475$ ,  $\gamma_3^{fl}=1.60419$ ,  $a_3^{ch}=0.61943$ ,  $a_3^{fl}=0.29288$ . The uncertainties of approximation are less than 4% at  $P=0.45$  and are fast decreased at lesser  $P$ . The interesting fact is the strong dependence of triplet configurations ratio  $W_3^{ch}/W_3^{fl}$  on porosity (from 2.11 at  $P=0$  to 1.18 at  $P=0.45$ ) that can be explained by the difference in "guard zone" parameters  $\gamma_3^i$  and their weights  $a_3^i$ . Such effect proves to be a good test on the approach validity.

The approach was able to evaluate the probability area distribution functions  $G(S)$  of duplex pores and triplex ones and their first moments and the linear sizes of multiple holes. When hole multiplicity  $m$  rises the calculated functions  $G_m(S)$  tend to Gaussian form according to the statistical law of large numbers that confirms the conclusions [2] for quadratic holes. The functions of average sizes of duplex holes and triplex ones vs porosity were obtained by numerical integration up to  $P=0.45$ . It has been found that the mean values of multiply hole area  $\langle S_m \rangle$  (in units of  $S_1$ ) at  $P=0$  were equal to the next

ones namely  $\langle S_2 \rangle^0 = (7/4) = 1.75$ ;  $\langle S_3^{ch} \rangle = 2.6562$ ;  $\langle S_3^{fl} \rangle = 2.1547$ ;  $\langle S_3 \rangle = 2,495$  (for quadratic holes  $\langle S_2 \rangle = 1.775$ ,  $\langle S_3 \rangle = 2.55$  [3]). When  $P$  increases the values  $\langle S_m \rangle$  decrease slowly (by 3.6% for  $m=2$  and 5.3% for  $m=3$  at  $P=0.45$ ) and the rms value raises by 9.3% at  $P=0.45$  for duplets. The triplex area dispersions were found to be approximately constant namely  $(D_3^{ch})^{1/2} = 0.2101$ ;  $(D_3^{fl})^{1/2} = 0.284$ . The largest linear size of triplex holes  $D_{||}$  for “chains” changes from 2.495 ( $P=0$ ) to 2.438 ( $P=0.45$ ). The analytical approach results can be useful both for understanding the observed picture of nuclear pore overlaps and give good tests for MC calculations.

### References

1. Barashenkov V.S. //JINR Reports. R14-10532. Dubna, in Russian).
2. Riedel C., Spohr R. //Rad.Effects. 1979, v.42, No.1/2, p.69.
3. Shorin V.S.// Preprint IPPE – 2835. Obninsk, 2000 (in Russian); //High energy chemistry, 2001, v.35, No.3, p.201

### 3. ACCELERATORS COMPLEX

During 2000 four accelerators were operated for nuclear physics and to study irradiation effects on metals, semiconductors and dielectrics. The main parameters of accelerators are given in Table.

Accelerator type	Singly-charged ion energy (MeV)	Ions type	Operation conditions	Ion beam parameters	Operation time
EG-1	1.5-4.0	p,d	Pulsed	Pulse duration-2 ns Pulse repetition-1-2 MHz Pulse beam current-2,5 mA	1590 h
KG-2,5	0.2-2.0	p,d	Continuous	Beam current 10-100 $\mu$ A	1850 h
EGP-10M	4.0-9.2	p	Continuous	Beam current 0,1-2,0 $\mu$ A	1050 h
EGP-15	5.0-11.5	p	Pulsed	Pulse duration-1,0 ns Pulse repetition-2,5 MHz Pulse beam current-0,5 $\mu$ A	430 h

## 4. PUBLICATIONS

### THEORETICAL NUCLEAR PHYSICS DIVISION

1. Borzov I.N., Avdeenkov A.V., Gruen B., Oberhummer H. Direct neutron capture in microscopical models. Proc. Conf. Nuclei in the Cosmos VI, Aarhus, Denmark, June 2000, to be publ.
2. Borzov I.N. Electron-neutrino capture rates for astrophysical applications. Proc. Conf. Nuclei in the Cosmos VI, Aarhus, Denmark, June 2000, to be publ.
3. Borzov I.N.  $\beta^+$ -strength functions in heavy nuclei and electron-antineutrino capture. Sent to Nucl. Phys., 2000.
4. Камерджиев С.П., Литвинова Е.В. Некоторые вопросы обобщенной теории конечных ферми-систем // Ядерная физика. 2001. Т. 64, № 4.
5. Kamerdzhiev S., Liotta R., Tselyaev V. Random phase approximation for odd nuclei and its application to description of the electric dipole modes in  $^{17}\text{O}$ . Phys. Rev.C, 2001, to be publ.
6. Kamerdzhiev S., Speth J., Tertychny G. Microscopic description of total spectra in  $^{40}\text{Ca}$  ( $\alpha, \alpha'$ ) at  $E_\alpha = 240$  MeV. Annual Report, 2000, IKP (Jülich), 2001.
7. Ignatyuk A.V., Lunev V.P., Shubin Yu.N., Gai E.V., Titarenko N.N., Gudowski W. Neutron and proton cross section evaluations for Th-232 up to 150 MeV. Nucl. Sci. Engin., 2000, submitted.
8. Gai E.V., Ignatyuk A.V., Lunev V.P., Shubin Yu.N. Radiological aspects of heavy metal liquid targets for ADS as intense neutron sources. In: Proc. Conf. on Structure of Nucleus at the Dawn of Century, Bologna, May 2000, World Scientific, to be publ.
9. Ignatyuk A.V. Systematics of low-lying level densities and radiative widths. Ibid.
10. Blokhin A.I., Storozhenko A.N., Vdovin A.I., Ventura A. Microscopic description of properties of hot nuclei. Ibid.
11. Ignatyuk A.V., Schmidt K.-H., Benlliure J. et al. New results on structure effects in nuclear fission. Proc. XV-Workshop on Physics of Nuclear Fission, Obninsk, October, 2000, to be publ.
12. Ignatyuk A.V., Kulagin N.T., Lunev V.P., Schmidt K.H. Analysis of spallation and fission reaction product yields within intranuclear cascade models. Ibid.
13. Ignatyuk A.V. Nuclear Data Needs for Accelerator Driven Subcritical Reactors. Proc. Meeting on Long Term Needs for Nuclear Data Development. IAEA, Vienna, to be publ.
14. Shubin Yu.N. Model calculations and evaluation of nuclear data for medical radioisotope production. J. Radiochimica Acta, 2000, to be publ.
15. Szelecsenyi F., Tarkanyi F., Takacs S., Hermanne A., Sonck M., Shubin Yu., Mustafa M.G., Youxiang Zhuang. Excitation function for  $^{nat}\text{Ti}(p,x)^{48}\text{V}$  nuclear process: evaluation and new measurements for practical applications. Nucl. Instr and Meth. (NIMB), 2000, to be publ.
16. Takacs S., Szelecsenyi F., Tarkanyi F., Sonck M., Hermanne A., Shubin Yu., Dityuk A., Mustafa M.G. and Youxiang Zhuang. New cross sections and intercomparison of deuteron monitor reactions on Al, Ti, Fe, Ni and Cu. Nucl. Instr and Meth. (NIMB), 2000, to be publ.
17. Manokhin V.N., Odano N., Hasegawa A. Consistent evaluation of (n, 2n) and (n, np) reaction excitation function for some even-even isotopes using empirical systematics. Report JAERI (in press).

18. Золотарев К.И., Пащенко А.В. АСТ-1000. Библиотека групповых сечений активации для реактора ВВЭР-1000 // ВАНТ. Сер. Ядерные константы. 2000. Вып. 2. С. 8–19.
19. Zolotarev K.I., Pashchenko A.V. Evaluation of  $^{54}\text{Fe}(n,2n)$  reaction cross sections for high energy dosimetry applications // VANT, ser. Nuclear Constants, 2000, is. 2, p. 20.
20. Хорасанов Г.Л., Блохин А.И., Прусаков В.Н., Чельцов А.Н. Высокообогащенный свинец-206 для малой атомной энергетики // Тр. 5-й Межд. конф. “Физико-химические процессы при селекции атомов и молекул”, 2–6 окт. 2000, Звенигород.
21. Хорасанов Г.Л., Блохин А.И., Сеница В.В. Выжигание трансурановых элементов в жестком спектре нейтронов: Препринт ФЭИ-2843. Обнинск, 2000. Направлена в Известия ВУЗов.
22. Markovskij D.V., Chuvilin D.Yu., Zagryadsky V.A., Nefedov Yu.Ya., Semenov V.I., Shmarov A.E., Savin M.V., Livke A.V., Shvetsov A.M., Blokhin A.I., Manokhin V.N. Evaluation and benchmarking the nuclear data of vanadium in integral experiments with 14-MeV neutrons. Journal for Fusion Energy and Technology, 2000, submitted.
23. Nefedov Yu.Ya., Semenov V.I., Shmarov A.E., Orlov R.A., Savin M.V., Livke A.V., Shvetsov A.M., Nagorny V.I., Zhitnik A.K., Chirkin V.A., Blokhin A.I. Benchmark experiments on measurement of neutron and gamma-ray leakage spectra and yields from three vanadium spheres. Report to the 21 SOFT, September, 2000, Madrid, submitted.

## EXPERIMENTAL NUCLEAR PHYSICS DIVISION

1. Деменков В.Г., Журавлёв Б.В., Лычагин А.А., Трыкова В.И. Двухканальное устройство отбора событий в спектрометрии быстрых нейтронов по времени пролёта // Приборы и техника эксперимента, 2000. № 2. С. 66–69.
2. Журавлёв Б.В., Титаренко Н.Н. Поиск параметров плотности уровней ядер для расширенного интервала энергий возбуждения: Препринт ФЭИ–2819, Обнинск, 2000.
3. Журавлёв Б.В. Плотность уровней ядра  $^{59}\text{Ni}$  // Известия Акад. наук. Сер. Физическая, 2000. Т. 64, № 3. С. 414–421.
4. Zhuravlev B.V., Titarenko N.N., Trykova V.I. “Spin dependence of the nuclear level density of  $^{165}\text{Er}$  and  $^{181}\text{W}$ ”. Report on 8 Inter.Seminar on Interaction of Neutrons with Nuclei (Dubna, May 17–20, 2000). Abstracts of contributed papers, JINR, E3-2000-71, p. 43.
5. Журавлёв Б.В., Титаренко Н.Н., Трыкова В.И. “Спиновая зависимость плотности уровней  $^{165}\text{Er}$  и  $^{181}\text{W}$ ” // Тезисы докладов межд. конф. по ядерной физике “Кластеры в ядерной физике” (Санкт-Петербург, 14–17 июня 2000 г.) Санкт-Петербург, 2000. С. 131.
6. Grigoriev Yu.V., Kitaev V.Ya., Sinitsa V.V., Zhuravlev B.V. et al. “Investigation of the  $^{232}\text{Th}$  neutron cross-section resonance structure in the energy range 1 eV–10 keV”. Report on 8 Inter. Seminar on Interaction of Neutrons with Nuclei (Dubna, May 17–20, 2000). Abstracts of contributed papers, JINR, E3-2000-71, p. 45.
7. Borzakov S.B., Faikov-Stanchik H., Panteleev Ts.Ts., Grigoriev Yu.V. “Energy dependence of neutron cross-section  $\sigma(n,\gamma)$  and  $\sigma(n,f)$  for  $^{235}\text{U}$  in the 0.003–2.0 eV energy interval”. Report on 8 Inter. Seminar on Interaction of Neutron with Nuclei

- (Dubna, May 17–20, 2000). Abstracts of contributed papers, JINR, E3-2000-71, p. 94 // ВАНТ. Сер. Ядерные константы. 2000. Т. 1, С. 3.
8. Borzakov S.B., Faikov-Stanchik H., Panteleev Ts.Ts., Telezhnikov S.A., Grigoriev Yu.V., Smotritsky L.M. "Gamma-ray transitions of  $^{118}\text{Sn}$  observed in radiative capture of thermal neutrons". Report on 8 Inter. Seminar on Interaction of Neutrons with Nuclei (Dubna, May 17–20, 2000). Abstracts of contributed papers, JINR, E3-2000-71, p. 98.
  9. Borzakov S.B., Panteleev Ts.Ts., Strelkov A.V., Grigoriev Yu.V. "Search for dineutron in interaction of thermal neutrons with deuterons". Report on 8 Inter. Seminar on Interaction of Neutrons with Nuclei (Dubna, May 17–20, 2000). Abstracts of contributed papers, JINR, E3-2000-71, p. 101.
  10. Kornilov N.V., Kagalenko A.B. "Investigation of scintillator light output with two dimension experiment". Report on 8 Inter. Seminar on Interaction of Neutrons with Nuclei (Dubna, May 17–20, 2000). Abstracts of contributed papers, JINR, E3-2000-71, p. 82.
  11. Kornilov N.V., Kagalenko A.B., Baryba V.Ya., Demenkov V.Ya., Pupko S.V., Androsenko P.A. "Inelastic neutron scattering and prompt fission neutron spectra for  $^{237}\text{Np}$ ". Annals of Nuclear Energy, 27 (2000), p. 1643–1667.
  12. Корнилов Н.В., Кагаленко А.Б. "Предразрывные нейтроны и интегральный спектр нейтронов деления". Послана в редакцию журнала "Ядерная физика".
  13. Kornilov N.V., Kagalenko A.B., Hamsch F.J. "New evidence of scission neutron existence". Послана в редакцию журнала "Nuclear Physics".
  14. Kornilov N.V., Kagalenko A.B., Hamsch F.J. "Scission neutrons for  $^{235}\text{U}$  and  $^{252}\text{Cf}$ ". Report on 15 Inter. Workshop on Nuclear Fission Physics, Obninsk, October 2–6, 2000.
  15. Лунёв В.П., Проняев В.Г., Симаков С.П., Шубин Ю.Н. Анализ сечений и механизма реакций  $(n, xn)$  и  $(n, \chi\gamma)$  на ядрах Pb и Bi // Известия Акад. наук. Сер. Физическая, 2000. Т. 64, № 1. С. 95.
  16. Grigoriev Yu.V., Kitaev V.Ya., Sinitsa V.V., Zhuravlev B.V., Borzakov S.B., Faikov-Stanchik H., Ilchev G.L., Panteleev Ts.Ts., Kim G.N. "Investigation of the  $^{232}\text{Th}$  neutron cross-sections in resonance energy range". Report on the 2 Workshop for Nuclear Data Production and Evaluation.
  17. Zhuravlev B.V. Nuclear level density of  $^{165}\text{Er}$  and  $^{181}\text{W}$ . 1) Report on the 2 Workshop for Data Production and Evaluation, Pohang Accelerator Laboratory, Pohang, Korea, August 25–26, 2000. 2) Report on the Eurasia Conference on Nuclear Science and Application, Izmir, Turkey, 23–27 October 2000.
  18. Григорьев Ю.В., Журавлёв Б.В., Китаев В.Я., Сеница В.В., Борзаков С.Б., Илчев Г.Л., Файков-Станчик Х., Пантелеев Ц.Ц., Ким Г.Н. Измерение сечения радиационного захвата тория-232 в диапазоне энергий 20 эВ–10 кэВ // ВАНТ. Сер. Ядерные константы. 2000. Вып. 2.
  19. Grigoriev Yu.V., Kitaev V.Ya., Sinitsa V.V., Faikov-Stanchyk H., Mezentsova J.V., Ilchev G.L. Study of a resonance self-shielding effect in the  $\alpha$ -value of  $^{235}\text{U}$  and  $^{239}\text{Pu}$  in the resonance energy range. Report on 15 Inter. Workshop on Nuclear Fission Physics, IPPE, Obninsk, October 2–6, 2000.
  20. Grigoriev Yu.V., Kitaev V.Ya., Moiseev K.V., Panteleev Ts.Ts., Faikov-Stanczyk H. Investigation of a resonance self-shielding effect in the  $\alpha$ -value of  $^{239}\text{Pu}$ . Proc. of 14 Inter. Workshop on Nuclear Fission Physics. (Obninsk, October 12–15, 1998), Obninsk-2000, p. 203.
  21. Back W.Y., Kim G.N., Cho M.N., Ko I.S., Namkung W., Grigoriev Yu.V., Faikov-Stanczyk H., Shvetsov V.N., Furman W.I. Investigation of  $\gamma$ -multiplicity spectra and

- neutron capture cross-section of  $^{232}\text{Th}$  in the energy region 21.5–215 eV. Nucl. Instr. and Method in Phys. Res., B168, (2000), p. 453–461.
22. Григорьев Ю.В. Гравитационный монохроматор нейтронов и монохроматор на основе эффекта силы Кориолиса: Препринт ФЭИ-2797, Обнинск, 2000.
  23. Григорьев Ю.В. О возможности исследования нейтрон-нейтронного взаимодействия по методу догоняющих нейтронов: Препринт ФЭИ-2815, Обнинск, 2000.
  24. Simakov S.P., Fisher U., Moellendorff U. Testing and updating of MoDoLi Monte Carlo code. Report of FZK, Karlsruhe, 2000.
  25. Simakov S.P., Devkin B.V., Kobozev M.G., Talalaev V.A., Fisher U., Moellendorff U. Validation of evaluated data libraries against an iron shell transmission experiment and the Fe (n, xn), reaction cross-section with 14 MeV neutron source. Report on Workshop of Fusion Nuclear Data and Neutronics, NEA Data Bank, Paris, 5–6 December 2000.

## CONDENSED MATTER PHYSICS LABORATORY

1. Блохин В.А., Ивановский М.Н., Кувшинчикова Т.А., Кузин В.В., Морозов В.А., Новиков А.Г., Савостин В.В., Шимкевич А.Л., Шимкевич И.Ю. Структура, атомная динамика, термодинамика и примесное состояние расплавов свинца и висмута: Обзор ФЭИ-290. Обнинск, 2000. 78 с.
2. Кузин В.В., Новиков А.Г., Савостин В.В., Шимкевич А.Л., Шимкевич И.Ю. Атомная динамика жидкого калия и расплава калий-кислород из данных молекулярно-динамического моделирования и экспериментов по неупругому рассеянию нейтронов // Известия ВУЗов. Атомная энергетика, 2000. № 1. С. 40.
3. Beldiman A., Ion M., Kozlov Zh.A., Novikov A.G., Padureanu I., Radulescu A., Savostin V.V. Collective dynamics of liquid gallium studied by inelastic neutron scattering. FLNP Annual Report 1999, Dubna 2000, p. 119.
4. Новиков А.Г., Родникова М.Н., Соболев О.В. О диффузии больших ионов в водных растворах // Письмо в редакцию “Ж. физ. химии”.
5. Novikov A.G., Rodnikova M.N., Sobolev O.V. On the diffusion of big ions in aqueous solutions. FLNP Annual Report 1999, Dubna 2000, p. 143.
6. Новиков А.Г., Селиверстов Д.И., Соболев О.В. Микродинамические характеристики жидкой хлорокиси фосфора  $\text{POCl}_3$ : Препринт ФЭИ-2841, Обнинск, 2000, 22 с.
7. Благовещенский Н.М., Морозов В.А., Новиков А.Г., Савостин В.В., Шимкевич А.Л. Исследование микроструктуры и атомной динамики расплавов свинца и эвтектики свинец-калий методом рассеяния нейтронов: Препринт ФЭИ-2861. Обнинск, 2000.
8. Blagoveshenskii N.M., Morozov V.A., Novikov A.G., Savostin V.V., Shimkevich A.L. Neutron scattering study of the structure and dynamic of liquid lead and lead-potassium: Preprint IPPE-2861. Obninsk, 2000, (in Russian).
9. Bogoyavlenskii I.V., Puchkov A.V. and Skomorokhov A. The association between temperature dependence of liquid  $^4\text{He}$  scattering law and the phenomena of the Bose condensation, Physica B276–278 (2000) 465.
10. Bogoyavlenskii I.V., Puchkov A.V. and Skomorokhov A. Some results of investigation of liquid  $^4\text{He}$  dynamics, FLNP Annual Report 1999, Dubna 2000, p. 121.
11. Дубовский О.А. Щелевой кинематический биэкситон Френнеля // ФТТ. 2000. Т. 42. С. 440.

12. Дубовский О.А. Бризерные солитоны нового типа при Ферми-резонансе оптических колебаний в кристаллах // ФТТ. 2000. Т. 42. С. 665.
13. Agranovich V.M., Dubovsky O.A., Basko D.M., LaRocca G.C., Bassani F. Kinematic Frenkel Biexcitons, *Journal of Luminescence*, 85 (2000) 221.
14. Дубовский О.А. Нелинейные бризерные самоорганизованные колебания ангармонических кристаллитов. Направл. в ред. журн. ФТТ. Исх. 47-03/135 от 24.03.2000.
15. Radulescu A., Padureanu I., Rapeanu S.N., Beldiman A., Ion M., Kozlov Zh.A., Semenov V.A. Low-Frequency Collective Modes in the Superionic Phase of Lead Fluoride FLNP Annual Report 1999, Dubna 2000, p. 147.
16. Ishmaev S.N., Lisichkin Y.V., Puchkov A.V., Semenov V.A. Neutron study of dynamic atomic correlations in amorphous isotopic Ni-B alloys, *Materials Science Forum*, Vols. 321-324 (2000) pp. 502-506.
17. Padureanu I., Kozlov Zh.A., Rotarescu Gr., Semenov V.A. and Radulescu A. High temperature investigation of the dynamics and the thermodynamics of ZrH-U system by neutron scattering: Препринт ОИЯИ Е14-2000-120, Дубна, 2000.
18. Radulescu A., Padureanu I., Beldiman A., Rapeanu S.N., Kozlov Zh.A., Semenov V.A. Observation of Low-frequency excitations of hydrogen in zirconium, *Physica B* 276-278 (2000) 841.
19. Danilkin S., Fuess H., Graf H.A., Hoser A., Wieder T. Phonon dispersion and elastic constants in Fe-Cr-Mn-Ni austenitic steel, *J. of Materials Science*, in print.
20. Danilkin S., Graf H.A., Hoser A., Wieder T. Phonon dispersion in Fe-Cr-Mn(Ni) austenitic steel, BENCS Experimental Report 1999, Hahn-Meitner Institute, Berlin, p. 147.
21. Danilkin S., Jung M. Phonons in nanocrystalline and plastically deformed vanadium and niobium, *ILL Experimental Reports and Theory Activities*, 2000, exp. № 7-01-61.
22. Danilkin S., Fuess H., Gavriljuk V., Hoelzel M., Wipf H. Hydrogen vibrations in austenitic stainless steels, *ILL Experimental Reports and Theory Activities*, 2000, exp. № 4-05-372.
23. Danilkin S., Konstantinov V., Novikov A., Puchkov A., Solovjev B., Zeinalov Sh., Wiedenmann A. "SANS Spectrometer for 1 MW NUR Reactor at URGN, Algeria", *Physica B* 276-278 (2000) 100.
24. Кнотько А.В., Путляев В.И., Морозов С.И. Фононные спектры La - содержащих твердых растворов на основе  $\text{Bi}_2\text{Sr}_2\text{CaCu}_2\text{O}_8$ , измеренные методом неупругого рассеяния нейтронов // Направлено в ред. журнала ФТТ.
25. Дубовский О.А., Орлов А.В., Семенов В.А. Нелинейные бризерные колебания кристаллических материалов вблизи порога потери их структурной устойчивости. Препринт ФЭИ-2870, Обнинск, 2000.

## MATHEMATICS AND SOFTWARE DIVISION

1. Artemyev V.K., Ginkin V.P., Gusev N.V., Folomeev V.I., Lyukhanova T.M., Kartavykh A.V., Milvidskii M.G., Rakov V.V. Numerical simulation of anomalous doping effect in Ge single crystals grown by FZ-technique aboard the spacecrafts // *Proceedings of Third International Conference "Single crystals growth, strength problems, and heat mass transfer" (ICSC-99)*. Obninsk, IPPE, 2000, Vol. 1, p. 26-36.
2. Artemyev V.K., Ginkin V.P., Gorev N.A., Gusev N.V., Folomeev V.I., Lukhanova T.M., Rakitin A.Yu., Senchenkov A.S., Sleptsova I.V. Numerical and experimental study of heat transfer processes in modular furnace "Polizon"//

- Proceedings of Third International Conference "Single crystals growth, strength Problems, and heat mass transfer", (ICSC-99). Obninsk, IPPE, 2000, Vol. 1, p. 15–25.
3. Sviridenco V.P., Shishulin V.P., Kamensky Ya.V., Artemyev V.K., Gusev N.V., Ginkin V.P. Numerical and experimental study of high temperature heat zones in growth devices based on the Bridgman and zones methods//Proceedings of Third International Conference "Single crystals growth, strength problems, and heat mass transfer" (ICSC-99). Obninsk, IPPE, 2000, Vol. 2, p. 477–491.
  4. Артемьев В.К., Гинкин В.П., Земсков В.С., Раухман М.Р., Шалимов В.П. Численное исследование влияния трехмерной конвекции на концентрационную и температурную однородность расплава при выращивании кристаллов в космосе методом бестигельной зонной плавки // Тезисы докладов IX Национальной конференции по росту кристаллов (НКРК-2000), Москва, 16–20 октября, 2000 / М.: ИК РАН. С. 506.
  5. Артемьев В.К., Гинкин В.П., Картавых А.В., Мильвидский М.Г., Раков В.В., Фоломеев В.И. Расчетные исследования влияния конвекции Марангони на распределение примеси в монокристаллах Ge, выращенных в космосе. Там же. С. 507.
  6. Артемьев В.К., Гусев Н.В., Свириденко И.П., Шишулин В.П. Расчетно-экспериментальное обоснование конструкции и параметров тепловых зон космических ростовых установок, основанных на использовании методов Бриджмена и зонной плавки. Там же. С. 520.
  7. Гинкин В.П., Артемьев В.К., Гусев Н.В., Люханова Т.М., Науменко О.М., Фоломеев В.И. Математическое моделирование процессов кристаллизации расплавов в условиях микрогравитации // Труды регионального конкурса научных проектов в области естественных наук. Выпуск 1. Калуга: Издательский дом "Эйдос". 2000. С. 25–47.
  8. Корниенко Ю.Н., Артемьев В.К. Одномерное математическое моделирование и замыкающие соотношения для программ расчета аварийных режимов ЯЭУ// Тез. докладов 4-го Сибирского конгресса по прикладной и индустриальной математике (ИНПРИМ-2000), Новосибирск, 2000. Ч. 4, С. 29.
  9. Корниенко Ю.Н., Артемьев В.К., Зайцев С.И. Метод расчета аварий с потерей теплоносителя в ЯЭУ для программного комплекса "ТРАП-97". Там же. С. 77.
  10. Artemyev V.K., Kornienko Yu.N., Zaitsev S.I. Modernization of Numerical Scheme and Calculation Algorithm for Accidental Regimes in the Code TRAP-97 // Transactions of the Fourth International Exchange Forum "Safety Analysis for NPPs of VVER and RBMK Type", 11–15 October, 1999, Obninsk. US Department of Energy, Office of Nuclear Energy, Science and Technology, p. 1023–1032.
  11. Корниенко Ю.Н., Ниноката Х. К обоснованию одномерных моделей замыкающих соотношений для кодов поканального анализа сборок твэлов // Труды 4-го Минского Международного форума: 22–26 мая, 2000. Минск, 2000. Т. 10, С. 226–233.
  12. Корниенко Ю.Н., Ниноката Х. Аналитические оценки вклада поперечного изменения параметров потока на поведение коэффициентов трения и теплообмена в кольцевых каналах и сборках стержней. Там же. С. 234–242.
  13. Kornienko Yu. On development of Analytical Closure Relationships for Local Wall Friction, Heat and Mass Transfer Coefficients for Sub-Channel Codes // IAEA, TECDOC-1157, "LMFR core thermohydraulics: Status and prospects", June 2000, Vienna, Austria.
  14. Забудько М.А. Точные и численные решения нелинейных уравнений теплопроводности и кинетических уравнений для моделирования процессов

- кристаллизации. Диссертация на соискание ученой степени кандидата физ.-мат.наук. Обнинск, 2000.
15. Галкин В.А., Забудько М.А. Точные и численные решения нелинейных уравнений теплопроводности и кинетических уравнений // Известия вузов. Ядерная энергетика. Т. 1. 2000. С. 19–28.
  16. Cole C.R., Hoover K.A., Foley M.G., Gerhardstein L.H., Williams M.D., Wurstner S.K., Drozhko E.G., Samsonova L.M., Vasil'kova N.A., Zinin A.I., Zinina G.A. Development and calibration of a tree-dimensional regional Hydrogeologic model for the Mayak site // Hydrological Science and Technology, AIH, Urals. Vol. 16, № 1–4, 2000, p. 79–100.
  17. Shimkevich I.Yu. and Shimkevich A.L. Molecular-Dynamics Investigation for Oxygen Effect on Atomic Dynamics in Liquid Potassium: Preprint IPPE–2830. Obninsk, 2000, p. 1–17 (Russian).
  18. Kuzin V.V., Novikov A.G., Savostin V.V., Shimkevich I.Yu., Shimkevich A.L., Zaezjev M.V. Atomic Dynamics of Liquid Potassium and Potassium-Oxygen Melt// Izvestia VUZ, Yadernaya Energetica (Communications of Higher Schools. Nuclear Power Engineering), № 1, 2000.
  19. Кузин В.В., Новиков А. Г., Савостин В.В., Шимкевич А.Л., Шимкевич И.Ю. Цепочечные кластеры растворенного кислорода в расплаве калия // Теплофизические исследования / Под ред. А.Д.Ефанова, Ф.А.Козлова. Обнинск, ФЭИ. 2000. С. 171.
  20. Ginkin V.P., Kulik A.V., Naumenko O.M. An efficient preconditioning procedure in the conjugate gradient method for 3D HEX-Z geometry // Proceedings of the Fourth International Conference on Supercomputing in Nuclear Applications (SNA2000), September 4–7, 2000, Tokyo, Japan.
  21. Гинкин В.П., Кулик А.В., Науменко О.М. Эффективный преобуславливатель в методе сопряженных градиентов для трехмерной HEX-Z геометрии // Тез. докладов 4-го Сибирского конгресса по прикладной и индустриальной математике (ИНПРИМ-2000), Новосибирск, 2000. Ч. 2. С. 80–81.
  22. Artemiev V.K., Ginkin V.P., Folomeev V.I., Kartavykh A.V., Milvidskii M.G., Rakov V.V. Numerical Simulation of Anomalous Doping Effect in Ge Single Crystals Grown by FZ-Technique Aboard the Space Crafts. International Conference on Solid State Crystals - Materials Science and Applications // Abstracts, October 9–13, 2000, Zakopane, Poland, p. 81.

## HIGH-VOLTAGE ACCELERATORS DIVISION

1. Kouzminov B.D. The role of accelerator complex of SSC RF-IPPE in providing nuclear data for nuclear technologies. In: Proceedings of the XIII International Conference on Electrostatic Accelerators, Obninsk: SSC RF-IPPE, 2000, p. 5–12 (in Russian).
2. Gorbich A.F. New modifications of traditional methods of nuclear micro-analysis. Ibid, p. 13–23.
3. Sokovikov V.V., Konstantinov I.O. On the feasibility of studying wear and corrosion of ceramics by the surface activation method. Ibid, p. 81–87.
4. Khorasanov G.L. Light ion radioactive beams at tandem accelerators. Ibid, p. 122–124.
5. Romanov V.A., Ekomasov V.V., Bazhal S.V., Feygin A.S. Accelerating tube of EG-1 (UTPPEG-1-99) ESA. Ibid, p. 146–149.
6. Glotov A.I., Bazhal S.V., Bashmakov V.S., Volodin V.I., Debin V.K., Koupriyanov B.V., Malygin A.A., Nikitin V.A., Romanov V.A., Spirin V.I.,

- Feygin A.S., Chaly Yu.R. Recent works at tandem accelerator EGP-15 at the IPPE for the fundamental and applied investigations. *Ibid*, p. 150–156.
7. Bazhal S.V., Faarinen Mirko, Hellborg Ragnar, Magnusson Carl-Erik, Romanov V.A. Design of the beam optics for a new injector of the Lund Pelletron. *Ibid*, p. 160–166.
  8. Koupriyanov B.V., Bashmakov V.S., Bazhal S.V., Glotov A.I., Matveyev V.M., Chaly Yu.R. Preliminary results of up-grading of EGP-15 accelerator injector. *Ibid*, p. 204–206.
  9. Kanaki V.N., Dudkin N.I., Chaly Yu.R. Electrostatic accelerator EG-1 of SSC RF-IPPE for fast neutron spectrometry. *Ibid*, p. 236–240.
  10. Резвых К.А., Глотов А.И. Полярный эффект пробивного напряжения газовой изоляции высоковольтного ускорителя. Количественная оценка. Тез. докладов сб.: XVII Совещания по ускорителям заряженных частиц. Протвино: ИФВЭ, 2000, 90 с.
  11. Резвых К.А., Глотов А.И., Романов В.А. Расчетная математическая модель пробивного напряжения газовой изоляции и учет показателя шероховатости  $\eta_z$  электродов ускорителя. Там же. С. 90–91.
  12. Резвых К.А., Романов В.А. Эффективность оптимизации геометрии (формы и размеров) электродов высоковольтного ускорителя. Там же. С. 89–90.
  13. Романов В.А., Спирин В.И., Экомасов В.В. Новый ленточный транспортер зарядов для электростатических ускорителей. Там же. С. 89.
  14. Романов В.А., Бажал С.В., Экомасов В.В. Ускоряющая трубка спектрометра быстрых нейтронов на базе электростатического ускорителя. Там же. С. 89.
  15. Glotov A.I., Koupriyanov B.V., Chaly Yu.R., Lura F., Babben St. The accelerator complex "SPRUT" for simulation of space environment at the facility КОBE. In: Proceedings of the 8<sup>th</sup> International Symposium on "Materials in a Space Environment" / 5<sup>th</sup> International Conference on "Protection of Materials and Structures from the LEO Space Environment", Arcachon, France, 5–9 June 2000.
  16. Соковиков В.В., Константинов И.О. Мониторинг малых скоростей изнашивания и коррозии методом радиоиндикаторов: Препринт ФЭИ-2825, Обнинск, 2000, 28 с.
  17. Резвых К.А., Глотов А.И. Количественная оценка влияния полярности на пробивное напряжение газовых промежутков ускорителя: Препринт ФЭИ-2842, Обнинск, 2000, 30 с.
  18. Хорасанов Г.Л., Блохин А.И. Выжигание трансураниевых элементов в жестком спектре нейтронов: Препринт ФЭИ-2843, Обнинск, 2000, 12 с.
  19. Хорасанов Г.Л., Блохин А.И., Сеница В.В. Выжигание трансураниевых элементов в жестком спектре нейтронов // Известия вузов. Ядерная энергетика, 2000. № 3. С. 76–81.
  20. Хорасанов Г.Л., Блохин А.И., Прусаков В.Н., Чельцов А.Н. Высокообогащенный свинец-206 для малой атомной энергетики // Тр. 5-ой Международной научной конференции "Физико-химические процессы при селекции атомов и молекул", 2–6 октября 2000 г., Звенигород. С. 186–189.
  21. Хорасанов Г.Л., Иванов А.П., Коробейников В.В. Выжигание америция в реакторах с жестким спектром нейтронов // Материалы XI семинара по проблемам физики реакторов, Москва, 4–8 сентября 2000 г. М: МИФИ, 2000. С. 200–202.
  22. Khorasanov G.L., Ivanov A.P., Blokhin A.I. et al. Molten lead enriched with isotope Pb-206 as a low activation coolant for emerging nuclear power systems. In: Proc. of the 8<sup>th</sup> Int. Conf. on Nucl. Engineering, ICONE-8, Baltimore, USA, April 2–6, 2000. Paper # ICONE- 8385, 8 p.

## 5. PARTICIPATION IN INTERNATIONAL AND NATIONAL CONFERENCES AND MEETINGS

1.	8 <sup>th</sup> International Symposium on "Materials in a Space Environment" / 5 <sup>th</sup> International Conference on "Protection of Materials and Structures from the LEO Space Environment"	June 5-9 2000	Arcachon, France
2.	XVII Совещание по ускорителям заряженных частиц	17-20 октября 2000	Протвино, Россия
3.	5-я Всероссийская (Международная) научная конференция "Физико-химические процессы при селекции атомов и молекул"	2-6 октября 2000	Звенигород, Россия
4.	XI семинар по проблемам физики реакторов "Физические проблемы эффективного использования и безопасного обращения с ядерным топливом", Волга-2000	4-8 сентября 2000	Москва, Россия
5.	8 <sup>th</sup> International Conference on Nuclear Engineering, ICONE-8	April 2-6, 2000	Baltimore, USA
6.	ANS International Topical Meeting on "Advances in Reactor Physics and Mathematics and Computation into the Next Millenium", PHYSOR-2000	May 7-11, 2000	Pittsburg, USA
7.	FIRST MEETING "Development and practical utilization of small angle neutron scattering (SANS) applications"	November 13-16, 2000	IAEA Vienna, Austria
8.	International Workshop "New Perspectives of Pairing Phenomena in Nuclear Systems"	January 31-February 11, 2000	Trento, Italy
9.	International Conference "Clustering Phenomena in Nuclear Physics"	June 14-17, 2000	St. Peterburg, Russia
10.	IX International Seminar "Electromagnetic Interactions of Nuclei at Low and Medium Energies"	September 20-22, 2000	Moscow, Russia

## 6. COOPERATION

№№	Topic	Organization	Country
1.	Condensed matter study and the neutron spectrometry methods development.	Frank Laboratory of Neutron Physics, Joint Institute on Nuclear Research	Dubna, Russia
2.	The partial dynamical structure factors study of the crystalline and amorphous compounds Ni-B by the inelastic neutron scattering.	Russian National Centre - "Kurchatov Institute"	Moscow, Russia
3.	Study of the microscopic dynamics of the aqueous and nonaqueous solutions by the inelastic neutron scattering.	Kurnakov Institute of General and Inorganic Chemistry, Russian Academy of Sciences	Moscow, Russia
4.	Investigation of the influence of high frequency nonlinear vibrations - biphonons, biexcitons, solitons - with the energy near the lattice stability barrier on the phase transition kinetic in the crystalline and the disordered solid materials.	Institute of Spectroscopy, Academy of Sciences of Russian Federation	Troitsk, Moscow Region
5.	Study of lattice dynamic of high temperature superconductors.	Chemical faculty of MSU	Moscow, Russia
6.	The investigation of the quantum liquids fundamental properties by neutron scattering.	National Scientific Centre of Ukraine - "Kharkov Institute of Physics and Technology"	Kharkov, Ukraine
7.	The investigation of hydrogen effect on the crystal structure and lattice dynamics of the austenitic Fe-Cr-Mn steels by the neutron diffraction and inelastic neutron scattering.	Institute for Metal Physics, Ukraine Academy of Science	Kiev, Ukraine
8.	Surface excitations in thin helium film in silica aerogels.	Institute of Laue-Langevin	Grenoble, France
9.	A study of the lattice dynamics of fast ion conductors with the fluorite structure at the transitions temperatures.	Institute for Physics and Nuclear Engineering	Bucharest, Romania

10.	Interstitial atom effect on the crystal structure and lattice dynamics of the triple Nb-O-H(D) solid solutions and high nitrogen steels.	Darmstadt University of Technology	Darmstadt, Germany
11.	X-ray diffraction and inelastic neutron scattering study of the substitutional alloying additions effect on the crystal structure and lattice dynamics of the austenitic steels.	Institute of Solid State Physics, Bulgarian Academy of Science	Sofia, Bulgaria
12.	The investigation of nanocrystal materials and the elastic deformed metals by neutron scattering.	Hahn-Meitner-Institute	Berlin, Germany
13.	Accelerator system "SPRUT" with overlapping low energy electron and proton beams for use in simulating complex KOBE	Deutsches Zentrum für Luft-und Raumfahrt e.V.	Berlin, Germany
14.	Charging belt system for electrostatic accelerators	Institute of Ion Beam Physics and Materials Research	Rosendorf, Germany
15.	Application of Electrostatic Accelerators in Basic and Applied Research	University of Lund, Department of Physics	Lund, Sweden
16.	Extended theory of finite Fermi systems. Calculations of $^{40}\text{Ca}(\alpha, \alpha')$ cross sections	Forschungszentrum Jülich	Jülich, Germany